

The University of Maine

DigitalCommons@UMaine

---

Electronic Theses and Dissertations

Fogler Library

---

Fall 12-18-2020

## Understanding Biomass Upgrading Through Hydrogenolysis Reactions: Kinetics and Mechanism

Jalal Tavana

University of Maine, [jalal.tavana@maine.edu](mailto:jalal.tavana@maine.edu)

Follow this and additional works at: <https://digitalcommons.library.umaine.edu/etd>



Part of the [Catalysis and Reaction Engineering Commons](#), and the [Materials Chemistry Commons](#)

---

### Recommended Citation

Tavana, Jalal, "Understanding Biomass Upgrading Through Hydrogenolysis Reactions: Kinetics and Mechanism" (2020). *Electronic Theses and Dissertations*. 3304.

<https://digitalcommons.library.umaine.edu/etd/3304>

This Open-Access Thesis is brought to you for free and open access by DigitalCommons@UMaine. It has been accepted for inclusion in Electronic Theses and Dissertations by an authorized administrator of DigitalCommons@UMaine. For more information, please contact [um.library.technical.services@maine.edu](mailto:um.library.technical.services@maine.edu).

**UNDERSTANDING BIOMASS UPGRADING THROUGH  
HYDROGENOLYSIS REACTIONS: KINETICS AND MECHANISM**

By

Jalal Tavana

B.Sc. Chemical Engineering Tehran Polytechnic, 2011

M.Sc. Chemical Engineering Tehran Polytechnic, 2014

A DISSERTATION

Submitted in Partial Fulfillment of the

Requirements for the Degree of

Doctor of Philosophy

(in Chemical Engineering)

The Graduate School

The University of Maine

December 2020

Advisory Committee:

Thomas J. Schwartz, Assistant Professor of Chemical Engineering, Advisor

M. Clayton Wheeler, Professor of Chemical Engineering

William J. DeSisto, Professor of Chemical Engineering

Carl P. Tripp, Professor of Chemistry

Caitlin Howell, Assistant Professor of Biomedical Engineering

# UNDERSTANDING BIOMASS UPGRADING THROUGH HYDROGENOLYSIS REACTIONS: KINETICS AND MECHANISM

By Jalal Tavana

Dissertation Advisor: Thomas J. Schwartz

An Abstract of the Dissertation Presented  
in Partial Fulfillment of the Requirements for the  
Degree of Doctor of Philosophy  
(in Chemical Engineering)  
December 2020

This dissertation involves several hydrogenolysis reactions but is mainly focused on hydrodechlorination (HDC) of chlorobenzene (PhCl) and hydrodeoxygenation (HDO) of 2-furancarboxylic acid (FCA). Hydrodechlorination of PhCl has been the subject of research for some time. Here, we used a Pd/C catalyst to study this reaction through rigorous kinetics and mechanistic analyses in a CSTR reactor. The  $H_2/D_2$  kinetic isotope effect (KIE) experiment revealed that  $H_2$  is not involved in a rate controlling step. The kinetics data are in agreement with similar systems reported before and follow a first-order dependence on chlorobenzene, half order for hydrogen and an inverse first order with respect to HCl. These data suggest a mechanism that involves C-Cl cleavage in the rate controlling step preceded by adsorption of reactant and followed by desorption of products from the surface. The derived rate expression was used in a microkinetic model to predict the observed rates of this reaction. This model successfully captures the experimental trends observed in the kinetic studies. Moreover, motivated by the applications of *in situ* spectroscopic techniques, the detailed design of an FTIR cell which enables both steady state and transient studies to measure kinetics and investigate the mechanism of reactions at a molecular level, is included.

Hydrodeoxygenation of 2-furancarboxylic acid was investigated to produce  $\delta$ -valerolactone, which represents a series of functionalized lactone molecules that have a potential to be used in prospective polymers. Motivated by excellent HDO activity reported for Ru/TiO<sub>2</sub> catalysts, and with the aim of taking advantage of the built-in bifunctionality of this catalyst when introduced to hydrogen, we have used Ru/TiO<sub>2</sub> to quantitatively synthesize the functionalized lactone monomer (FDHL). The focus of our work has been to optimize process parameters, including temperature, solvent, catalyst support, metal loading, weight of the catalyst and reaction time, to achieve an acceptable yield for the target product. The yield of 53% to  $\delta$ -hexalactone (DHL) for a simple 5-methyl-2-furancarboxylic acid was significantly greater than the previous reports.

## DEDICATION

*Dedicated*

*to*

*My parents, Mohammadali Tavana and Fatemeh Yusefian who  
encouraged me to take this adventure.*

*The love of my life, Atefeh Rajaei for her continued support and  
sharing this journey with me.*

## ACKNOWLEDGEMENTS

I would like to express my appreciation to Prof. Thomas J. Schwartz for being a great mentor, his support and for all the encouragements he provided.

I would like to acknowledge Mohammed Z. Algharrawi for his part in collecting kinetics data on hydrodechlorination of chlorobenzene.

I would like to thank Dr. Brian G. Fredrick for allowing to use his instruments and taking every opportunity as a moment to teach, excellent discussions in our group meetings and precious feedback.

I would like to thank Timothy J. Thibodeau, Françoise G. Amar, and Brian G. Fredrick for data on hydrodeoxygenation of Acrolein over  $WO_x$  and DFT calculations.

I would like to thank Dr. William Gramlich and his student Atik Faysal for their collaboration on creating bio-based polymers. It has been a wonderful experience getting to know another research area.

I would like to thank my friends at the University of Maine Catalysis Research Group for their support and making my PhD an interactive learning experience.

I would like to thank the UMaine Vice President for Research for providing start-up funds, ACS-PRF grant# 56712 DNI-5 and USDA grant# 2018-67010-279 for this work.

I would also like to thank Keith Hodgins for his help in the machine shop for construction of FTIR cell described in Chapter A.

Finally, I would like to acknowledge the presence of some wonderful people including Nayereh, Koorosh, Azadeh, Kasra and Atefeh for being there for me. It is always nice to have people to share a smile with or to talk to, especially in a time that politics keeps people separated from the loved ones and you have no other defence than to keep smiling.

## TABLE OF CONTENTS

DEDICATION .....	ii
ACKNOWLEDGEMENTS .....	iii
LIST OF TABLES .....	v
LIST OF FIGURES .....	vi
1. INTRODUCTION .....	1
1.1 Motivation.....	1
1.2 C-Cl Catalytic Hydrogenolysis .....	2
1.2.1 Gas Phase Hydrodechlorination .....	3
1.2.2 Liquid Phase Hydrodechlorination .....	11
1.3 C-O Catalytic Hydrogenolysis.....	16
1.4 Thesis Scope .....	28
2. HYDROGENOLYSIS OF CHLOROBENZENE.....	30
2.1 Introduction .....	30
2.2 Experimental.....	31
2.2.1 Catalyst Preparation .....	31
2.2.2 Catalyst Characterization.....	32
2.2.3 Reaction Kinetics Studies .....	33
2.3 Results and Discussion.....	35
2.3.1 Reaction Selectivity and Catalyst Stability .....	35
2.3.2 Reaction Order Measurements.....	36

2.3.3	Hydrogen-Deuterium Isotope Effect.....	38
2.3.4	Proposed Reaction Sequence.....	39
2.4	Summary .....	44
3.	C-O HYDROGENOLYSIS .....	46
3.1	Introduction .....	46
3.2	Materials and Methods .....	49
3.2.1	Preparation of catalysts .....	49
3.2.2	Catalyst Activity .....	50
3.3	Results and Discussion.....	51
3.3.1	Hydrogenolysis of FCA Over Various Catalysts .....	51
3.3.2	Solvent Effect .....	52
3.4	Lactone Yield Improvement .....	54
3.5	Conclusion.....	58
4.	REACTION KINETICS ANALYSIS OF ACROLEIN HYDRODEOXYGENATION OVER A TUNGSTEN OXIDE CATALYST: MICROKINETIC MODELING .....	59
4.1	Introduction .....	59
4.2	Theoretical Methods .....	61
4.3	Results .....	63
4.3.1	Hydroxyl Formation and Surface Oxygen Vacancy Creation.....	63
4.3.2	Microkinetic Modeling.....	63
4.4	Discussion .....	66
4.5	Summary .....	68
	REFERENCES .....	70

APPENDIX – REACTOR CONFIGURATION FOR FTIR STUDIES.....	96
BIOGRAPHY OF THE AUTHOR.....	103

## LIST OF TABLES

2.1	Sequence of elementary steps for HDC of PhCl.....	42
2.2	Thermodynamic values for rate constants calculation.....	43
3.1	Optimizing reaction conditions to maximize DHL.....	56
3.2	Recent reports on reduction of FCA and similar structures to their prospective lactone compounds. ....	57
4.1	Sequence of elementary steps on the bronze surface.....	66
4.2	Modification to parameters adopted from DFT.....	67
4.3	Degree of rate control analysis for routes leading to acrolein, propene an propanol and the overall turn over frequency. ....	69

## LIST OF FIGURES

1.1	Calculated structures of 4-CP on Pd(111).....	8
1.2	Reduction of 4-NP and HDC of 4-CP.....	14
2.1	TEM micrograph of the reduced 5wt% Pd/C catalyst.....	35
2.2	Product selectivity of PhCl HDC over Pd/C .....	36
2.3	Reaction order plots of PhCl HDC.....	38
2.4	Kinetic isotope effect.....	39
2.5	Experimental and predicted chlorobenzene HDC TOF associated with Pd/C: P <sub>H<sub>2</sub></sub> =10-97 kPa; T=323-353K.....	44
3.1	Hydrogenolysis of FCA using Ru over various supports. ....	52
3.2	Effect of Solvent in Hydrodeoxygenation of FCA over 5%Ru/TiO <sub>2</sub> catalyst .....	54
3.3	Concentration profile for the reduction of FCA.....	55
4.1	Proposed catalytic cycle for the reduction of acrolein to propene, allyl alcohol, and 1-propanol on a model W <sub>3</sub> O <sub>9</sub> cluster.....	60
4.2	The fully oxidized W <sub>3</sub> O <sub>9</sub> cluster used in the calculations.....	62
4.3	Energy and free energy of species in PES relative to structure of 12 + Acrolein + 2 H <sub>2</sub> . ....	64
4.4	Extracting kinetics of oxygen vacancy creation from TGA data.....	65
4.5	Initial oxygen coverage calculated from microkinetic model assuming the reactor is a transient CSTR. ....	65

4.6	Microkinetic model prediction of the product distribution based on raw DFT data.....	67
4.7	Microkinetic model captures the trends of product distribution. ....	68
A.1	FTIR experimental set-up.....	97
A.2	Pd insertion stages into C-Cl bond in chlorobenzene. <sup>1</sup> .....	98
A.3	3D CAD assembly of the operando transmission IR reactor .....	101

## LIST OF SCHEMES

1.1	Reaction scheme for HDC of PhCl proposed by Coq et al. <sup>2</sup> .....	4
1.2	Reaction mechanism on a bimetallic surface.....	5
1.3	Step wise and concerted mechanisms of HDC for DCB proposed by Chen and Liu <sup>3</sup> .....	10
1.4	Reaction pathways for the HDC of 2,4-DCP <sup>4</sup> .....	11
1.5	Proposed reaction mechanism of the Mg metal mediated dechlorination of aromatic chlorides. ....	15
1.6	Reaction pathways for HDC of PhCl proposed by Yakovlev et al. <sup>5</sup> .....	16
1.7	Mechanism of direct deoxygenation of 2-ethylphenol over CoMoS/Al <sub>2</sub> O <sub>3</sub> . <sup>6,7</sup> .....	19
1.8	Mechanism of deoxygenation of m-cresol over Ni, Fe and Ni-Fe Catalysts. <sup>8</sup> .....	20
1.9	Proposed mechanism for anisole hydrodeoxygenation over La <sub>0.8</sub> Sr <sub>0.2</sub> CoO <sub>3</sub> . ....	22
1.10	Mechanism of phenolic model compound adsorption over (a) silica and (b) alumina supports. Extracted from Popov et al. <sup>9</sup> .....	23
1.11	Hydrodeoxygenation mechanism of oxygenated compounds over metallic catalysts with active supports. Extracted from Mendes et al. <sup>10</sup> , van Duijne et al. <sup>11</sup> , He and Wang <sup>12</sup> . ....	24
1.12	Proposed molecular mechanism of DDO pathway for phenol over Ru/TiO <sub>2</sub> .....	25
1.13	Reaction mechanism of FCA reduction over Pt–MoO <sub>x</sub> /TiO <sub>2</sub> catalyst. ....	27
3.1	2-Furancarboxylic acid (FCA) reduction to tetrahydro-2-furancarboxylic acid (THFCA) and $\delta$ -valerolactone (DVL).....	48
3.2	5-methyl-2-Furancarboxylic acid (5MFCA) reduction to 5-methyltetrahydro-2-furancarboxylic acid (5MTHFCA) and $\delta$ -hexalactone DHL). ....	56

# CHAPTER 1

## INTRODUCTION<sup>1</sup>

### 1.1 Motivation

Biomass is the only renewable organic carbon-neutral source with many advantages including abundance and low price.<sup>13</sup> Ever increasing research revolving around biomass in the past decades has been focused on the selective conversion of highly functionalized sugars and lignin-derived chemicals into aliphatic fuels and aromatics. Heterogeneous catalysis is a highly efficient chemical process to efficiently transform biomass to meet the market demand while keeping its environmental impact minimal. Biomass catalysis may have been born from existing knowledge of petroleum industries,<sup>14</sup> initially with traditional catalytic materials employed in the industry while research has already steered towards discoveries of new catalytic materials,<sup>15</sup> with the help of computational<sup>16,17</sup> and experimental techniques<sup>18,19</sup> tailored for biomass conversion. Since current infrastructure for petroleum-based refineries is in place, it is reasonable to think that this effort will likely be focused on trying to replace petroleum-derived analogues.<sup>20</sup> Cheap production of North American shale gas comes at a historic moment since it might be viewed as a potential market competitor, however, shale gas and biomass in fact have a symbiotic relationship.<sup>21,22</sup> Bio-based feedstocks are made of large molecules that are highly oxidized, demanding the use of upgrading technologies such as hydrotreating and hydroprocessing to be suitable for market demands especially in the energy industry; therefore, hydrogen has been identified as the major economic cost for implementation of catalytic biomass processes. On the other hand, shale gas is made of light alkanes, mostly methane and small

<sup>1</sup>This is from a paper, J. Tavana, D. V. Stück, T. J. Schwartz. “Hydrogenolysis of C-X bond through heterogeneous catalysis: A Review” (In preparation)  
My contribution is equal to the second author in research and writing the paper.

(<C4) hydrocarbons, and can provide cheap hydrogen right now instead of waiting for sustainable alternative energy sources in the future.<sup>23</sup>

Important components of biomass, *e.g.* cellulose and lignin, can be depolymerized into important platform chemicals like 5-hydroxymethylfurfural (HMF) and 5-chloromethylfurfural (CMF) that are especially important because their structures contain reactive groups with a strong chemical reactivity that paves the way to be upgraded to a wide range of value-added chemicals.<sup>24</sup> Upgrading reactions of these platform structures involves removal of chlorine and oxygen namely hydrodechlorination (HDC) and hydrodeoxygenation (HDO), respectively. There are even reports for the confluence of these reactions improved reactivity and selectivity of the target chemicals.<sup>25</sup>

## 1.2 C-Cl Catalytic Hydrogenolysis

Chloroarenes are used in many industries from dyes, herbicides, pesticides, solvents to their application as intermediates in organic synthesis;<sup>26</sup> therefore, these compounds are one of the main sources of chlorine released to the environment.<sup>27</sup> On the other hand, removal of chlorine before HDO in reactions like production of 2,5-dimethylfuran (DMF) from CMF, opens routes to intermediates, like ether products that are not easily degradable and can even improve the kinetics of the HDC reaction.<sup>24</sup> Studying hydrodechlorination (HDC) is usually performed on compounds like chlorobenzene (PhCl) and chlorophenol (CP) since they represent the halogenated species found in many organic wastes,<sup>28</sup> and in turn this knowledge could be applied to HDC of pseudo-aromatics like CMF.

Catalytic hydrodechlorination (HDC) of chloroaromatics is a non-destructive, low energy approach for the removal of chloride in the production value added products,<sup>29-32</sup> as intermediates in organic synthesis<sup>33</sup> and for treatment of hazardous wastes.<sup>34-38</sup> hydrodechlorination can be performed in both the liquid- and gas-phase; however the latter has some advantages over the former in terms of improved catalyst stability, such as no requirement for additional solvent and high efficiency.<sup>39</sup> hydrodechlorination of chlorinated

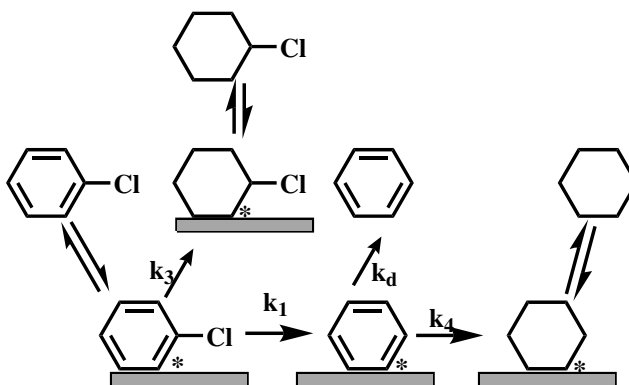
organics is usually performed with supported transition metal catalysts such as Pd,<sup>2,40-42</sup> Pt,<sup>43</sup> Rh,<sup>2,44</sup> Ru,<sup>45,46</sup> Ni<sup>42,47-49</sup> and bimetallic catalysts that modify the electronic properties of the metal phase (*e.g.* Pd-Fe,<sup>50,51</sup> Pd-Ni,<sup>52,53</sup> Cu-Ni,<sup>54</sup> Pd-Rh<sup>44</sup>). However, non-noble metal catalysts tend to deactivate due to surface poisoning by HCl, which forms inactive surface metal halides<sup>55,56</sup> The support has been reported to play a role in the activity, selectivity and stability of some catalysts used for HDC.<sup>47,57</sup> Basically, inorganic and organic materials can be selected as supports as long as they are stable under corrosive conditions (*i.e.* high concentrations of HCl and HF and/or high temperatures) and avoid secondary reactions such as Cl/F exchange or coupling reactions.<sup>28</sup> Urbano and Marinas<sup>28</sup> have categorized catalytic supports suitable for hydrodehalogenation (HDH) reactions into organic and inorganic supports. Inorganic supports are mainly alumina,<sup>38,43,51,53,58-61</sup> silica,<sup>38,41,43,62-64</sup> and other metal oxides such as MgO,<sup>65</sup> ZrO<sub>2</sub><sup>66</sup> etc. The main disadvantage of these supports is that they are readily attacked by hydrogen halides formed during the reaction and they favor unwanted reactions leading to selectivity loss. Activated carbons<sup>40,41,45,52,63,67,68</sup> are the main organic supports and most widely used for this reaction due to their chemical resistance, high surface area and low cost.<sup>57</sup> Diverse reaction conditions for HDH reactions (*e.g.* gas-phase versus liquid-phase, aliphatic halides versus aromatics, etc.) might make it difficult to draw general conclusions about the reaction mechanism.<sup>28</sup> This chapter will deal with kinetics and mechanism of catalytic HDC reactions chlorinated aromatics in gas and liquid phase.

### 1.2.1 Gas Phase Hydrodechlorination

In one of the earlier studies on the mechanism of gas phase HDC of PhCl, Coq et al.<sup>2</sup> used Pd/Al<sub>2</sub>O<sub>3</sub> and Rh/Al<sub>2</sub>O<sub>3</sub> catalysts at 353K. The authors propose a reaction scheme similar to the Mars-van Krevelen (MvK) mechanism for oxidation of hydrocarbons through which PhCl interacts with the surface and forms an adsorbed chloride and gaseous benzene; hydrogen recovers a site and HCl competes with the reactant for chlorination

step. They conclude that the rate determining step is the reaction between dissociated hydrogen and PhCl, and adsorption of HCl and PhCl is competitive.

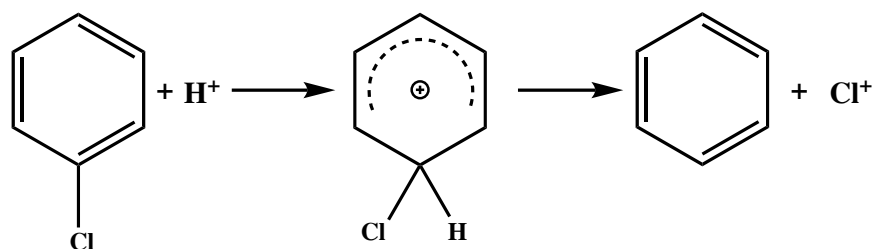
Palladium possesses intrinsic resistance to poisoning and usually is reported to have minor or no deactivation;<sup>69</sup> however, other catalysts exhibit lower activity and are believed to be strongly structure sensitive. Recent studies have shown improved activity (up to 70 times faster reactions) for Pd-decorated Au catalyst for aqueous phase HDC.<sup>70,71</sup> Klokov et al.<sup>72</sup> observed better reactivity for Co/C nanocomposites when compared with cobalt in C shell structure and Co/CNT composites. Jujjuri and Keane<sup>41</sup> argue that Pd/SiO<sub>2</sub> catalysts with bigger particle sizes show better reactivity. The reason for these observations is attributed to the electrodeficient character of small particles causing a susceptibility to chlorine attack which in turn leads to deactivation and selectivity loss.



Scheme 1.1: Reaction scheme for HDC of PhCl proposed by Coq et al.<sup>2</sup>.

Due to the concerns around stability of monometallic catalysts, some research is focused on the modification of monometallic catalytic systems by combining it with another transitional metals. Hagh and Allen<sup>73</sup> used NiMo/ $\gamma$ -Al<sub>2</sub>O<sub>3</sub> for hydrodechlorination of chlorobenzene and drew an analogy between the HDC mechanism of chlorinated aromatics and hydrodesulfurization (HDS) where sulfur anion vacancies exposing Mo<sup>+3</sup> are the active sites responsible for HDS reaction. The surface anion vacancies are believed to have a *pi* bond interaction with the aromatic ring. Seshu Babu et al.<sup>53</sup> assumed the same role for Ni in Pd-Ni/Al<sub>2</sub>O<sub>3</sub> catalysts with the formation of a diadsorbed chloroaromatic species. The

resonant structure of the benzene ring is weakened by adding electrons to the antibonding orbital followed by the attack of a proton which results in the formation of an arenium ion as the transition state. Despite the insufficiency of existing database on bimetallic catalysts in HDC reactions for drawing any generic conclusions, it is generally acknowledged that catalytic HDC, is strongly influenced by the electronic structure of the active metal sites.



Scheme 1.2: Reaction mechanism on a bimetallic surface.

The gas-phase HDC of a range of chlorinated aromatics was studied over the temperature range 473 K-573 K using Ni/SiO<sub>2</sub> catalysts.<sup>47,48,74</sup> Adsorption of chlorinated compound is reported to occur through the partially positive carbon atom connected to chlorine while another hydrogen adatom attacks the adsorbed molecule to cleave the C-X (X= Cl, Br<sup>74</sup>) bond which is assumed to be the rate determining step. When considering polychlorinated products such as dichlorophenol (DCP), it is expected that due to the high electronegativity of the chlorine atom, the dissociation energy of C-Cl increases proportionately.<sup>48</sup> Moreover, the activity and selectivity would be affected by steric effects when chlorine is close to the substitution (*i.e.* ortho position), the chlorine removal occurs in a concerted step.

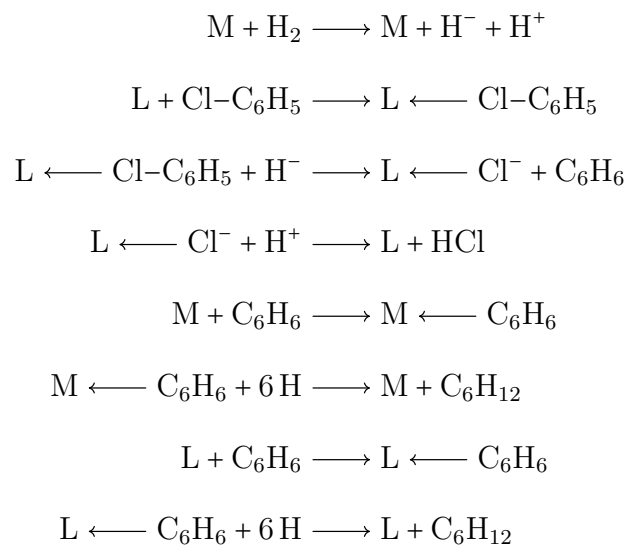
Keane and Murzin<sup>47</sup> compared different mechanistic assumptions offered in the literature.<sup>2,48,50,62,73</sup> Their results suggest a non-uniform surface is involved in the reaction, which highlights the role of spillover hydrogen from the support as necessary to explain the experimental observations. Amorim and Keane<sup>75</sup> even considered improving the activity by increasing the spillover hydrogen through adding Al<sub>2</sub>O<sub>3</sub> component to Ni and Pd. They

found no significant changes when using Pd, which is intrinsically active for the reaction, while Ni showed an increased activity.

Cobalt-based amorphous catalysts have been reported to demonstrate low activity in HDC of chlorobenzenes and chlorophenols.<sup>31</sup> Since non-noble metal catalysts are more likely to deactivate in the presence of HCl in HDC reaction, encapsulation of the active metal nanoparticles by a thin layer of carbon is suggested to be a promising solution to prevent deactivation.<sup>72</sup> Cecilia et al.<sup>55</sup> suggest a synergic metallic effect in cobalt phosphide catalysts that leads to the activation of the C–Cl bond facilitated by spillover hydrogen.

Hydrodechlorination of chlorobenzene and 1,3-dichlorobenzene was performed over Pd/SiO<sub>2</sub> (1.4-8.3 wt% Pd loading) over the temperature range of 373-423K.<sup>41</sup> In a chemically controlled condition, varying inlet H<sub>2</sub> partial pressure affects HDC rate according to a Langmuir–Hinshelwood type model, suggesting competitive dissociative hydrogen adsorption and associative chlorinated aromatic adsorption with no product limitation. They observed better reactivity when the Pd loading and particle size increased possibly indicating a structure sensitive reaction.

Platinum and palladium supported on alumina, silica, titania, and silica-alumina at 298K was carried out in gas phase for HDC of PhCl.<sup>43</sup> The observed activity for supports with Brønsted acidity such as SiO<sub>2</sub>–Al<sub>2</sub>O<sub>3</sub> and titania was not sufficient, and even for very weak Lewis acidic supports such as aerosil-silica, only moderate activities were observed. However, alumina supports with Lewis acidic sites showed good activities for the HDC of HACs. The dipole moment in chlorobenzene, a polar bond (C<sup>δ-</sup>–Cl<sup>δ+</sup>), leads to adsorption on the Lewis acid site (L). This adsorbed PhCl is then attacked by dissociated hydrogen on or spilled over the metal. Similar trend was observed for the case DCB and TCB; however, increasing the contact time was necessary to overcome higher bond strength of multiple chlorines in their structure which resulted in more hydrogenated products.



Pd supported on mesoporous silica-carbon nanocomposites (Pd/MSiC) showed high activity for HDC of chlorophenyl at 258-313K.<sup>64</sup> A combination of density functional theory (DFT) technique and using triethylamine as a probe confirmed that Pd defects are mainly responsible for HDC of chlorophenols at low temperature. Chlorophenyl adsorption on Pd(III) is through either  $\pi$  or  $\sigma$  complex (Figure 1.1), where hydrogen adatoms play an important role in the HDC reaction.

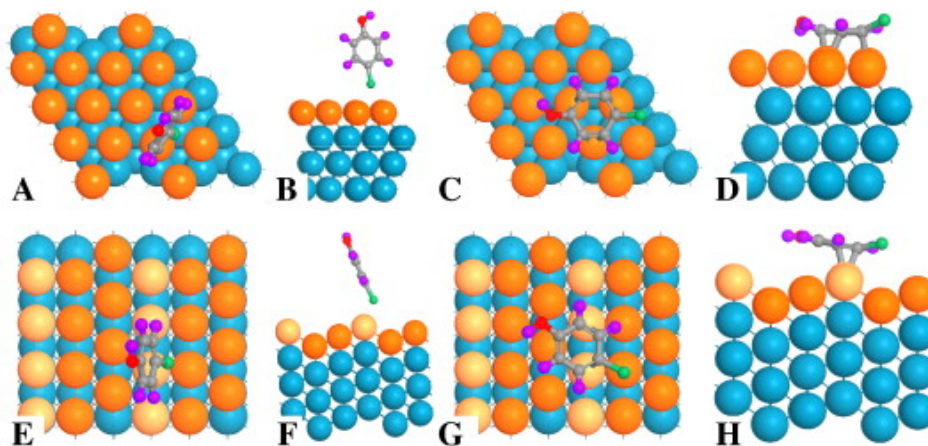


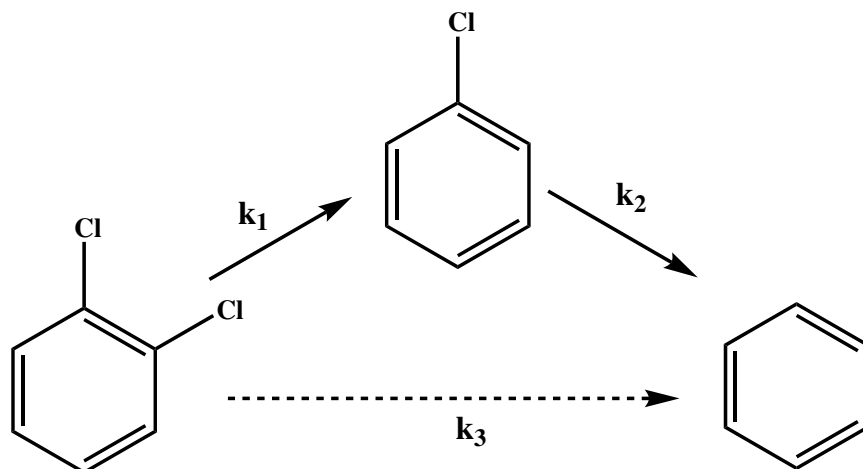
Figure 1.1: Calculated structures of 4-CP on Pd(111), ((A) top and (B) side views of  $\sigma$  adsorption, (C) top and (D) side views of  $\pi$  adsorption) and Pd (211), ((E) top and (F) side views of  $\sigma$  adsorption, G top and H side views of  $\pi$  adsorption surfaces); the H atoms are purple, the C atoms are gray, the O atoms are red and the Cl atoms are green. Reprinted by permission from Elsevier.<sup>64</sup>

Nickel and NiP catalysts supported on silica were used for gas phase HDC of PhCl.<sup>56</sup> The small positive charge on Ni in NiP catalyst along with the ensemble effect of P, helped decrease deactivation by lowering the coverage of chlorine on Ni.<sup>56,76</sup> The ensemble effect is a dilution of surface by another element. Decreased chlorine coverage on NiP surface is reported to lower the energy barrier of hydrogen spillover on the silica-supported NiP which, in turn, causes an abundant spillover hydrogen from the silica support that can promote the HDC. However, studies showed that NiP catalysts exhibit an induction period during hydrodenitrogenation (HDN) and hydrodesulfurization (HDS) which was attributed to blocking of Ni sites by P which will be adjusted during the course of the reaction when P content decreases and more active site will be recovered.<sup>77</sup> This induction period can be controlled by manipulating the initial Ni/P ratio, increasing the H<sub>2</sub> flow rate, higher temperature and longer reduction time when preparing the catalyst.

The study of HDC reaction of chlorobenzene with a presulfided hexagonal-Mo<sub>2</sub>C-(001) catalyst was performed using DFT calculations.<sup>78</sup> A weaker adsorption of chlorobenzene was observed as a result of adsorbed sulfur which prevents  $\pi$ -type bonding; therefore, avoiding carbonation and chlorination of the catalyst. Their results show that HDC

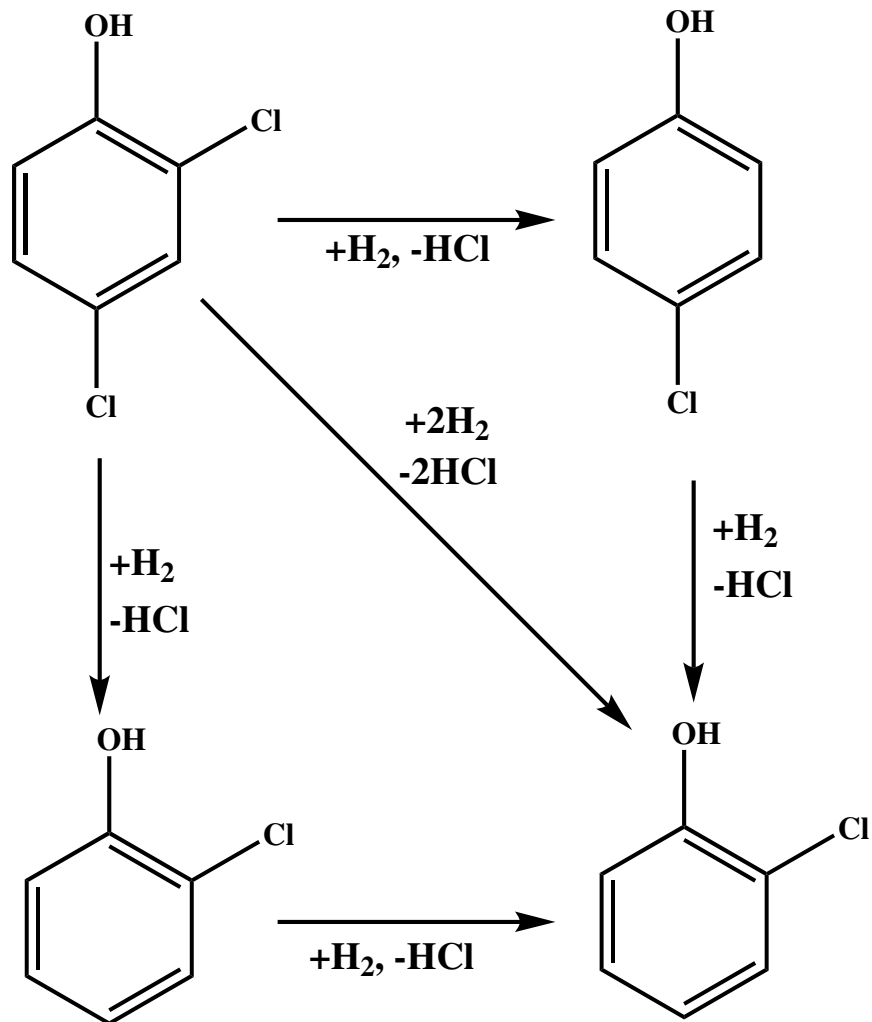
reaction can follow two reaction mechanisms, the direct mechanism involving hydrogenation of PhCl from a Mo-H species and two steps mechanism involving formation of S-H from an adjacent hydride and hydrogenation of PhCl from S-H. The energetics favor the direct mechanism; however, the authors do not rule out the possibility of the two-step mechanism, since extra energy consumption of about 0.6 eV is required, which could be achieved under the reaction conditions (623 K).

The addition of small quantities of Fe to Pd/Al<sub>2</sub>O<sub>3</sub><sup>51</sup> improves the catalyst resistance to HCl poisoning which can be related to the formation of positive Pd active species on the Pd-O-Fe interfaces to facilitate weak adsorption of chlorine. Bimetallic Pd-Fe was used by Chen and Liu<sup>3</sup> in the dechlorination of dichlorobenzene and investigated the kinetics. Their contribution considers deviations from Langmuirian adsorption as a result of interactions between adsorbates or between adsorbate and adsorbent, and utilized the cooperative adsorption theory. The theory is based on multi-layer adsorption, like BET except for surface reactions, as in a surface reaction, chemicals are reactive only if they are attached to the catalyst surface. Apparent multi-layer adsorption was utilized to model this theory mathematically. This model considers active sites as consisting of multiple potential energies and chemicals will attach to these sites based on their energies, highest energy as the first layer, if the highest energy sites are occupied then the second layer will be formed for the second highest energy site and so on. A kinetic model was developed based on this theory which is the summation of two rates from the first layer and the second layer.



Scheme 1.3: Step wise and concerted mechanisms of HDC for DCB proposed by Chen and Liu<sup>3</sup>

The gas phase (1 atm, 423 K) catalytic HDC of 2,4-DCP over Au/Fe<sub>2</sub>O<sub>3</sub> was carried forward through a step-wise electrophilic mechanism<sup>4</sup> and the main product was 4-CP mainly because the chlorinated reactant adsorbed from the -OH group promoting activation of the ortho-C-Cl bond and selective catalytic hydrogenolysis of sterically constrained Cl substituents.



Scheme 1.4: Reaction pathways for the HDC of 2,4-DCP<sup>4</sup>.

In spite of recent attempts to explain the mechanism of HDC of HACs, there is no consensus on whether the mechanism is radically or ionic, including nucleophilic or electrophilic attack.

### 1.2.2 Liquid Phase Hydrodechlorination

Many researchers are devoted to the palladium catalyzed liquid-phase HDH of aromatic compounds,<sup>31,37,40,52,68,79,80</sup> some deal with the decontamination of the environment from chlorinated compounds,<sup>31,52</sup> while others are focused on theoretical approaches to shed

some light on the reaction including kinetics, mechanism, catalysts, influence of the solvent, addition of base compounds, etc.

The liquid-phase catalytic HDH reaction suffers from strong deactivation of catalysts, caused from the hydrogen halide formed in the reaction.<sup>28</sup> Therefore, increasing the resistance to chlorine by incorporating basic supports, using basic solvents as proton scavengers,<sup>81</sup> and switching to more active catalysts such as Pd, with a more inherent resistance to HCl along with adjusting the particle size are necessary.<sup>37</sup>

HDC of PhCl in liquid phase at 313 K was studied using Pd on four different supports of different acid-base properties consisting zirconium oxide, magnesium oxide, a mixed system from aluminum orthophosphate and silica,<sup>65</sup> to find an optimum support that inhibits deactivation caused by Cl poisoning of the active site. Catalyst supports such as ZrO<sub>2</sub> can immobilize chloride species; therefore, choosing the right support has a significant effect in the stability of the catalyst. A higher resistance to chloride poisoning was observed for lower dispersion and higher particle size caused from refreshing the outer surface for further reaction by the migration of chloride species into large particles.

Ma et al.<sup>68</sup> investigated Pd/C and Raney Ni catalysts and compared for HDH of HACs. As C–X cleavage is the rate determining step in HDH of HACs, they expected the reactivity of these catalysts to follow C–X bond energies, C–I ( $\Delta H = 222 \text{ kJ mol}^{-1}$ ) > C–Br ( $\Delta H = 280 \text{ kJ mol}^{-1}$ ) > C–Cl ( $\Delta H = 339 \text{ kJ mol}^{-1}$ ) > C–F ( $\Delta H = 456 \text{ kJ mol}^{-1}$ ), which was followed in the case of Raney Ni. However, because of halogens inductive effect, appearance of partial charges on the neighboring bonds of carbon-halogen at short distances caused by electronegativity difference,<sup>82</sup> iodoarenes adsorbs more strongly on Pd/C catalyst which caused the reactivity to be in order of C–Br > C–Cl > C–I > C–F.

Multi-substituted chlorinated phenols have been reported to have preferential adsorption through the less steric sterically hindered group in para position. The adsorption of 2,4–DCP occurs on defect atoms of Pd nanoparticles in palladium supported on mesoporous silica carbon nanoparticles (MSCN).<sup>63</sup> Their observations suggested that

the product desorption should be the rate limiting step following an ionic reaction mechanism. Moreover, since HCl formed in this reaction has an inhibiting effect, more polar solvents such as methanol, are better for the reaction since they facilitate the transfer of chloride species from the catalyst surface into the reaction media.

It is believed that surface chemistry of the supports governs adsorptivity of reactant on the catalysts.<sup>81</sup> The HDC reaction of chlorinated benzenes using Ni over inactive supports, activated carbon, SiO<sub>2</sub>, Al<sub>2</sub>O<sub>3</sub> and Raney Ni showed that Ni on activated carbon shows the highest activity because PhCl adsorbs better on this support. Their kinetics studies suggest a near zero and 1.9 order reaction with respect to PhCl and hydrogen pressure, respectively. The fact that the reaction only proceeds in the presence of NaOH suggests that the rate limiting step involved desorption of chlorine.

Several reports on structure sensitivity of the reaction and significant role of the support on the activity and stability, inspired some researchers to find a creative solution to synthesize better supports. Le et al.<sup>79</sup> synthesized high surface area Fe<sub>3</sub>O<sub>4</sub>@SiO<sub>2</sub>@m-SiO<sub>2</sub> support that can be recovered using a magnetic field from the reaction mixture. Authors believe that catalytic HDC of 4-CP and 4-nitrophenol (4-NP) using Pd/Fe<sub>3</sub>O<sub>4</sub>@SiO<sub>2</sub>@m-SiO<sub>2</sub> starts with dissociative adsorption of hydrogen on the active site, followed by C–Cl bond dissociation through adsorbed hydrogen attack to form phenol<sup>83</sup>.

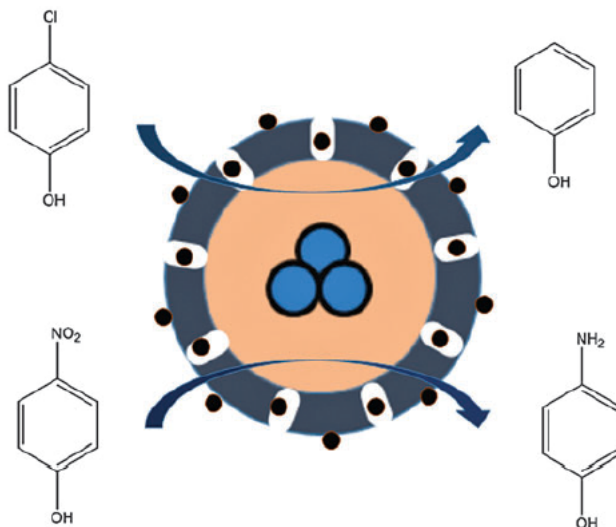
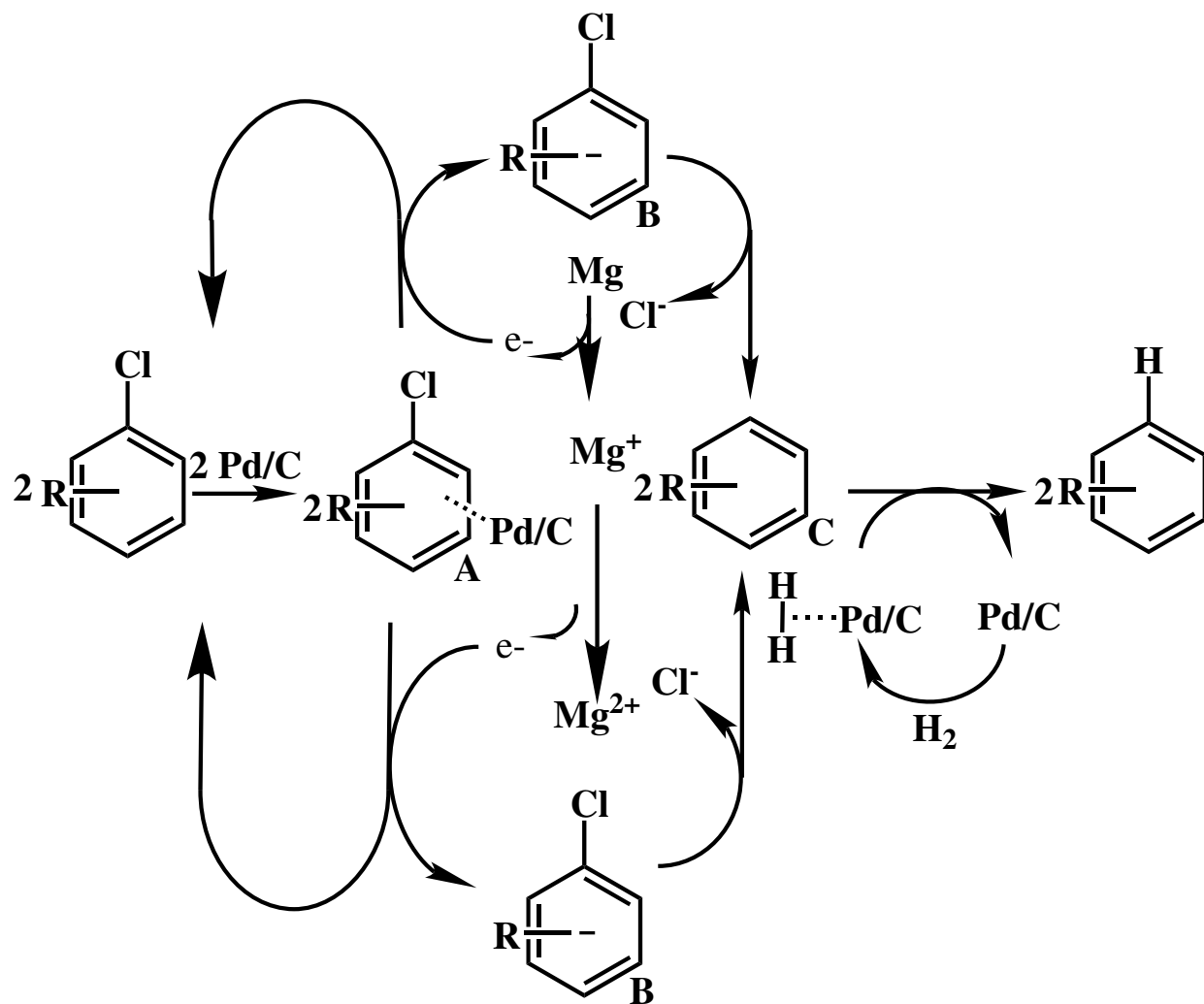


Figure 1.2: Reduction of 4-NP and HDC of 4-CP catalyzed by the Pd/Fe<sub>3</sub>O<sub>4</sub>@SiO<sub>2</sub>@m-SiO<sub>2</sub> catalyst.

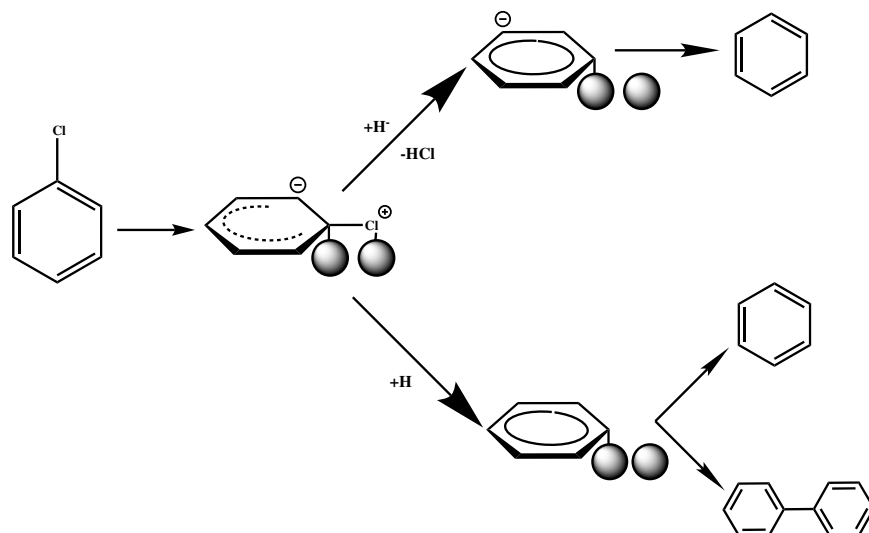
HDC of chlorinated aromatic as well as polychlorinated biphenyls (PCBs) were investigated using bimetallic 10% Pd/C–H<sub>2</sub>–Mg catalyst at low temperatures and pressures<sup>84</sup> in which 10% Pd/C can be reused and will be active after five cycles. The reaction response to the addition of 7,7,8,8-Tetracyanoquinodimethane (TCNQ) as a single electron scavenger drastically reduced the HDC; therefore, the authors believe that Mg functions as a single electron donor (Scheme 1.5) to create anion radical (B) which will undergo dechlorination to create dechlorinated product (C).



Scheme 1.5: Proposed reaction mechanism of the Mg metal mediated dechlorination of aromatic chlorides.

The electrophilic attack of activated hydrogen onto the aromatic ring was suggested by some researchers<sup>35,37</sup> while the possibility of nucleophilic or radical attacks were also put forth in HACs by Yakovlev et al.<sup>5</sup> Isotope exchange experiments were performed and the presence of biphenyl in product is indicative of a radical mechanism of dechlorination. Moreover, the results from D-NMR suggests the presence of both deuterated products as well as non-isotopic products which suggested competition for hydrogen supply from

adsorbed hydrogen and the solvent. The structure sensitivity of the reaction was also suggested based on the experimental data where larger Pd particles had more activity.



Scheme 1.6: Reaction pathways for HDC of PhCl proposed by Yakovlev et al.<sup>5</sup>

### 1.3 C-O Catalytic Hydrogenolysis

C-O bond cleavage in aromatics is a widely used reaction for lignin depolymerization to phenolic compounds and deoxygenation to most suitable chemicals. In this context, hydrogenolysis of lignocellulosic compounds has been previously studied and reviewed.<sup>12,85-92</sup> Model substrates from lignin-derived bio-oils were widely used, most commonly phenol, m-cresol, guaiacol, anisole, vanillin and eugenol have been studied.<sup>93</sup>

Catalytic systems that were developed for this reaction include metals, like Ru, Pt, Pd and Ni,<sup>58,94</sup> and bimetallic systems like combination of noble with transition metals like Fe, Ni, Cu, Zn or Sn form highly selective catalysts.<sup>93,95,96</sup> Moreover, alloying group VIII with oxophilic metals such as Sn, Re, or Fe will decrease the interaction with the ring and enhance the interaction with the carbonyl or hydroxyl group.<sup>8</sup>

The selectivity for hydrodeoxygenation (HDO) can be influenced by the properties of the support.<sup>97</sup> Noble metals over acidic supports can offer good selectivity for direct deoxygenation (DDO) of the C-O bond, but also oxophilicity, metal dispersion, strength of

metal-support interactions and deactivation effects by coking formation needs to be considered for the selection of the right metal-support combination. Based on Sabatier's rule, an oxide support with moderate metal-oxygen bond strength is ideal.<sup>6</sup> If the the bond between metal and oxygen is too strong, it is difficult to create surface vacancies for oxygenated groups adsorption, but if the metal-oxygen bond strength is too low it would make the catalyst unable to abstract oxygen effectively.<sup>98</sup> In this regard, the strength of metal-oxygen bond were evaluated as follow:  $Mg > Al > Zr > Ti > W > Cr > Zn > V > Sn > Fe > Ge > Mn > Ni > Bi > Cu > Pb$ .<sup>93</sup>

Some combinations of metals and supports in heterogeneous catalysts are known to exhibit what known as strong metal-support interactions (SMSI) and being about physicochemical properties that were not present when metals and supports were just physically mixed. SMSI generally arises due to the electronic perturbation of metallic atoms by surrounding atoms from the supports, which would result in the change of electronic properties of the metal catalyst.<sup>93</sup> Therefore, mild to moderate acidic supports such as  $TiO_2$ ,  $ZrO_2$ , zeolites,  $Al_2O_3$  and  $CeO_2$  are often used for HDO process due to their ability to catalyze C-O bond hydrogenolysis with minimal coking effect.<sup>98</sup> Basic support (CoMo/MgO) catalyst are more likely to resist sintering and coking effects but offers significantly lower HDO activity.<sup>93</sup>

- Oxygenated groups can be adsorbed through Lewis acid/base interaction and activated on:<sup>6</sup>
  - Coordinate unsaturated metal sites: For bimetallic catalysts, instead of the presence of an active support, the second metal act as the enhancement agent for oxygen adsorption.<sup>99</sup>
  - Oxygen vacancies on the support
  - Exposed cations on the support

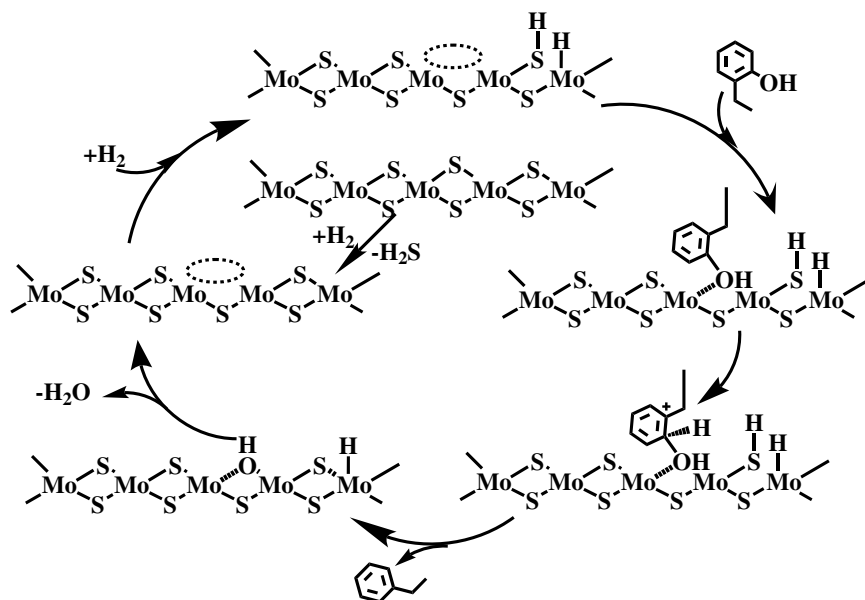
- An oxygenated aromatic with more than one oxygen atom may have different adsorption sites on the supports.<sup>100</sup>
- At the same time, the aromatic ring is easy to bond into a catalytic surface.<sup>101</sup>
- H<sup>+</sup> donation is available directly from
  - Phosphides, carbides, nitrides
  - Brønsted acid -OH groups
  - -SH groups
  - Metals and noble metals by H spillover.<sup>6</sup> Noble metals are particularly efficient catalysts in activating molecular hydrogen.

Cresol deoxygenation over Pt/Al<sub>2</sub>O<sub>3</sub> catalysts at atmospheric pressure generates toluene and benzene but methylcyclohexane remains as the main reaction products.<sup>102</sup> In the conversion of m-cresol over Pd/SiO<sub>2</sub>, hydrogenation of the aromatic ring is favored, but using ZrO<sub>2</sub> as a support helps create oxophilic sites favoring direct deoxygenation (DDO) pathway.<sup>103</sup>

Particularly, Ni/SBA-15 catalyst exhibit higher catalytic performance for hydrodeoxygenation of the aromatic ring (HYD) of anisole. On the contrary, the direct hydrogenolysis of the methoxy group from anisole is favored over Co/SBA-15, leading to much higher aromatic selectivity.<sup>104</sup>

A mechanism for HDO of 2-ethylphenol over a CoMoS/Al<sub>2</sub>O<sub>3</sub> catalyst was proposed in Scheme 1.7. On MoS/Al<sub>2</sub>O<sub>3</sub> catalysts vacancy sites are created by the removal of H<sub>2</sub>S in presence of H<sub>2</sub><sup>6</sup>. H<sub>2</sub> is activated by heterolytic dissociation forming one S-H and one Mo-H groups; the oxygenated group is adsorbed on those vacancy sites formed an adsorbed carbocation after receiving a proton from the S-H group. This intermediate undergoes direct C-O bond cleavage and generates ethylbenzene. The vacancy site is recovered by the formation of H<sub>2</sub>O from the adsorbed OH and H groups. The addition of

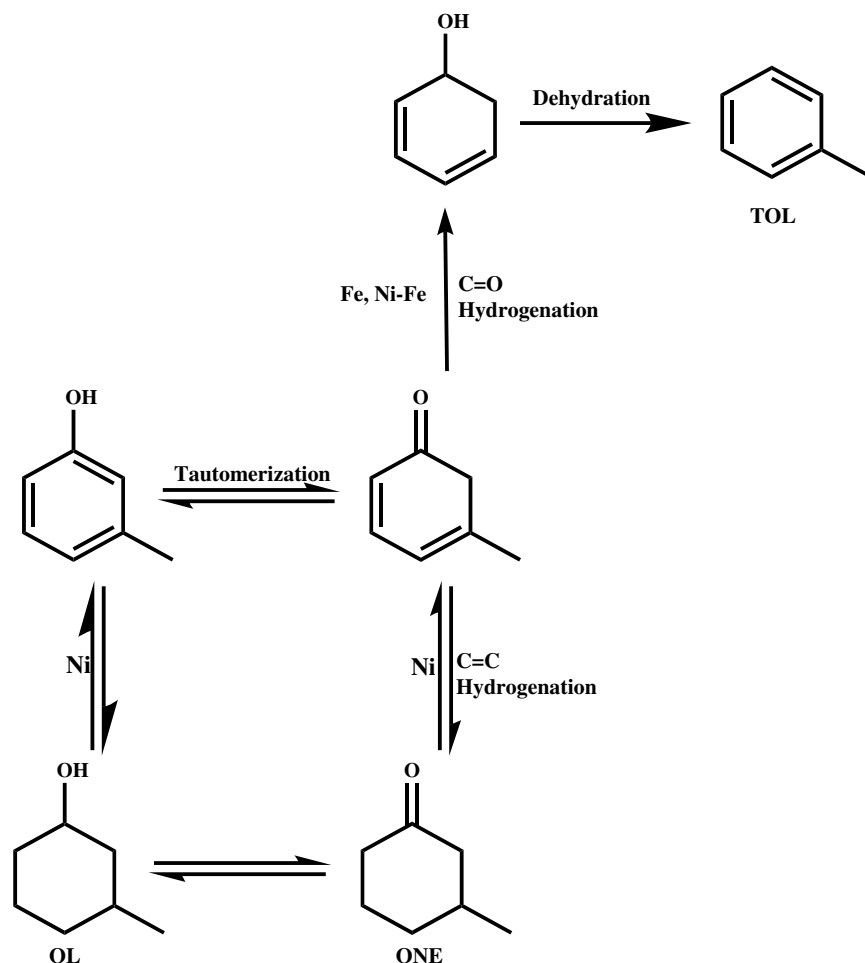
cobalt to this catalyst CoMoS/Al<sub>2</sub>O<sub>3</sub> enhances the direct C–O bond scission, because of an increment in the number of active sites, some of them being new sulfur vacancies<sup>7</sup>.



Scheme 1.7: Mechanism of direct deoxygenation of 2-ethylphenol over CoMoS/Al<sub>2</sub>O<sub>3</sub>.<sup>6,7</sup>

ReS<sub>2</sub>/ZrO<sub>2</sub> is greatly active for guaiacol DDO, reactions with H<sub>2</sub> breaks in first instance the C–O bond for the methoxy group and then breaks the formed hydroxyl group, producing mostly catechol and phenol. Here, demethoxylation occurs on the vacancies of the sulfide metal ReS<sub>2</sub>. The use of sulfated ZrO<sub>2</sub> as support provides a stronger interaction with Re precursor leading to a highly dispersed catalyst.<sup>105</sup> The mechanism for HDO over sulfided NiW is similar to the previously proposed.<sup>11</sup>

Bifunctional catalyst have been lately studied for DDO reactions. The presence of Fe and Ni–Fe bimetallic catalysts supported on SiO<sub>2</sub> promotes the hydrogenation of the C–O group of m-cresol. Hydrogenation of the non-aromatic tautomer produces a reactive alcohol, which is further easily dehydrated (Scheme 1.8). The favorable sites for this process come from Lewis acids associated with the incomplete reduction of Fe and/or Ni cations. Here, the aromatic ring is repulsed from the catalyst surface, while the oxygenated group strongly interact with the acid sites, promoting the oxygen removal reaction pathway.<sup>8</sup>



Scheme 1.8: Mechanism of deoxygenation of m-cresol over Ni, Fe and Ni-Fe Catalysts.<sup>8</sup>

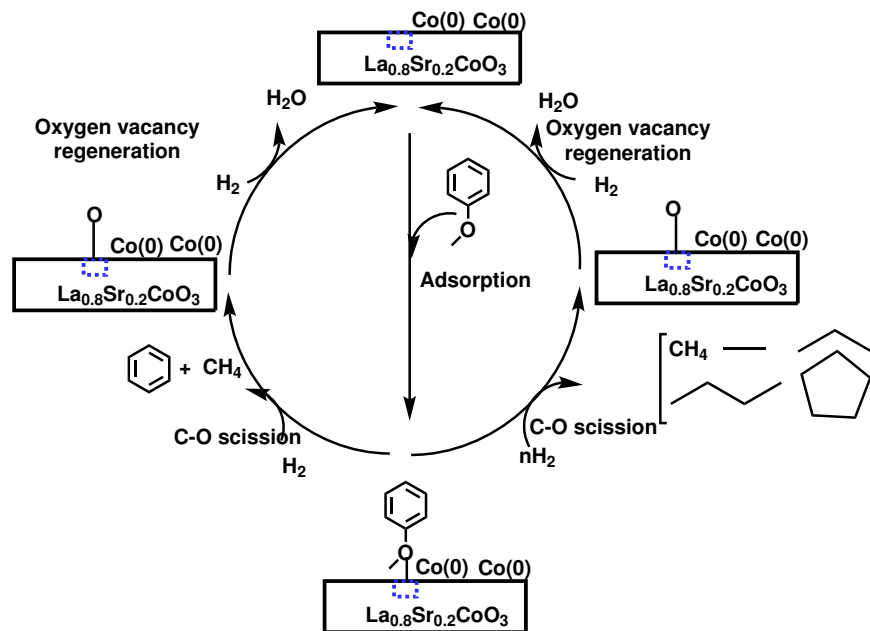
When studying Hydrodeoxygenation (HDO) of m-cresol over Pt/C and Pt-WO<sub>x</sub>/C, the latter was much more active and selective towards DDO.<sup>99</sup> Hydrodeoxygenation reaction on Pt-WO<sub>x</sub>/C proceeds selectively in m-cresol, because of the synergic effect between the Pt and the redox supported WO<sub>x</sub> complexes. Pt stabilizes the partially reduced tungsten oxide sites and favors the formation of oxygen vacancies, where the hydroxyl group is adsorbed, by forming a Pt-W bond. These sites are very important for selective C-O scission, because they limit the interaction of the aromatic ring with the Pt surface, avoiding its parallel adsorption that could cause ring hydrogenation.<sup>99</sup>

Selective C-O hydrogenolysis of vanillin was also found over Au-Pt/CeO<sub>2</sub> using formic acid as the hydrogen source. Pt interact with Au forming Au-Pt alloys showing excellent

performance. Presence of small nanoparticles, the  $\text{CeO}_2$  support, the good dehydrogenation ability of formic acid and the hydrogenolysis of  $\text{C}=\text{O}$  species are also key factors for this reaction. The strong activity of this catalyst is, again, because of oxygen vacancies that interacts with the hydroxyl groups, which facilitates the  $\text{C}-\text{O}$  bond cleavage. The remaining oxygen is removed by hydrogenation forming water, thus leading to the formation of new oxygen defects.<sup>100</sup>

Some supports are discovered to be active in the molecular mechanism of  $\text{C}-\text{O}$  bond hydrogenolysis, those will be called active support and its performance were in some cases very well studied. Improvements of inert supports like carbon modified into a nitrogen-doped hierarchical porous carbon (NHPC), has also been developed, reaching higher performances for  $\text{C}-\text{O}$  cleavages. On vanillin It was proposed a direct hydrogenolysis or hydrogenation-hydrogenolysis reaction mechanism for vanillin. Here, Ni/NHPC favors full oxygen removal of a broad set of oxygenated aromatics. The reason of its high activity is the structure of the modified nickel interacting with nitrogen dopant contributed by the hierarchical porous structure of the carbon.<sup>103</sup>

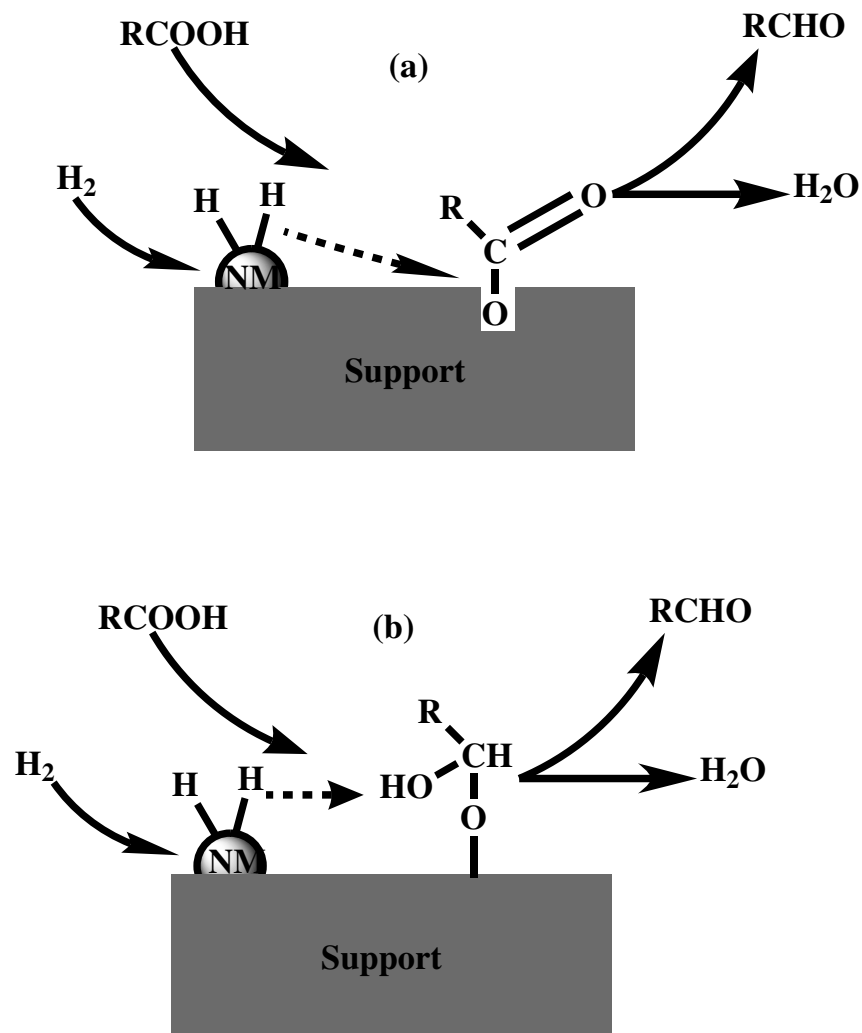
A strontium (Sr)-substituted lanthanum cobaltite ( $\text{La}_{0.8}\text{Sr}_{0.2}\text{CoO}_3$ ) was recently found to be selective towards  $\text{C}-\text{O}$  and  $\text{C}-\text{C}$  hydrogenolysis on anisole by stabilizing the  $\text{Co}^0/\text{Co}^{\text{II}}$  sites. This stabilization effect plays an important role on the activity of the catalyst.  $\text{Co}^{\text{II}}$  sites were favored at low temperatures and performed selective  $\text{C}-\text{O}$  hydrogenolysis by existence of oxygen vacancies generated Sr-substitution. With the participation of  $\text{Co}^0$  sites in close proximity to  $\text{Co}^{\text{II}}$  sites, the adsorbed anisole can also form H-deficient intermediates.<sup>104</sup>



Scheme 1.9: Proposed mechanism for anisole hydrodeoxygenation over  $\text{La}_{0.8}\text{Sr}_{0.2}\text{CoO}_3$ .

Phenolic compounds could be very strong adsorbed on oxides. Adsorption of phenolic compounds over  $\text{SiO}_2$  and  $\text{Al}_2\text{O}_3$  was studied. As seen in Scheme 1.10, over silica the main interaction mechanism is H-bonding, while over alumina the main adsorption mode is chemisorption.<sup>9</sup> Despite that a hydroxyl adsorption on the surface could be beneficial for HDO processes, the strong interaction between the phenolic compounds and the alumina support could also generates severe catalyst poisoning.<sup>106</sup>



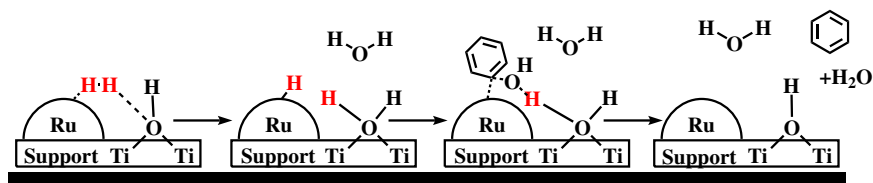


Scheme 1.11: Hydrodeoxygenation mechanism of oxygenated compounds over metallic catalysts with active supports. Extracted from Mendes et al.<sup>10</sup>, van Duijne et al.<sup>11</sup>, He and Wang<sup>12</sup>.

As a particular example for C–O bond hydrogenolysis, Ru/TiO<sub>2</sub> demonstrated an outstanding performance: unusual and high selectivity towards direct deoxygenated component, without the hydrogenation of the aromatic ring.<sup>107</sup> This is due the active nature of the support TiO<sub>2</sub>. Different groups<sup>107,108</sup> have investigated the catalytic conversion on model compounds over this catalyst. It is been demonstrated that the direct deoxygenation pathway of phenol and guaiacol on titania involves a bifunctional catalyst,

where the metal-support interface is participating in the reaction, while there is no apparent support, pore size or morphology effects for the HYD pathway.<sup>109</sup>

For the DDO pathway, the overall activity and selectivity is higher for catalysts with larger interfacial sites.<sup>107,108</sup> Previous contributions,<sup>109,110</sup> demonstrate the interfacial direct deoxygenation mechanism.



Scheme 1.12: Proposed molecular mechanism of DDO pathway for phenol over Ru/TiO<sub>2</sub>

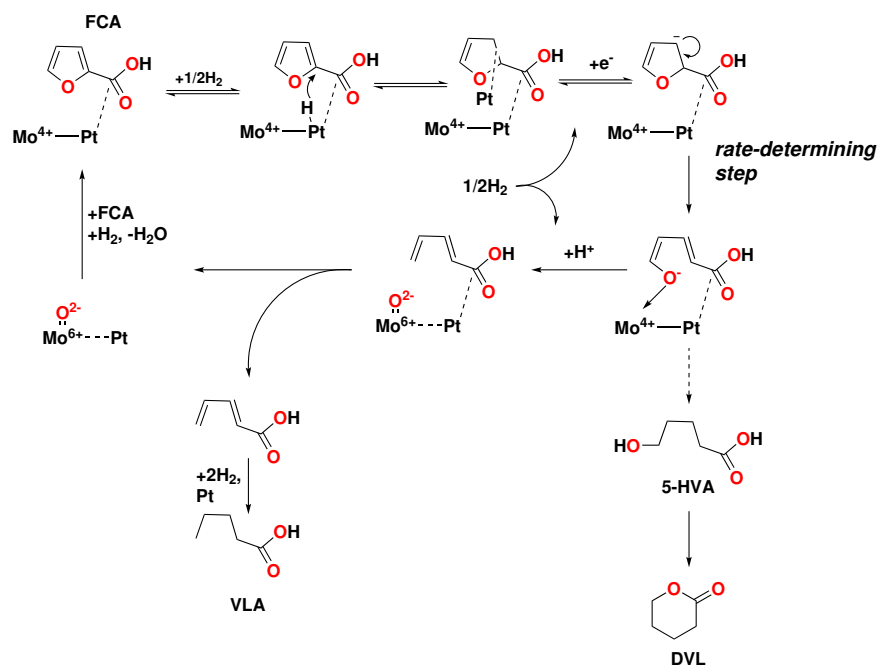
The mechanism shown in Scheme 1.12 starts with a surface hydroxyl in the support. This hydroxyl group facilitates, in first instance, the adsorption of a H<sub>2</sub> molecule on the interface and its further heterolytic cleavage, by acting as a Brønsted base (1). This cleavage generates an active site consisting of a Brønsted acid, (H<sup>+</sup> donor) on the support in close proximity to a reductive ruthenium hydride (2). The DDO of phenol begins with its adsorption at the interface. The aromatic ring is adsorbed by the metal and the phenolic oxygen is adsorbed by the now protonated surface hydroxyl. Here the surface hydroxyl functions as a Brønsted acid that protonates the phenolic oxygen, weakening the C–O bond (3). The weakened C–O bond is then cleaved, while the Brønsted base donates a proton to the released hydroxyl group generating a desorbed water molecule. Finally, the adsorbed benzene is protonated by the ruthenium hydride, and desorbed out of the metal. Now the catalyst is in the same initial state ready to start a new catalytic cycle (4). Under this mechanism, it's been demonstrated that the presence of a water molecule in close proximities of the interface avoid the formation of an oxygen vacancy sites and generates the surface hydroxyl groups that favor direct deoxygenation pathways, lowering the activation barrier of the process. Water act as a co-catalyst of the reaction, favoring the

hydrogen cleavage and stabilizing the adsorbed molecule of phenol at the interface, as long as water concentration is not high enough to act as a site blocking term.

The enhancement in DDO activity of  $\text{TiO}_2$  was also proposed for other metals, even if the reaction mechanism is not demonstrated to happen at the interface. The use of  $\text{TiO}_2$  support shows a preferential activation of C–O bond. HDO reactants formed activated complexes with higher orderly bonding configurations. Their proposed kinetic model confirmed that phenol hydrogenolysis and hydrogenation are the respective rate-limiting steps for DDO and HYD pathways respectively.<sup>111</sup>

Furanic platform chemicals like HMF and furfural have been the subject of many contributions because of their ease of production and can easily be upgraded to bio-based products; however, unsaturated aldehyde group make them rather unstable which is one of their major shortcomings. Research on the production of their oxidized analogues that are stable solid crystalline compounds, 2,5-furandicarboxylic acid (FDCA) and 2-furancarboxylic acid (FCA), respectively, has been an attractive field while the use of FCA and FDCA as sources of biobased compounds is extremely limited except application of FDCA as a monomer as an alternative to terephthalic acid in production of polyesters.<sup>112</sup> Reactions that involve the reduction of carboxylic acid in these molecules are not attractive since FDCA and FCA are produced through oxidation of their reactive sources. The production of adipic acid from FDCA was first discussed in a patent, Boussie et al.<sup>113</sup> and later improved systems were reported.<sup>114,115</sup> These reactions involve hydrogenation of the furan ring and subsequent C–O cleavage of tetrahydrofuran ring with HI as the key intermediate in the C–O dissociation step. Direct HDO of FCA into valeric acid using bifunctional catalysts,  $\text{Pt}-\text{MoO}_x/\text{TiO}_2$ <sup>116,117</sup> and  $\text{Pt}/\text{Al}_2\text{O}_3$ ,<sup>118</sup> were performed; although the target products (VA or 5-HVA derivatives) were not accessible through formation of tetrahydro-2-furancarboxylic acid (THFCA, *c.f.* Scheme 1.13). In another report, THFCA was converted to DVL+5-HVA using  $\text{Rh}-\text{WO}_x/\text{SiO}_2$  with the highest conversion of 61.8% and extremely low yield of 8.8% which was only achieved after

optimizing process conditions. Limited publications on the subject of reduction of FCA like molecules with the intention of retention of carboxylic acid heavily relies on the usage of bifunctional systems which often leads to bimetallic catalysts that suffer greatly from instability during real process conditions. In this regard, there is a need to explore catalysts that show a built-in bifunctionality when introduced to hydrogen. Therefore, we have explored previously studied catalyst Ru/TiO<sub>2</sub><sup>107</sup> that exhibit unusually high activity towards DDO of phenolic compounds for HDO of FCA and functionalized FCA (FFCA). This reaction takes place with the intention of production of monomer, functionalized  $\delta$ -hexalactone (FDHL). This monomer is then employed in successful polymerization of functionalized molecules with retention of carboxylic acid in the target polymer while the functionality, phenolic compounds, gives a tunable characteristic to the process and enables us to practice a range of different polymers.



Scheme 1.13: Proposed reaction mechanism of FCA reduction over Pt-MoO<sub>x</sub>/TiO<sub>2</sub> catalyst.<sup>116</sup>

It is important to notice that many different mechanisms had been proposed for direct deoxygenation of aromatic and pseudo-aromatic compounds some of which are in close agreement with each other, like the presence of an oxygen vacancy site that favor the adsorption of the oxygenated group. Others may have been suggested to go through a tautomerization mechanism as a different point of view for this reaction. These reactions pose an attractive pathway to alternative chemical goods with the same quality of petroleum-based analogues. With the shale gas boom on the horizon as a cheap source of hydrogen it is expected that biomass catalysis to shift towards more and more hydrogen assisted processes like HDO and HDC and graduate from their parent catalysts that were adopted from petroleum industry.

#### 1.4 Thesis Scope

Considering the lack of consensus on the mechanism of HDC reactions, it is necessary to perform the reaction in a simplified system where the outcome is not affected by the perturbation of factors like effect of support and transport limitation. Therefore, the first target of my thesis is to work on HDC of a simple chlorinated aromatic, chlorobenzene (PhCl) over Pd on an inert support which will be performed in detailed kinetic study in Chapter 2. For future investigation, Appendix A will consider the need for a molecular observation of such reaction and is focused on the design of an quartz cell that allows for infrared (IR) observations of the reaction in steady state with the option of performing transient experiments.

Converting biomass into bio-based thermoplastics with the objective of improving characteristics like glass transition temperature ( $T_g$ ) is the focus of Chapter 3. This work is essentially divided into two thrusts, 1) producing the monomer from biomass; and 2) polymerization. The first thrust is carried out by me which is discussed in detail to study the possibility of monomer production quantitatively, and the second thrust is carried out by Dr. William Gramlich and his group from the UMaine Department of Chemistry.

Therefore, Chapter 3 is focused on the process optimization of monomer production rather than kinetics or mechanistic studies.

Chapter 4 summarized the results in a collaboration with Dr. Brian G. Fredrick from the UMaine Department of Chemistry on acrolein HDO over tungsten oxide bronze catalysts. I will discuss the details of a microkinetic model using Matlab<sup>®</sup> software.

## CHAPTER 2

### HYDROGENOLYSIS OF CHLOROBENZENE<sup>1</sup>

#### 2.1 Introduction

Chlorinated aromatics have been used extensively for the production of herbicides, pesticides, intermediates for organic synthesis, pharmaceuticals, and dye<sup>33,119–121</sup>. However, there is a significant environmental concern associated with the use of chloroaromatics if they are not treated appropriately at the end of their life cycle<sup>119</sup>. In particular, these molecules exhibit high toxicity due to the strength of the C–Cl bond ( $\Delta H = 399.6 \text{ kJ mol}^{-1}$ )<sup>122</sup>, and this toxicity increases nonlinearly as more chlorine atoms are added to the structure<sup>26</sup>. There is, thus, an impetus to mitigate the toxicity of waste chlorocarbons, and one way this can be accomplished is via reductive dechlorination (*i.e.*, hydrogenolysis of the C–Cl bond).

The selective hydrogenolysis of C–Cl bonds in organohalogen compounds is typically accomplished using noble metal catalysts<sup>26,123–125</sup>, with cleavage of the C–Cl bond in chlorobenzene (*i.e.*, phenyl chloride, PhCl) often used as a model reaction<sup>47,49</sup>. This reaction is also referred to as hydrodechlorination (HDC), in a reference to the related classes of hydrotreating reactions (*e.g.*, hydrodesulfurization, hydrodenitrogenation, hydrodeoxygenation, etc.). Group VIII metals are typically active for this class of reaction, including Ni, Pt, Rh, Ru and Pd<sup>1,2,121,126–128</sup>. Among these metals, Pd is reported to be the most active and selective for dechlorination of chloroaromatics<sup>2,40,47,48,61,64,68,69,129,130</sup>, although it is often reported to be susceptible to deactivation<sup>2,69,76,125,130,131</sup>. In addition to careful choice of the metal, there is some evidence that judicious choice of the support can inhibit poisoning by chloride ions<sup>65</sup>, and more generally the support must be chosen to

<sup>1</sup>This chapter is from a paper: J. Tavana, M. Algharrawi, M.C. Wheeler and T. J. Schwartz, “Chlorobenzene hydrodechlorination: reaction mechanism and kinetic modeling”, *Journal of Applied Catalysis A*, **2020**. (In preparation)

My contribution is doing kinetics measurements, data analysis and writing the paper.

withstand corrosion caused by HCl, which is formed as a byproduct of the reaction. Moreover, it has been reported that common supports such as alumina and silica can participate in the reaction<sup>2,47–49,64,68,69,132</sup>, while carbon is an inert support that can withstand corrosive environments<sup>133,134</sup>. Although, the published contributions on HDC of chlorinated chemicals have contributed to understanding of the underlying kinetics and a compilation of rate data for specific systems, the mechanism of C–Cl hydrogenolysis is still unresolved and authors have appealed to different models to explain the observed kinetic behavior<sup>132,135,136</sup>.

The difference between the proposed mechanisms seems to be rooted in the assumed nature of reactive adsorbed species<sup>73</sup>. Keane and Murzin<sup>47</sup> suggest that HDC of PhCl occurs on a non-uniform surface which requires spilled over hydrogen from the support. In contrast, according to Sinfelt<sup>137</sup>, hydrogenolysis of carbon-heteroatom bonds (*i.e.*, scission of C-X bonds by addition of H<sub>2</sub>, where X= C, O, N, or Cl) in simple molecules can all be explained by a similar mechanism wherein cleavage of the C-X bond is the rate-controlling step. Ribeiro *et al.*<sup>130</sup> extended the application of this mechanism to chlorofluorocarbons, suggesting a transition state structure where Pd inserted into the C–Cl bond, forming Pd–C and Pd–Cl on the same active site. In this study, the gas-phase hydrodechlorination of chlorobenzene over Pd/C in atmospheric conditions and low temperatures, is subjected to a kinetic and mechanistic study through kinetic isotope effect, temperature and partial pressure effects experiments, and the proposed mechanism have been modeled to predict the experimental data.

## 2.2 Experimental

### 2.2.1 Catalyst Preparation

A 5 wt% palladium catalyst was prepared by incipient wetness impregnation of an aqueous solution of Pd<sub>2</sub>(NO<sub>3</sub>)·xH<sub>2</sub>O (Strem Chemicals, 99.9%) onto a carbon black support (Cabot Corporation, Vulcan XC-72). The Vulcan XC-72 support used here was

chosen for its inertness and lack of S and N impurities that may influence the reaction kinetics. The catalyst was dried overnight at 383 K, after which it was reduced directly in a 50 sccm stream of flowing dihydrogen (Matheson, 99.999%) for 4 hours at 533 K (10 K min<sup>-1</sup>). The catalyst was passivated for 12 hours at room temperature in a dilute mixture of air and argon.

### 2.2.2 Catalyst Characterization

CO chemisorption measurements were performed in a Micromeritics ASAP 2020 instrument. The passivated catalysts were placed in a quartz sample tube between two layers of quartz wool, the sample was then evacuated, after which it was re-reduced at 673 K for 2 hr. Adsorbed hydrogen atoms were removed by desorption under vacuum (10<sup>-5</sup> torr) at 673 K for 1 hr. CO chemisorption was performed at 308 K using CO equilibrium pressures ranging between 0.5 to 313 torr. Pd dispersion and the average Pd nanoparticle size was obtained from the CO saturation coverage assuming a CO:Pd stoichiometry of 1:2<sup>138,139</sup> and a relationship between dispersion,  $D$ , and particle size,  $d$ , of  $d = \frac{1.1}{D}$ <sup>140</sup>.

The catalyst morphology and particle size distributions were evaluating using transmission electron microscopy (Philips CM10) at 200 kV. A few milligrams of the catalyst sample was dispersed in water and the suspension was sonicated for 10 min to prevent possible agglomeration. A small droplet of sample suspension was transferred onto an amorphous carbon film, coated by a 200 mesh Cu grid, glow discharged for 30 sec to improve hydrophilicity of the grid, and dried at room temperature before TEM analysis. TEM micrographs were acquired from different samples to capture a variety of particle sizes; 1540 particles were analyzed using ImageJ . The size analysis was carried out on the converted grayscale (TEM) images into black and white by thresholding which makes it possible for the program to identify the outlines of the particles. These outlines correspond the 2D projection of a particle and its characteristics such as size, the data were analyzed in Origin software (Figure 2.1 inset).

### 2.2.3 Reaction Kinetics Studies

Reactions were carried out at ambient pressure in a glass stirred tank reactor (Chemglass Model CG-1949-X-303) configured to operate as a continuous reactor in a Carberry configuration, with the feed stream being preheated to reaction temperature. The reactor vessel was originally designed for liquid-phase reactions. To modify it for gas-phase reactions, the impeller blades were replaced with four PEEK mesh baskets (mesh size = 50) affixed to the glass impeller shaft using a custom-machined Teflon bracket. These baskets are designed to receive the powder catalyst and spin it through the bulk vapor phase in a Carberry reactor configuration. The anchor stirrer at the bottom of the impeller shaft was kept to facilitate additional mixing. All standard taper joints were greased with H-grease (Apiezon). A pressure relief valve (Chemglass Part No. CG-999-02) was set to 3 psig and used to prevent over-pressurization of the glass vessel. A pressure gauge (Ashcroft Part No.94575XLL) was affixed to a Teflon stopper and used to monitor the pressure in the reactor vessel. Heating was provided in the jacketed portion of the vessel using a circulating heating bath (Fisher Scientific, Isotemp Model 6200 H7) containing propylene glycol antifreeze purchased from a local hardware store. Heating of the vessel head was provided by a heating tape (HTS/Amptek), and the whole vessel was wrapped in ceramic insulation. The reactor temperature was measured by a Hastelloy-sheathed K-type thermocouple (Omega, Inc.). Temperature control was provided by a combination of the circulating heating bath, which was set at the reaction temperature, and by the heating tape on the reactor head, via a PID temperature controller (Automation Direct) using input from the main reactor thermocouple. Measurement of the temperature at several points in the reactor vessel (achieved by moving the main reactor thermocouple) showed there to be no temperature gradients in the bulk vapor phase of the reactor.

For a typical reaction, 0.05 g of catalyst was diluted in 0.75 g of carbon black using an agate mortar and pestle. This diluted catalyst was loaded into the four PEEK mesh baskets on the reactor impeller shaft. The catalyst was reduced in flowing dihydrogen (60

sccm, 99.999%, Matheson) at 353 K for 1 hour, after which the reactor was set to the desired temperature. Liquid PhCl (>99%, Acros Organics) was fed from a syringe pump (NE-1000, New Era Pump Systems) through a 1/8 inch Teflon tube into a stream of flowing dihydrogen mixed with helium (99.999%, Matheson). The dihydrogen and helium flowrates were controlled by calibrated metering valves (SS-SS2-VH, Swagelok). The liquid and gas flowrates were chosen to keep the partial pressure of PhCl in this gas stream below its vapor pressure at 298 K. The vapor feed was introduced to the reactor through a glass spiral tube condenser (Chemglass Part No. CG-1215-C-01) used to pre-heat the feed. Periodically the reactor was checked for inertness by feeding a mixture of PhCl and dihydrogen at reaction temperature to the reactor vessel in the absence of a catalyst; no conversion of PhCl was observed during these runs. The effect of HCl on the reaction rate was probed by co-feeding HCl gas (1000 ppm in He, Research Grade, Airgas), delivered through a Teflon line to the reactor vessel.

The reaction products were quantified using a gas chromatograph equipped with a flame ionization detector (GC-FID, MG-5, SRI Instruments) and a capillary column (MXT-1, Restek). Reaction rates were measured at four different temperatures (323K, 333K, 343K and 353K) and a variety of partial pressures of PhCl, dihydrogen, and HCl, controlled by varying the flowrates of each species and the flowrate of the He diluent. Turnover frequencies (TOFs) were obtained by normalizing the reaction rates,  $r$ , to the CO uptake,  $n_{CO}$ , as shown in Equation 2.1.

$$TOF(s^{-1}) = \frac{r(\mu mol g^{-1} s^{-1})}{n_{CO}(\mu mol g^{-1})} \quad (2.1)$$

Selectivities were calculated according to Equation 2.2, where  $F_i$  corresponds to the molar flowrate of species  $i$  leaving the reactor.

$$Selectivity_i = \frac{F_{prod,i}}{\sum_i F_{prod,i}} \times 100\% \quad (2.2)$$

## 2.3 Results and Discussion

### 2.3.1 Reaction Selectivity and Catalyst Stability

The Pd/C catalyst synthesized here ( $\sim 10$  nm particle size and 10% dispersion based on a CO:Pd stoichiometry of 1:2 with a CO uptake of  $24 \mu\text{molg}^{-1}$  (*c.f.* Figure 2.1))<sup>139</sup> converts chlorobenzene into benzene and cyclohexane, with a benzene selectivity greater than 95% and no indication of catalyst deactivation over the time period studied here (see Figure 2.2). This observation is justified for catalysts with large Pd nanoparticles as explained by Aramendía et al.<sup>65</sup>. They suggest that some of the Cl surface species that are formed during the reaction, which are responsible for catalyst deactivation, can migrate to the interior of the Pd nanoparticles; consequently, smaller Pd nanoparticles with higher surface-area-to-volume ratios are rapidly saturated with Cl while larger nanoparticles are stable for longer time-on-stream.

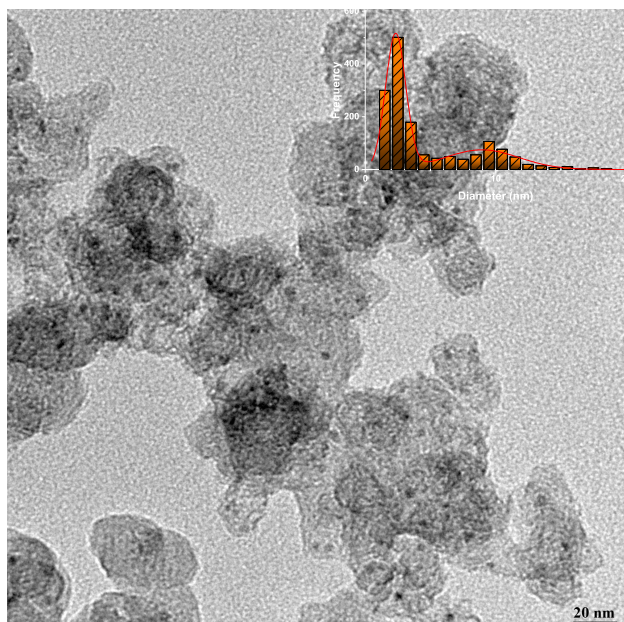


Figure 2.1: TEM micrograph of the reduced 5wt% Pd/C catalyst (inset: particle-size distribution of the corresponding samples).

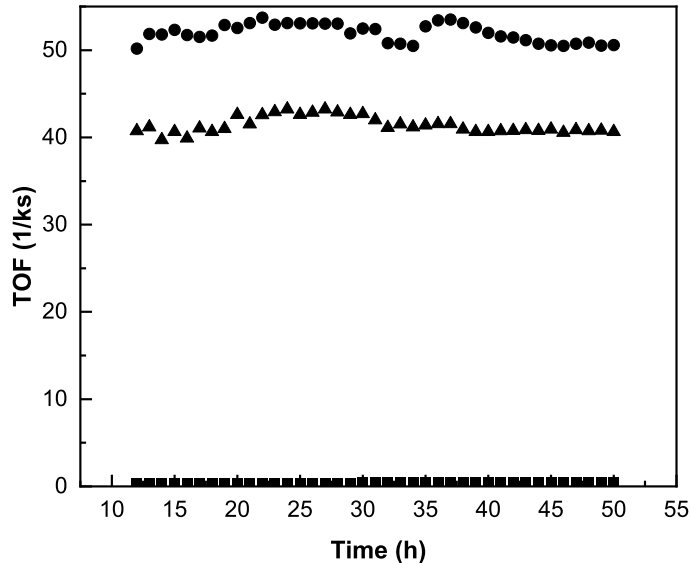


Figure 2.2: Production of benzene (▲) and cyclohexane (■) from chlorobenzene(●)with respect to time-on-stream. Reaction conditions: 5% Pd/C catalyst, 353 K, 97 kPa H<sub>2</sub>, 1.1 kPa PhCl, WHSV = 1.22 hr<sup>-1</sup>, PhCl ~50%.

### 2.3.2 Reaction Order Measurements

We evaluated the effects of the partial pressures of PhCl, H<sub>2</sub>, and HCl on the TOF for benzene production. All data were collected at ~50% PhCl conversion while varying only one pressure at a time. The reaction rates used to estimate the order with respect to HCl includes large variations of hydrogen pressure and therefore were normalized by H<sub>2</sub> pressure.

Representative reaction order plots depicting the response of the benzene TOF to variations in the partial pressure of PhCl at 323K, 333K, 343K, and 353K are shown in Figure 2.3a. The calculated reaction order with respect to PhCl increases with increasing temperature from 0.5 to 0.8, suggesting the surface is highly covered by PhCl-related species at low temperatures. Such an increase in reaction order with increasing temperature has previously been observed for other hydrogenation reactions of aromatic species,<sup>69</sup> which leads us to postulate that the Pd surface can become highly covered by PhCl at low temperatures. Figure 2.3b shows a similar plot for the influence of H<sub>2</sub> on the reaction,

again at 323K, 333K, 343K, and 353K. Reaction order with respect to  $H_2$  does not follow a particular trend with temperature and even at 323K it maintains 0.51 order dependency, suggesting that it is unlikely to saturate the Pd surface with hydrogen and despite previous report,<sup>141</sup> dissociated hydrogen is not weakly adsorbed to the catalyst surface. The effect of HCl partial pressure was studied to investigate product inhibition as it was suggested in several reports.<sup>2,69,130</sup> Because HCl is a byproduct of this reaction we cannot get to very low partial pressures and the nature of the experimental apparatus does not allow maneuvering with high partial pressures of HCl which lead us to measure in a limited pressure range while maintaining constant PhCl and  $H_2$  partial pressures at 353K (Figure 2.3c). Reaction order with respect to HCl is -0.99, which is in agreement with the literature.<sup>142</sup>

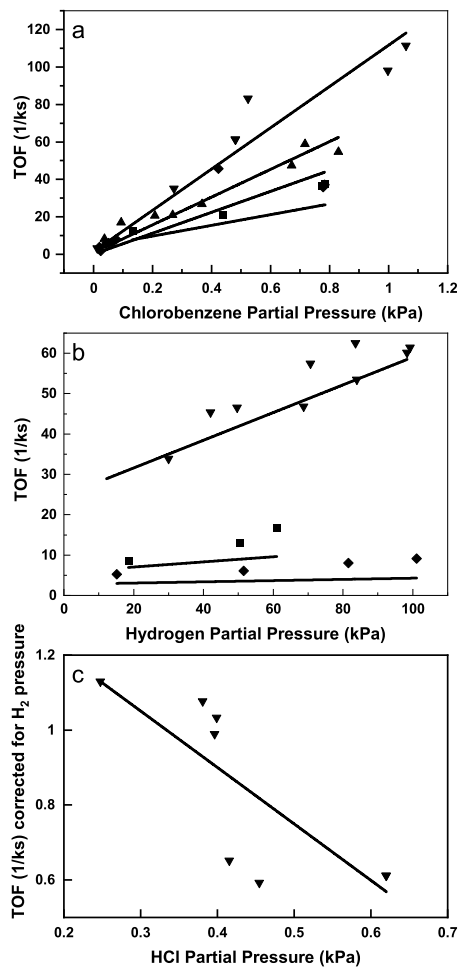


Figure 2.3: Reaction order plots for a) PhCl (with 100 kPa H<sub>2</sub>), b) H<sub>2</sub> (with 1 kPa PhCl), and c) reaction order plot for HCl at 353K. Temperatures include 323K (■), 333 K (◆), 343 K (▲), and 353 K (▲). Lines are predicted rates at experimental conditions. Reaction conditions: 5% Pd/C catalyst, WHSV = 1-6 hr<sup>-1</sup>. PhCl conversion in all cases ~50%.

### 2.3.3 Hydrogen-Deuterium Isotope Effect

To identify potential participation of H-related species in the rate-controlling step for PhCl hydrogenolysis, we performed the reaction using both D<sub>2</sub> and H<sub>2</sub>. The deuterium was obtained from Cambridge Isotope Laboratories, Inc. Figure 2.4 shows the TOF for benzene production as a function of time-on-stream in a D<sub>2</sub> environment (from t=0-6 hr) followed

by a switch to a H<sub>2</sub> environment (from t=6-12 hr). The TOF remains constant throughout this period, indicating that there is no significant hydrogen-deuterium isotope effect.

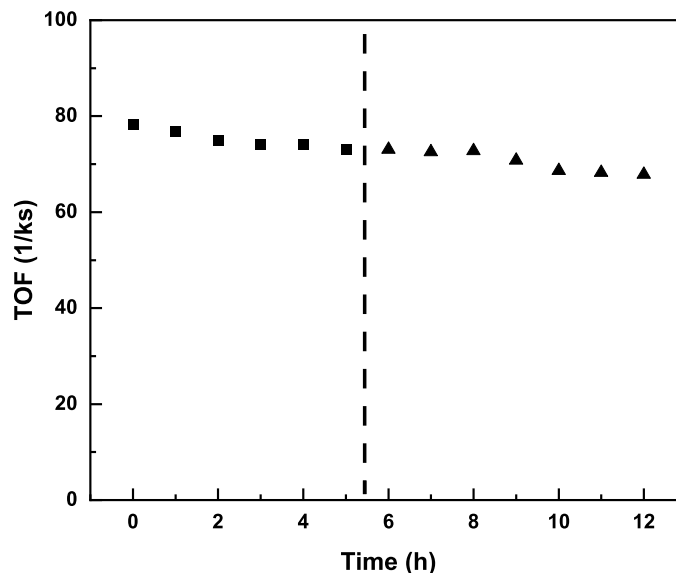


Figure 2.4: TOF for benzene production using both D<sub>2</sub> (■) and H<sub>2</sub> (▲) gasses. Reaction conditions: 5% Pd/C, 353 K, 0.7 kPa PhCl, 99.6 kPa H<sub>2</sub> or D<sub>2</sub>, WHSV = 2.44hr<sup>-1</sup>. PhCl conversion ~50%.

### 2.3.4 Proposed Reaction Sequence

The HDC of PhCl mechanism involves a transition state that leads to C–Cl cleavage, as well as several hydrogenation steps. There are several studies that focused the mechanism of hydrodechlorination reaction.<sup>4,30,133,143</sup> The chemisorption of simple alkyl halides on metals is reported not to proceed by dehydrogenation of C–H bonds.<sup>137</sup> Hydrogen adsorption is known to be quasi-equilibrated at these temperatures.<sup>144</sup> Chlorobenzene adsorption occurs molecularly at ambient temperature on Pd(111) surface.<sup>145</sup> It is also reported that adsorbed chlorine undergoes predominant desorption mechanism at temperatures above 320 K.<sup>146</sup> Therefore, we assume, as is generally the case for metal-catalyzed reactions, that adsorption and desorption steps are not kinetically significant. The lack of an observed primary kinetic isotope effect when using D<sub>2</sub> gas (*c.f.*, Figure 2.4) excludes the potential for any of the hydrogenation steps to be kinetically

significant. Accordingly, we consider the cases where C–Cl bond breaking is rate-controlling.

The first potential mechanism to consider involves the direct cleavage of the C–Cl bond following associative adsorption of PhCl on the Pd surface. Assuming C–Cl bond scission is irreversible and rate-controlling and is preceded by quasi-equilibrated adsorption of PhCl and H<sub>2</sub> and followed by quasi-equilibrated associative desorption of HCl and kinetically-insignificant desorption of benzene. If the surface is populated by a combination of adsorbed PhCl, HCl, and H and Cl adatoms, then the rate equation for benzene production is described by:

$$r_{direct-2} = \frac{k_{direct}P_{PhCl}}{(1 + K_{PhCl}P_{PhCl} + K_H P_{H_2}^{\frac{1}{2}} + K_{HCl}P_{HCl} + K_{Cl}P_{HCl}P_{H_2}^{\frac{-1}{2}})^2} \quad (2.3)$$

where  $k_{direct}$  is the effective rate constant for forming transition state for C–Cl cleavage relative to gas-phase PhCl and a bare surface.  $K_{PhCl}$ ,  $K_H$ ,  $K_{HCl}$ , and  $K_{Cl}$  are the equilibrium constants for adsorption of each surface species, and the site balance is given by  $[L] = [*] + [PhCl*] + [Cl*] + [H*] + [HCl*]$ . Notably, the site-blocking term of this rate expression is squared, implying that a surface species (*e.g.*, PhCl\*, Cl\*, H\*, or HCl\*) must desorb from the surface to make room for the Cl\* species being cleaved from the phenyl ring. It is possible, however, that this transition state occupies the same area as adsorbed PhCl\*, which would lead to a site-blocking term that is not squared as given by the usual Langmuirian depiction. The area of activation will be the same for both pathways,<sup>147</sup> suggesting that the effective rate constant remains  $k_{direct}$ . The resulting rate equation is given by:

$$\frac{r_{direct-1}}{[L]} = \frac{k_{direct}P_{PhCl}}{1 + K_{PhCl}P_{PhCl} + K_H P_{H_2}^{1/2} + K_{HCl}P_{HCl} + K_{Cl}P_{HCl}P_{H_2}^{-1/2}} \quad (2.4)$$

where the rate constants and site balance are the same as for Equation 2.3. Notably, this form of the rate expression is consistent with that proposed by Ribiero and

coworkers<sup>69,130</sup> for Pd-catalyzed C–Cl scission in chlorofluorocarbons, described as substitution of a surface Pd atom into the C–Cl bond.

A third potential mechanism would involve hydrogen-assisted removal of Cl from adsorbed PhCl. This mechanism is analogous to those described by<sup>2,50,148</sup> for a variety of hydrogenolysis reactions. In this pathway, C–Cl bond scission remains irreversible and rate controlling, but it is preceded not only by quasi-equilibrated adsorption of PhCl and H<sub>2</sub> but also by quasi-equilibrated addition of H\* to PhCl\*, forming a Ph-ClH\* species. HCl\* is formed upon cleavage of the C-Cl bond, implying that the surface would be populated only by PhCl, HCl, and H adatoms. The resulting rate equation is given by:

$$\frac{r_H}{[L]} = \frac{k_H P_{PhCl} P_{H_2}^{1/2}}{\left(1 + K_{PhCl} P_{PhCl} + K_H P_{H_2}^{1/2} + K_{HCl} P_{HCl}\right)^2} \quad (2.5)$$

where  $k_H$  corresponds to the effective rate constant for formation of the H-assisted transition state from gas-phase PhCl, H<sub>2</sub>, and a bare surface; the adsorption equilibrium constants are as above; and the site balance corresponds to

$$[L] = [*] + [PhCl*] + [H*] + [HCl*].$$

The apparent reaction orders presented in Figure 2.4 allow us to discriminate among these potential mechanisms. The two-site mechanisms given by Equations 2.3 and 2.5 each would lead to negative reaction orders with respect to PhCl if the surface were covered by PhCl at low temperature, while Figure 2.3a shows that the reaction order in PhCl approaches zero but remains positive at low temperatures. Moreover, neither rate equation can convincingly predict the observed inverse first-order dependence HCl pressure or the half-order dependence on H<sub>2</sub> pressure. However, the one-site mechanism given by Equation 2.4 is more promising: low-temperature coverage of the surface by PhCl\* would lead to the zero-order dependence on PhCl pressure at 323 K, and a surface covered by HCl\* would lead to inverse-first-order behavior with respect to HCl pressure and half-order behavior with respect to H<sub>2</sub> pressure.

Letting  $\text{PhCl}^*$  and  $\text{Cl}^*$  to be most abundant surface intermediates (MASI), with elementary steps delineated in Table 2.1, Equation 2.4 reduces to:

$$\frac{r_{\text{direct-1}}}{[L]} = \frac{k_{\text{direct}} P_{\text{PhCl}}}{1 + K_{\text{PhCl}} P_{\text{PhCl}} + K_{\text{Cl}} P_{\text{HCl}} P_{\text{H}_2}^{-1/2}} \quad (2.6)$$

where  $k_{\text{direct}}$  is  $k_{\text{Ph-Cl}} \times K_{\text{H}_2} \times K_{\text{HCl}}$ .

Table 2.1: Sequence of elementary steps for HDC of PhCl.

Step	Reaction
1	$\text{H}_2 + 2^* \xrightleftharpoons{K_{\text{H}_2}} 2\text{H}^*$
2	$\text{C}_6\text{H}_5\text{Cl} + ^* \xrightleftharpoons{K_{\text{PhCl}}} \text{C}_6\text{H}_5\text{Cl}^*$
3	$\text{C}_6\text{H}_5\text{Cl}^* \xrightarrow{k_{\text{Ph-Cl}}} \text{C}_6\text{H}_5\text{-Pd}^* \text{-Cl}$
4	$\text{C}_6\text{H}_5\text{-Pd}^* \text{-Cl} + \text{H}^* \rightleftharpoons \text{C}_6\text{H}_6 + \text{Cl}^*$
5	$\text{Cl}^* + \text{H}^* \xrightleftharpoons{K_{\text{HCl}}} \text{HCl} + 2^*$
Overall	$\text{H}_2 + \text{C}_6\text{H}_5\text{Cl} \rightleftharpoons \text{C}_6\text{H}_6 + \text{HCl}$

The rate constants involved in the expression above are evaluated from a combination of enthalpy and entropy values. Dissociative adsorption of hydrogen is a well-documented reaction step and binding energy of H-Pd is -2.65 (eV);<sup>149</sup> assuming  $\text{H}^*$  loses one directional freedom perpendicular to Pd(111) surface and acts a 2D gas one can calculate entropy of adsorbed hydrogen using statistical mechanic and therefore the change in entropy can be calculated:

$$S_{\text{trans},2D}^\circ = R \left( \ln \left( \frac{2\pi k_B T}{h^2} \right) + \ln \frac{SA}{N_{\text{sat}}} \right) \quad (2.7)$$

Where  $R$  is gas constant,  $k_B$  is the Boltzmann's constant and  $SA/N_{\text{sat}}$  is the area occupied per adsorbed molecule in standard condition. Natal-Santiago et al.<sup>150</sup> performed microcalorimetric experiments and reported an enthalpy value of -104 (kJ/mol) for hydrogen adsorption on Pd. Campbell and Sellers<sup>151</sup> have shown a linear relationship between the entropy of the molecularly adsorbed organic species and their gaseous counterparts. This relation is valid for molecules with less than 35 atoms; therefore,

entropy value for molecular adsorption of chlorobenzene can be calculated:

$$S_{ads}^{\circ}(T) = 0.7S_{gas}^{\circ}(T) - 3.3R \quad (2.8)$$

Surface science experiments have also been performed for desorption of HCl in step 5. Hunka et al.<sup>146</sup> used a combination of auger electron spectroscopy (AES) and thermal desorption spectroscopy (TDS) and reported a value of 70 (kJ/mol) for enthalpy change of this step consistent with previous work.<sup>130</sup> To be able to test the proposed rate expression (Equation 2.6) enthalpy of chlorobenzene adsorption (Step 2) and entropy of HCl desorption (Step 5) along with activation energy of the rate controlling step (C-Cl scission). These values were calculated using a microkinetic model which uses nlinfit function in MATLAB<sup>®</sup> over the entire range of experimental results (88 data points). Table 2.2 includes all the thermodynamic values required for determining rate constants.

Table 2.2: Thermodynamic values for rate constants calculation. *Fitted parameters are in gray cells.*

Parameter	$\Delta S/\Delta S^{\ddagger}$ (kJ/mol)	$\Delta H/\Delta H^{\ddagger}$ (kJ/mol)
$k_{Ph-Cl}$	$E_a^{\ddagger} = 86.77 \pm 2.09$	
$K_{H_2}$	-39	-104
$K_{PhCl}$	-147	$61.83 \pm 3.35$
$K_{HCl}$	$15.98 \pm 8.04$	70

Apparent activation energy reported in the literature is 18.8-18.9 kcal/mol (78.7-79.1 kJ/mol)<sup>152,153</sup> for C-Cl bond dissociation which is in agreement with the calculated value in Table 2.2. Enthalpy of adsorption of chlorobenzene was fitted to a value of  $-61.83 \pm 3.35$  (kJ/mol) which is in the reported range of  $-60 < \Delta H < -80$  (kJ/mol).<sup>154</sup>

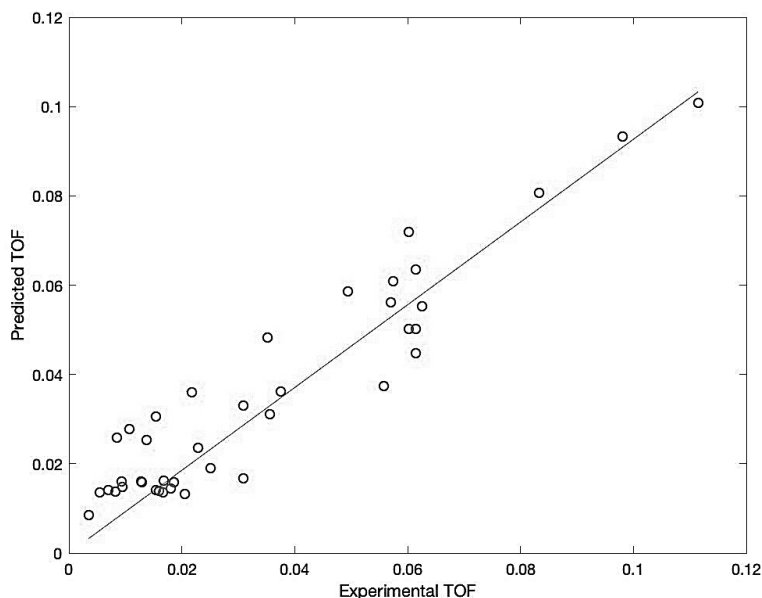


Figure 2.5: Experimental and predicted chlorobenzene HDC TOF associated with Pd/C:  $P_{H_2}=10-97$  kPa;  $T=323-353$ K.

The level of agreement between the calculated with the experimental TOF is illustrated in the parity plot in (*c.f.* Figure 2.5). Results from the model demonstrate that this model captures the trends of the experimental data (*c.f.* Figure 2.3a-c) which means the proposed mechanism in this work is consistent with the mechanism put forth by Sinfelt for hydrogenolysis of C-X bond ( $X = C, N, Cl$ ) in the molecules ethane, methylamine, and methyl chloride, respectively.

## 2.4 Summary

Kinetics of hydrodechlorination reaction of chlorobenzene (PhCl) was studied in a glass CSTR reactor at low temperatures. The results suggest a first order reaction in PhCl, half order in  $H_2$  and an inverse first order in HCl. The kinetics coupled with isotope labeling experiment suggest a reaction that is controlled by cleavage of C-Cl bond. Previous studies<sup>69</sup> along rate expression analysis suggest a one-site mechanism.

The microkinetic model successfully predicts thermodynamics of unknown elementary steps and the predicted rates of the reaction are in good agreement with observed kinetics.

This suggests that mechanism put forth by Sinfelt<sup>137</sup> which is also observed by Chen<sup>143</sup> may be one of the strong candidates to explain hydrodechlorination of chlorobenzene.

## CHAPTER 3

### C-O HYDROGENOLYSIS<sup>1</sup>

#### 3.1 Introduction

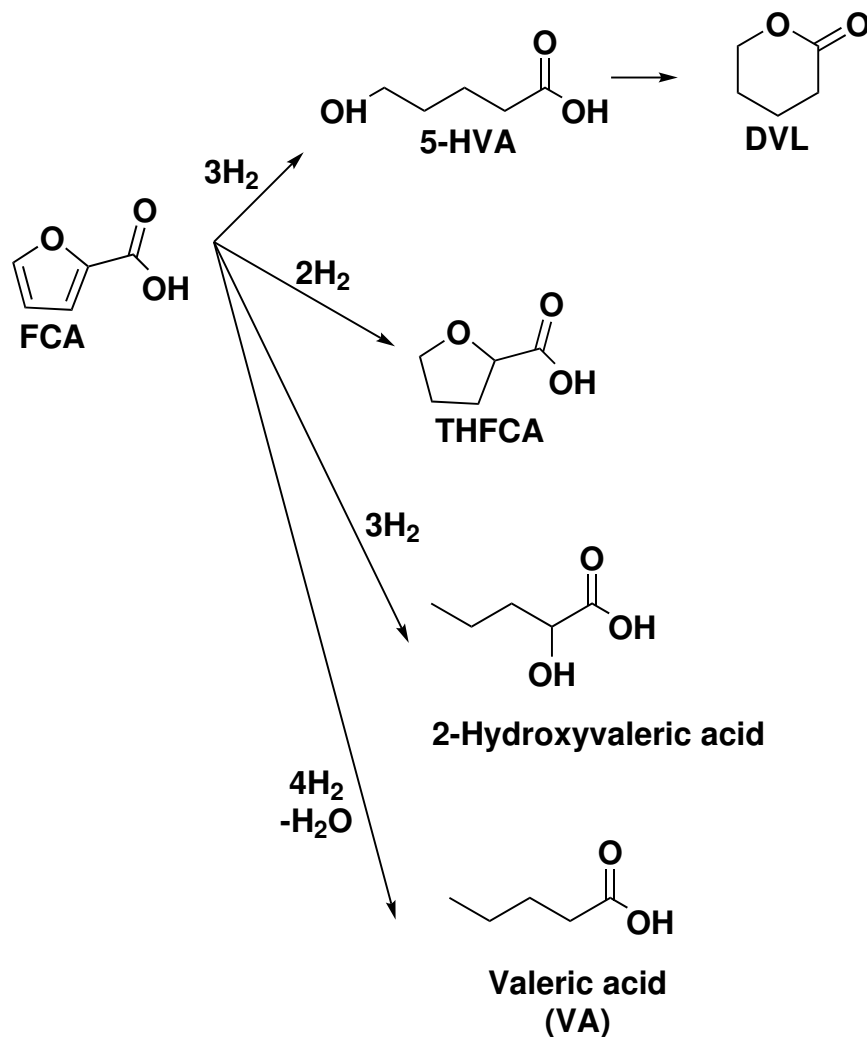
Utilization of biomass among other methods has been the focus of many groups in the scientific community to steer away from fossil resources, initially for energy production and continued in the production of engineering materials. While recent developments in shale gas make it a harder argument to look for alternative energy and lighter petrochemical resources,<sup>168</sup> products such as thermoplastics require higher carbon number and aromatic compounds as feedstocks.<sup>169</sup> Bio-based feedstocks can potentially not only replace petroleum-based materials that get their aromatic compounds from naphtha feedstocks through catalytic reforming, but also due to their oxygen content can produce materials that are not as easily available through petroleum-based feedstocks.<sup>170</sup>

Bio-based polymers have been the subject of many contributions; however, these polymers still have a long way to go before replacing their petroleum-based counterparts due to lower thermal or mechanical properties. For example, poly-lactic acid (PLA) polymers are the second most-used bio-renewable thermoplastic with a glass transition temperature ( $T_g=55-60$  °C) which is suitable for applications like plastic cups to 3D-printing, but market available for rigid materials like polymeric cement are more attracted to polystyrene like structures. Production of polymeric compounds typically require monomers with functional groups at their  $\alpha,\omega$ -positions namely diols, dicarboxylic acids and hydroxyl groups and their lactones.<sup>118</sup> Complex structures of bio-based feedstocks make it difficult to directly produce these monomers; therefore, choosing a

<sup>1</sup>This chapter is from a paper: Jalal Tavana, Faysal Atik, William Gramlich and Thomas J. Schwartz, "Functionalized  $\delta$ -hexalactone (FDHL): Bio-based Monomers to Synthesize Renewable Polyester Thermoplastics", ACS Sustainable Chemistry and Engineering, **2020**. (In preparation) My contribution is creating the monomer from biomass and equally contribute in the preparation of the manuscript.

chemical back bone from available platform chemicals in a biomass refinery with close structure to the target monomer is essential. For example, production of diols using furfural as platform molecule is well studied.<sup>171–177</sup> Biomass-derived platform chemical 5-hydroxymethylfurfural (HMF) with a hydroxyl and carboxyl group can be upgraded selectively through heterogeneous catalysis. Therefore, HMF functionalization with different pendant groups will allow the target polymer to have tunable characteristics and have the potential to functionalize bio-based polymers like PLA to achieve the desired thermal and mechanical properties.

Allen et al.<sup>178</sup> has recently developed etherification of HMF to introduce phenolic functionality to the compound. To yield the corresponding carboxylic acid into polymer, aldehyde group in HMF needs to be oxidized<sup>179</sup> to form FFCA which is similar to oxidation of furfural to furan-2-carboxylic acid (FCA).<sup>180–182</sup> Reduction of FCA are not attractive for researchers mainly because the products of these reactions including furfuryl alcohol can be synthesized with easier methods through hydrogenation of intermediates like furfural<sup>183–185</sup> that are obtainable with high yield. Recently, Tomishige's group<sup>116,118</sup> have focused on achieving products with retention of carboxyl group of FCA using a range of bimetallic catalysts (e.g. Rh–WO<sub>x</sub>/SiO<sub>2</sub>, Pt–MoO<sub>x</sub>/TiO<sub>2</sub>). Based on their observations, the catalyst can saturate the furan ring which leads to production of the hydrogenated species (THFCA) and is a primary product (*c.f.* Scheme 3.1). However, C–O cleavage at the  $\alpha$ -position of adsorbed carboxylate before the saturation leads to other primary products like valeric acid (VA) and 5-hydroxyvaleric acid (5-HVA) products. 5-HVA can dehydrate to yield  $\delta$ -valerolactone through an S<sub>N</sub>2 mechanism. In order to produce the lactone monomer (FDHL) from FFCA, hydrogenation of the furan ring followed by lactonization is required. While saturation of the furan ring is known to occur over hydrogenation catalysts including Pd,<sup>186</sup> Pt,<sup>187</sup> Ru,<sup>188</sup> the path to lactonization requires more complicated catalytic active sites which had led to numerous publications suggesting bimetallic catalysts.<sup>177,189–191</sup>



Scheme 3.1: 2-Furancarboxylic acid (FCA) reduction to tetrahydro-2-furancarboxylic acid (THFCA) and  $\delta$ -valerolactone (DVL) proposed by Asano et al.<sup>118</sup>.

Here we report hydrogenation and lactonization of biomass-derived FCA to DVL and use the knowledge to successfully synthesize functionalized hexalactone (FDHL) for further polymerization. The effect of catalyst and support were examined to find the catalyst that has a higher yield in DVL. Literature suggests that solvent impacts the stability of the transition state; here we study the solvent effect on the product distribution. Finally, the effect of reaction time on the product distribution was studied.

## 3.2 Materials and Methods

### 3.2.1 Preparation of catalysts

In case of titania supported Ru catalysts, Aeroxide<sup>®</sup> (TiO<sub>2</sub>) P25 (Evonik Degussa Co.) was used as support to prepare the catalyst. Ruthenium on P25 catalyst was prepared using incipient wetness impregnation achieving 1.5-5 wt% Ru loadings (1.5 Ru/TiO<sub>2</sub> and 5 Ru/TiO<sub>2</sub>, respectively). P25 was dried at 413 K for 6 h before impregnation to desorb water and some other species potentially present on the TiO<sub>2</sub> particles. A 31.3% Ru(III) nitrosyl nitrate (Alfa Aesar) was dissolved in deionized water to produce the different impregnating Ru concentrations. After measuring the wetness point of TiO<sub>2</sub> with water, a solution containing the precursor, with different concentrations as required by the desired ruthenium loading, was measured for 5 g of TiO<sub>2</sub>. In the first step, this precursor solution was drop-by-drop added to TiO<sub>2</sub> and a spatula was used to mix them thoroughly and ensure the solution filled all the pores in titania. Once the liquid addition was complete, the wet catalyst was dried at 373 K overnight. This allowed water evaporation from the TiO<sub>2</sub> support leaving Ru(NO)(NO<sub>3</sub>)<sub>3</sub> phase on the catalyst outer surface. The dried cake was crushed in a mortar until the resulting particles were fine enough, and reached size +50 of mesh filter. The catalyst was not calcined to ensure small particles and increased metal surface interface.<sup>107</sup> Pre-reduction was carried out in a quartz flow reactor unit following a purge using Ar at 60 sccm for 15 min, the unit was filled with H<sub>2</sub> gas, supplied from in house hydrogen generator (Parker-Dominick Hunter), at 60 sccm for 15 min to be reduced. Reduction steps involved the following: (a) a 1 °C/min temperature increase and (b) once 673 K was reached, this temperature was maintained for another 4 h (c) now the reactor was back-filled with Ar and slowly passivated with Air. The preparation procedure described in this section, ensures the formation of (Ru<sup>0</sup>) particles on the TiO<sub>2</sub> surface. The same method was followed for the synthesis of other catalysts (5 Ru/C and 5 Ru/Al<sub>2</sub>O<sub>3</sub>).

### 3.2.2 Catalyst Activity

Activity test for different catalysts were conducted in a 50 ml stainless steel autoclave Parr instrument . In a typical run, the passivated catalyst was put inside the autoclave and which was purged three times with N<sub>2</sub> and filled with 4 MPa of H<sub>2</sub> at room temperature. The catalyst was reduced *in situ* to get to M<sup>0</sup> state in the metal and remove remaining oxygen left from passivation step in the catalyst synthesis explained before. This reduction was carried out at 1°C/min from room temperature to 200 °C which was maintained for 4h. Then the reactor was cooled to the target reaction temperature (typically 150 °C) and the 30 ml of solution with the substrate (e.g. 5% FCA in 1,4-dioxane) was injected into the reactor using an HPLC pump (Chrom Tech, M1 Class). The solution was mixed using a magnetic stirrer at 500 rpm. Reagents, include 2-furancarboxylic acid (98% FCA, Acros Organics), tetrahydro-2-furancarboxylic acid (98+% THFCA, Acros Organics), 5-methyl-2-furancarboxylic acid (98% 5M2FCA, Combi-Blocks),  $\delta$ -valerolactone (98% DVL,Alfa Aesar),  $\delta$ -hexalactone (>99% DHL, TCI), 5-phenoxy-2-furancarboxylic acid (97% 5Ph2FCA, Maybridge) and isobutanol, as internal standard, were used as received.

After the reaction time which was up to 25 h (typically 8h), the autoclave was cooled down to room temperature, the gases were put into the vent and the solution was filtered and put into a vial. The internal standard (isobutanol) was added into vial along with the product solution. Products were analyzed by GC/MS (Agilent Technologies, 5977B MSD and 7820A GC systems) equipped with HP-5 column, and after identification of products their standard were acquired and quantification was carried out using a GC/FID unit manufactured by Agilent equipped with a DBWAX column mesh (9.1 m  $\times$  2 mm  $\times$  2  $\mu$ m nominal) was used to separate 1,4-Dioxane, FCA, (THFCA), and Lactone product. The H<sub>2</sub> gas produced in house and is highly pure(99.99%). Calibration of GC-FID detector was made using several mixtures of known concentrations with the internal standard.

conversion, yield and selectivity were calculated by the following equations:

$$\text{conversion}[\%] = \left(1 - \frac{\text{amount of detected reactant [mM]}}{\text{amount of loaded reactant [mM]}}\right) \times 100 \quad (3.1)$$

$$\text{yield}[\%] = \frac{\text{products [mM]}}{\text{loaded reactant [mM]}} \times 100 \quad (3.2)$$

$$\text{selectivity}[\%] = \frac{\text{amount of detected product molecule [mM]}}{\text{amount of loaded reactant [mM]}} \times 100 \quad (3.3)$$

### 3.3 Results and Discussion

#### 3.3.1 Hydrogenolysis of FCA Over Various Catalysts

Several reports<sup>116–118,191,192</sup> that focused on FCA upgrading with retention of carboxyl group suggest that hydrogenolysis of C-O bond at the  $\alpha$ -position requires activation of the substrate from the carboxylic acid on an active functionality on the catalyst and a hydrogen attack from the metallic surface. Newman et al.<sup>107</sup> have reported selective HDO activity of Ru/TiO<sub>2</sub> without the hydrogenation of the aromatic ring. Different groups,<sup>107,108</sup> that investigated the catalytic C-O hydrogenolysis of different model compounds including phenol and m-cresol, believe that Ru on titania involves a bi-functional catalyst, where the metal-support interface is participating in the reaction while Ru/Al<sub>2</sub>O<sub>3</sub> and Ru/C perform a moderate direct deoxygenation and some ring saturation product. Figure 3.1 compares the performance of different catalysts supports. This result shows that at a similar conversion (~60-80%), while hydrogenation seems a primary route, the DVL yield increases with TiO<sub>2</sub> as opposed to an inert and a Lewis acid support, C and Al<sub>2</sub>O<sub>3</sub>, respectively. The lower Ru loading, 1.5% Ru/TiO<sub>2</sub>, should provide more metal-support interface;<sup>107</sup> therefore, it is possible that the Brønsted sites created from hydrogen spillover could favor more selective C-O cleavage of FCA to DVL. However, 5 Ru/TiO<sub>2</sub> shows more selectivity to both lactone and THFCA which could be explained by the fact that adsorption mode of FCA on larger Ru particles plays a role in the

observed DVL yields. Moreover, 5 Ru/C and 5 Ru/Al<sub>2</sub>O<sub>3</sub> show similar results in hydrogenation and DVL selectivities to 1.5 Ru/TiO<sub>2</sub> which is another reason that Ru plays more important role than the support. In order to investigate this hypothesis requires mechanistic studies of the reaction beyond the scope of this contribution.

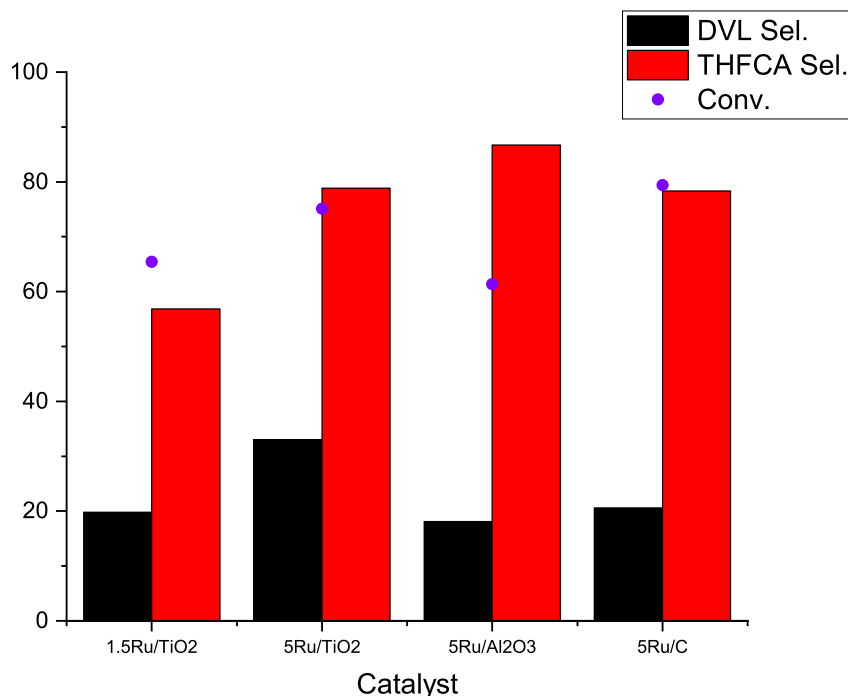


Figure 3.1: Hydrogenolysis of FCA using Ru over various supports. Reaction conditions: FCA=10 mmol, solvent=1,4-dioxane, T=423 K, P<sub>H<sub>2</sub></sub> = 4 MPa, t= 8h

### 3.3.2 Solvent Effect

Brønsted acid-catalyzed reactions are common in biomass upgrading and it is well known that these reactions are affected by the solvent composition, thus this property has been used to favor reaction rates, selectivities, stability of desired products and even the economics of downstream separations.<sup>193</sup> One of the reasons for the solvent effect in these reactions is stability of the acidic proton, in that a polar solvent like water stabilizes the proton to a greater extent than an aprotic solvent like tetrahydrofuran (THF) or 1,4-dioxane.<sup>194,195</sup> Schwartz and Bond<sup>196</sup> state that solvation can affect the selectivity either by stabilizing a reactant or a kinetically relevant transition state. Asano et al.<sup>116</sup>

have examined a range of solvents, from water to 1,4-dioxane, acetic acid to alcohols, for the reduction of FCA. They observed more THFCA in less polar solvents like 1,4-dioxane and t-butyl alcohol; however, when they used alcohols as solvent, they reported a decrease in DVL yield as they moved toward more polar solvents. The choice of solvent should include avoiding structures that contain similar reacting bonds, e.g. both THF and FCA have a furan ring and solvent can also participate in the reaction, or avoid competitive adsorption on the active site, e.g. methanol and t-butyl alcohol are known for adsorption on metal oxides.

In this study, we examined a polar solvent (water), and a polar aprotic solvent (1,4-dioxane). Figure 3.2 shows the selectivity of 5 Ru/TiO<sub>2</sub> in 1,4-dioxane, water and a mixture of 50% water and 1,4-dioxane at ~70% conversion. The results show that the choice of polar aprotic solvent leads to highest THFCA (~64%) and DVL (~32%) while water opens new routes for the reaction and degrades the products. Contrary to Asano et al.<sup>116</sup> the mixture of 1,4-dioxane and water did not lead to an average performance of the neat solvents, 1,4-dioxane prevents side reactions and we only observe two main products, THFCA(~80%) and DVL.

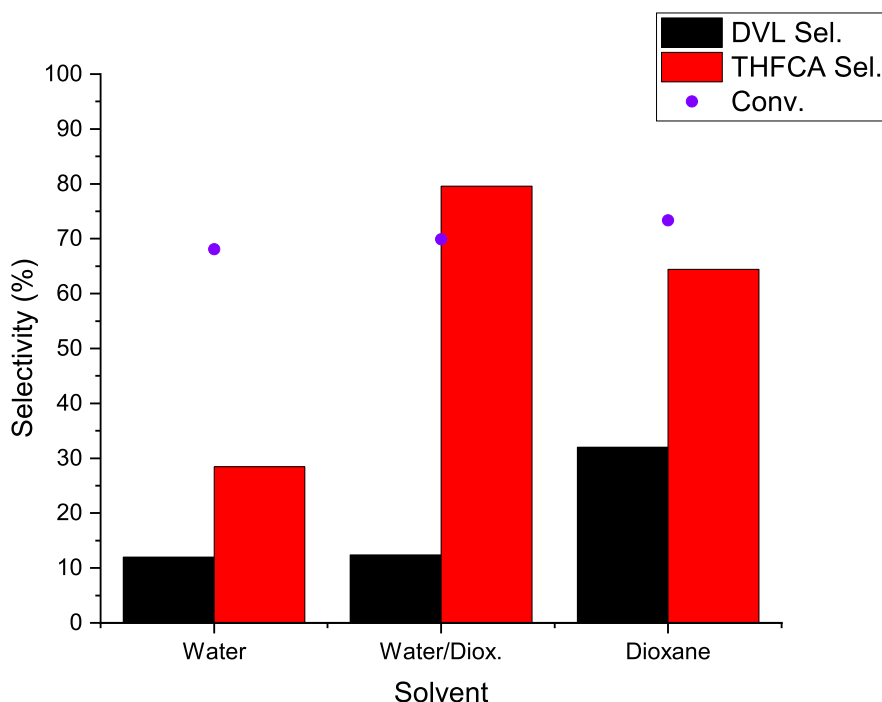


Figure 3.2: Effect of Solvent in Hydrodeoxygenation of FCA over 5%Ru/TiO<sub>2</sub> catalyst. Reaction conditions: FCA= 10 mmol, 50 (mg), 4 MPa H<sub>2</sub>, 423 K, 8h.

### 3.4 Lactone Yield Improvement

Tomishige's group<sup>116–118</sup> specifically focused on catalytic reduction of FCA propose that in order for the C-O cleavage at 2 position to be carried out, furan ring saturation is not necessary. They tested this theory with different substrates including THFCA and found very low activity (~18%) and extremely low yield for DVL (~1%). Figure 3.3 shows the concentration profile for the reduction of FCA using 5 Ru/TiO<sub>2</sub>. This figure shows that after ~6h there is not much change in the concentrations and there is no significant sign of converting THFCA to DVL. When we used THFCA as the substrate, we got a similar conversion of ~20% and ~3% yield in DVL. Tetrahydrofuran-2-carboxylic acid's lack of desire to convert to anything useful in good yield is also confirmed in the literature.<sup>192</sup> From a process stand point it seems we cannot get to a high yield in DVL when THFCA is

a primary product. However, simple molecules have shown different reactivity trend when substituted by other functionalities.

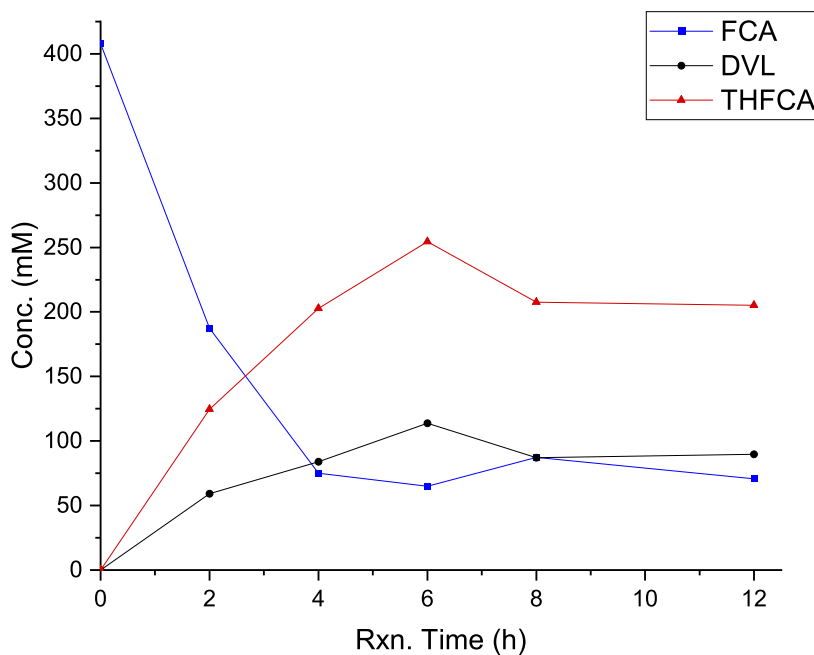
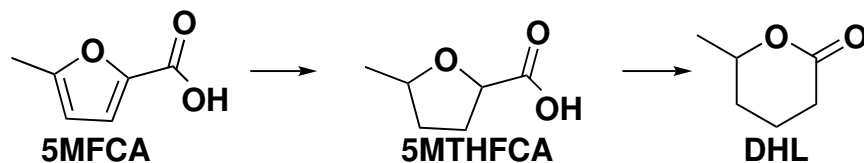


Figure 3.3: Concentration profile for the reduction of FCA. Reaction conditions: FCA= 10 mmol, solvent=1,4-dioxane, catalyst= 250 (mg) 5 Ru/TiO<sub>2</sub>, T= 423K, P<sub>H<sub>2</sub></sub>=4 MPa

Experimenting on phenol substituted FCA (our target monomer) is expensive and it is common practice to work on a similar, cheaper ingredients and apply the best knowledge we can gain to a minimized number of experiments on the more expensive substrate. Therefore, 5-methyl-2-furancarboxylic acid (5MFCA) could be a good candidate since it has a similar structure to FFCA but is not as expensive. Based on FCA hydrogenolysis reactions, we anticipated a better performance for 5 Ru/TiO<sub>2</sub> as opposed to 1.5 Ru/TiO<sub>2</sub> in similar reaction conditions; however, this catalyst exhibited a poor performance (Table 3.1 entry 1). Thermogravimetric (TGA) data on the spent catalyst confirms that there is no coking resulted from deactivation. On the other hand, 5MFCA was reported to react at high conversions it seems unlikely that we are at an equilibrium. Therefore, we tried to optimize the process parameters to tune the performance of the catalyst towards maximum

DHL product. The results show that running the reaction at higher temperature is will convert more of the substrate but it will also overcome some energy barriers that leads to degradation of the products (entry 4). Changing the space time by increasing the amount of catalyst and/or reaction time will improve the performance of the catalyst (entries 1 and 2 of Table 3.1). However, the most interesting fact is that when the same conditions were tried for 1.5 Ru/TiO<sub>2</sub> catalyst, it performed better than 5 Ru/TiO<sub>2</sub> which indicates that unlike our observation in FCA reaction, 5MFCA needs the catalyst-support interface to undergo a selective C-O hydrogenolysis. This indicates that 5-methyltetrahydro-2-furancarboxylic acid (5MTHFCA) might not be a primary product (*c.f.* Scheme 3.2) like THFCA was in FCA reduction as depicted in Scheme 3.1. In a final adjustment by doubling the catalyst used, the best performance was observed (entry 5) with almost all of the hydrogenated product consumed.



Scheme 3.2: 5-methyl-2-Furancarboxylic acid (5MFCA) reduction to 5-methyltetrahydro-2-furancarboxylic acid (5MTHFCA) and  $\delta$ -hexalactone (DHL).

Table 3.1: Optimizing reaction conditions to maximize DHL

Entry	Catalyst	Weight [mg]	Time [h]	Temp. [K]	Conv. [%]	DHL selectivity [%]
1	5 Ru/TiO <sub>2</sub>	250	8	423	14.19	16.02
2	5 Ru/TiO <sub>2</sub>	500	25	423	51.57	40.94
3	1.5 Ru/TiO <sub>2</sub>	500	25	423	90.98	47.28
4	1.5 Ru/TiO <sub>2</sub>	500	25	473	100	15.73
5	1.5 Ru/TiO <sub>2</sub>	1000	25	423	100	52.69

In an effort to elucidate the mechanism of FCA reduction over Pt–MoO<sub>x</sub>/TiO<sub>2</sub> catalyst, Asano et al.<sup>117</sup> have reported one entry for hydrogenolysis of 5MFCA with 91%

conversion and 17% yield in  $\delta$ -hexalactone (DHL). Table 3.2 compares results reported for similar reactions with our observations. The reduction of FCA with Ru/TiO<sub>2</sub> (entry 15) shows promising performance compared to other catalysts that are reported. However, 5MFCA reaction to DHL (entry 16) over 1.5 Ru/TiO<sub>2</sub> shows better performance than other report (entry 10) and we feel convinced to repeat this reaction conditions for the target molecule (5-phenoxy-2-furancarboxylic acid, 5PhFCA).

Table 3.2: Recent reports on reduction of FCA and similar structures to their prospective lactone compounds.

Entry	Substrate	Solvent	Catalyst	Conv.[%]	Selectivity <sup>a</sup> [%]	Yield <sup>a</sup> [%]	Ref.
1	FCA	Methanol	Pt/Al <sub>2</sub> O <sub>3</sub>	99	7	6.93	118
2	FCA	Methanol	Pt/CeO <sub>2</sub>	91	7	6.37	
3	FCA	Methanol	Ru/C	99	1	0.99	
4	FCA	Acetic Acid	Pt/Al <sub>2</sub> O <sub>3</sub>	55	66	36.3	
5	FCA	1,4-dioxane	Pt/Al <sub>2</sub> O <sub>3</sub>	88	34	29.92	
6	FCA	2-propanol	Pt/Al <sub>2</sub> O <sub>3</sub>	97	42	40.74	
7	THFCA	Water	Rh-WO <sub>x</sub> /SiO <sub>2</sub>	61.8	Nan	8.8	192
8	FCA	Water	Pt-MoO <sub>x</sub> /TiO <sub>2</sub>	82	Nan	9	116
9	FCA	Water	Pt-MoO <sub>x</sub> /TiO <sub>2</sub>	97	Nan	5	117
10	5MFCA	Water	Pt-MoO <sub>x</sub> /TiO <sub>2</sub>	91	Nan	17	
11	Succinic acid	1,4-dioxane	Re-Pd/SiO <sub>2</sub>	26	96	24.96	105
12	Adipic acid	1,4-dioxane	Re-Pd/SiO <sub>2</sub>	100	1.1	1.1	
13	Glutaric acid	1,4-dioxane	Re-Pd	22	93	20.46	197
14	1,5-PDO	Gas phase	Nan	99	94	93.06	198
15	FCA	1,4-dioxane	5 Ru/TiO <sub>2</sub>	83	37	30.71	This work
16	5MFCA	1,4-dioxane	1.5 Ru/TiO <sub>2</sub>	100	53	53	
17	THFCA	1,4-dioxane	5 Ru/TiO <sub>2</sub>	20	15	10.2	
18	FCA	1,4-dioxane	5 Pt/Al <sub>2</sub> O <sub>3</sub>	6	53	3.18	

<sup>a</sup>Reported for the lactone product.

After repeating the optimum reaction conditions for 5PhFCA, considering that the commercial standard of hydrogenated molecule is not available, we used the sensitivities of

phenol and 5MFCA derivatives and used a linear approximation to find the GC/FID sensitivity of the target molecule. The results show that after 25 h of reaction at 423 K over 1.5 Ru/TiO<sub>2</sub> we can get to a surprising conversion of 99%. The selectivity of phenoxy- $\delta$ -hexalactone (FDHL) requires meticulous GC/MS analysis of the products peaks; however, preliminary observations suggest ~60% selectivity to FDHL.

### 3.5 Conclusion

Hydrogenolysis of FCA to DVL lactone was studied and the results show that THFCA and DVL are both primary products which is in agreement with the literature<sup>116,118</sup> and while using different supports leads to similar selectivities Ru/TiO<sub>2</sub> with higher loading performs better in terms of producing more DVL. The 5 Ru/TiO<sub>2</sub> catalyst for FCA reaction was used for methyl substituted FCA and the results show increased activity and selectivity to the lactone with increasing the metal-support interface (1.5 Ru/TiO<sub>2</sub>) which indicates a different reaction mechanism than what is hypothesized for FCA reaction. Moreover, just by adjusting the reaction parameters we were able to successfully improve DHL yield to ~53% which is almost three times better than previous reports. These observations resulted in the production yield of 59.56% for FDHL at 99% conversion which could be used as monomer for polymerization by our colleagues.

**CHAPTER 4**  
**REACTION KINETICS ANALYSIS OF ACROLEIN**  
**HYDRODEOXYGENATION OVER A TUNGSTEN OXIDE CATALYST:**  
**MICROKINETIC MODELING<sup>1</sup>**

## 4.1 Introduction

Bio-oils, with a potential to reduce dependence on petroleum-based fuel,<sup>88,199–201</sup> produced by formate assisted fast pyrolysis (FAsP) are composed of a complicated mixture of oxygenated compounds including carboxylic acids, aldehydes, ketones, alcohols, and phenols.<sup>202,203</sup> Catalytic upgrading is necessary to remove oxygen in order to increase the energy density, make it less acidic, and lower the viscosity.<sup>92,204,205</sup>

Hydrodesulfurization (HDS) catalysts, such as sulfided, Mo-promoted cobalt or nickel,<sup>Elliott</sup><sup>204</sup> suffer from short catalyst lifetimes and downstream contamination of bio-oils with sulfur. Supported noble metal catalysts have been investigated for upgrading whole bio-oils,<sup>206</sup> show good activity for HDO reactions and usually take place via hydrogenation pathways. Catalyst lifetime and cost, and higher consumption of hydrogen are factors that must be justified on the basis of product value.

Transition metal oxides have displayed some activity for deoxygenation. Doornkamp and Ponc<sup>207</sup> have reviewed the evidence for a Mars-van Krevelen mechanism in the deoxygenation of nitrobenzene to nitrosobenzene, and carboxylic acids to aldehydes. The deoxygenation rate depend on the metal oxygen bond strength<sup>208</sup> and the relative strength of CO bond with respect to the metal oxygen bonds.<sup>209–211</sup>

Metal oxides used as selective oxidation catalysts<sup>212–215</sup> are reported to follow the Mars-van Krevelen (MvK) mechanism.<sup>7</sup> A previous report<sup>215</sup> used a bismuth molybdate

<sup>1</sup>This chapter will be part of a paper titled “Mechanism of Hydrodeoxygenation of Acrolein on a Cluster Model of WO<sub>3</sub>” and authors include Timothy J. Thibodeau, Christopher M. Goodwin, Jalal Tavana, François G. Amar, Thomas J. Schwartz and Brian G. Fredrick and the manuscript is in preparation. My role in the paper is on developing a microkinetic modeling of the proposed reaction sequences.

catalyst to selectively oxidize propene to acrolein. Propene first adsorbs on the bismuth oxide phase and forms surface  $\pi$ -allyl species which then migrates to the molybdenum oxide phase and becomes oxygenated to form C=O bond. In the final step, acrolein desorbs from the catalyst, which contains oxygen vacancies and surface hydroxyls, the surface is regenerated with O<sub>2</sub> to form a fully oxidized bismuth molybdate.

This contribution focuses on the reverse MvK mechanism displayed in Figure 4.1. Oxygen vacancies and hydroxyls are produced by pre-treating WO<sub>3</sub> in H<sub>2</sub> at 623 K for 10 hours<sup>216</sup> which leads to the production of a tungsten oxide bronze. This catalyst should selectively reduce the C=O bond while leaving the C=C bond in place, to minimize H<sub>2</sub> consumption, when feeding acrolein.

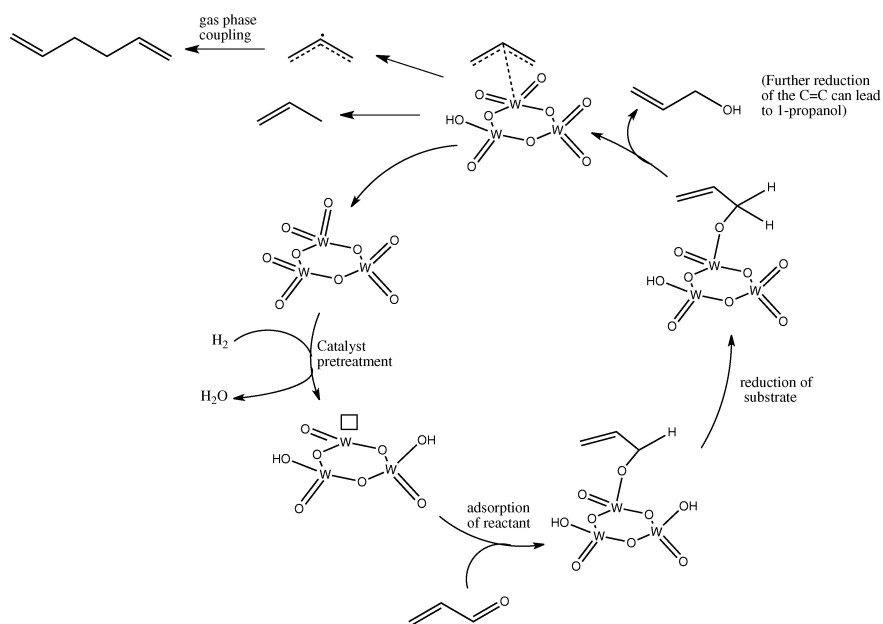


Figure 4.1: Proposed catalytic cycle for the reduction of acrolein to propene, allyl alcohol, and 1-propanol on a model W<sub>3</sub>O<sub>9</sub> cluster.<sup>216</sup>

Thibodeau et al.<sup>216</sup> has reported quantitative production of allyl alcohol with reducing the C=O bond to a C-O bond by formation of the active catalyst by heating WO<sub>3</sub> in H<sub>2</sub> for ten hours at 623 K producing a bronze: H<sub>1.29</sub>WO<sub>2.77</sub>. The HDO of allyl alcohol was performed at higher temperatures (600 K) to show conversion of allyl alcohol to propene.

The underlying surface mechanism of the hydrogenation (HYD) and HDO of allyl alcohol on a model  $W_3O_9$  cluster will be discussed here.

Moberg et al.<sup>217</sup> investigated the HYD and HDO of acrolein on a  $Mo_3O_9$  cluster and estimated that the reaction thermodynamics should be within 10 kJ/mol of the experimental values. Calculations of the electronic structure of the tungsten analogue ( $W_3O_9$ ) have been done and Huang et al.<sup>218</sup> suggest that this is a good model for bulk  $WO_3$ . These calculations were carried out at a similar level of theory to the work reported in this paper. Therefore, calculations investigating the mechanism of the formation of the active site is presented which most likely occurs by hydrogen adsorption and surface hydroxyl formation at terminal sites, followed by desorption of water on the  $W_3O_9$  cluster model. These calculation will be discussed in details when the paper is published and I will only present the result in Figure 4.3. My contribution to this project comes at developing a microkinetic model based on the DFT calculations performed by our collaborators, Dr. Brian G. Fredrick's group, to first calculate thermodynamics of each reacting species including the proposed transition states. These data will be used to calculate the reaction rate constants in each proposed step. Finally, the reaction product distribution at each temperature can be calculated which can be used to investigate the underlying mechanism by finding the degree of rate control of each step.

## 4.2 Theoretical Methods

Density functional theory calculations were done using Gaussian 03<sup>219</sup> and 09.<sup>220</sup> Initial geometry optimizations were performed with B3LYP functional and LANL2DZ effective core potential (ECP) and basis set for W and the 6-31G(d,p) basis set was used for all other atoms. This level of theory is consistent with our previous calculations,<sup>217</sup> and the work of Pudar et al.<sup>221</sup> for  $Mo_3O_9$  clusters. Using optimized structures from calculations at the LANL2DZ/6-31G(d,p) level, we performed single point calculations with the LANL2DZ basis set and ECP for tungsten and the 6-311+G(d,p) basis set for all other

atoms. SCF energy convergence utilized Gaussian's<sup>219,220</sup> quadratic convergence algorithm<sup>222</sup> and tight convergence criteria<sup>223</sup>. Gibbs free energies at 1 atm and either 325 K or 600 K were calculated using frequency calculations performed at the LANL2DZ/6-31G(d,p) level with the appropriate thermodynamic scaling factor.<sup>224,225</sup> These temperatures and pressures correspond to typical experimental conditions for hydrogenation<sup>216,226</sup> and hydrodeoxygenation,<sup>216</sup> respectively. Transition state searching was performed with the TS, QST2 or QST3<sup>227,228</sup> algorithms followed by frequency calculations to verify first-order saddle points and intrinsic reaction coordinate (IRC) calculations to confirm that the transition states led toward the correct reactant and product conformations. Rate constants<sup>229</sup> were calculated from classical energy barriers determined at the LANL2DZ/6-311+G(d,p) level of theory. Zero-point energy correction and partition functions were also calculated from frequency calculations at the LANL2DZ/6-31G(d,p) level of theory.

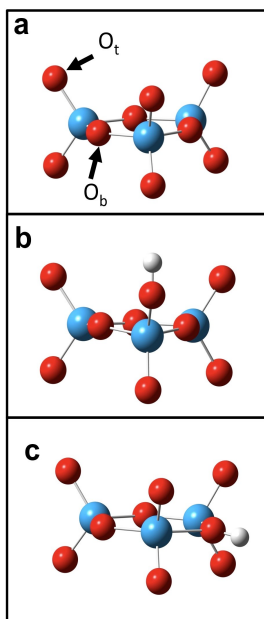


Figure 4.2: (a) The fully oxidized W<sub>3</sub>O<sub>9</sub> cluster used in the calculations, consisting of terminal and bridging oxygens. The red spheres are oxygen atoms, the blue spheres are tungsten atoms, and the white spheres are hydrogen atoms. (b) The W<sub>3</sub>O<sub>9</sub>H cluster with a terminal surface hydroxyl, H<sub>t</sub>. (c) The W<sub>3</sub>O<sub>9</sub>H cluster with a bridging surface hydroxyl, H<sub>b</sub>.

## 4.3 Results

### 4.3.1 Hydroxyl Formation and Surface Oxygen Vacancy Creation

The proposed active site of a tungsten oxide bronze HDO catalyst is a surface oxygen vacancy site at which acrolein can adsorb. Catalytic experiments<sup>216</sup> suggest that surface vacancies are produced during heating in hydrogen at 625 K. Based on our previous work,<sup>217</sup> we expect formation of vacancies to occur in two steps. First, hydrogen from the gas phase adsorbs dissociatively to form surface hydroxyls. Then, dehydroxylation leads to formation of surface oxygen vacancies and desorption of water. In the  $W_3O_9$  cluster there are two surface oxygen sites, terminal and bridging, as shown in Figure 4.2a, which can form terminal (Figure 4.2b) and bridging (Figure 4.2c) hydroxyls. Adsorption of hydrogen can occur at combinations of terminal and bridging sites. Results reported only for the unterminated cluster, because when accounting for bulk like oxygens, strong distortions of the cluster occurred during geometry optimization occurs.

### 4.3.2 Microkinetic Modeling

Moberg et al.<sup>217</sup> have shown that this reaction is more favorable towards less desirable HYD products when performed at low temperatures while at higher temperatures HDO products become thermodynamically more favorable. Therefore, the more desirable product, propene, production at 600 K will be discussed. Figure 4.3 contains the results of potential energy calculations, directly from DFT values, from which we can understand the mechanism for hydrogenation of acrolein into allyl alcohol and 1-propanol, as well as the further hydrodeoxygenation of allyl alcohol to propene, which will form the basis of a microkinetic model described in the 4.4. The same numbering was followed as previous publication<sup>217</sup> and in the work of Pudar et al.<sup>221</sup>

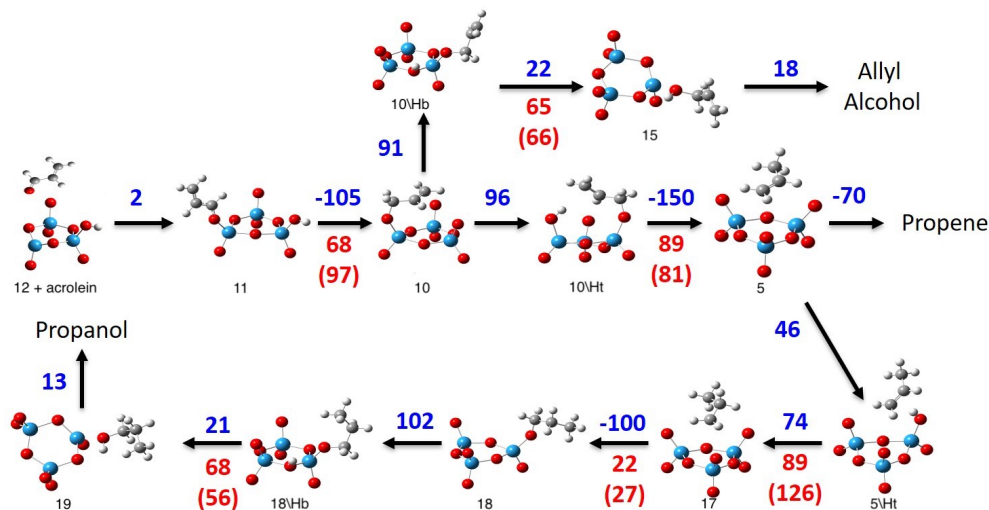


Figure 4.3: Energy and free energy of species in PES relative to structure of 12 + Acrolein + 2H<sub>2</sub>. Blue numbers represent  $\Delta G_{600\text{ K}}$  (kJ/mol) and red numbers represent energy of activation (or  $\Delta G^\ddagger$ ; kJ/mol). All energies refer to B3LYP/6-311+G(d,p) single point calculations for structures optimized at the B3LYP/6-31G(d,p) level for light atoms and LANL2DZ ECP and basis set for tungsten. Free energies refer to frequency calculations at the B3LYP/6-31G(d,p) level for light atoms and the LANL2DZ ECP and basis set for tungsten and energy calculations at the B3LYP/6-311+G(d,p) level .

One step is missing from these calculations and that is the activation energy for bronze formation which can be obtained through TGA data if the reactor is modeled as a batch reactor. By measuring the mass loss from the TGA data,<sup>216</sup> we can calculate the amount of oxygen on the surface of WO<sub>3</sub> as a function of time at different temperatures. Moreover, integrated design equation for batch reactor gives plots for oxygen vacancy concentration as a function of time which in turn can be used to extract rate constants at different temperatures (*c.f.* Figure 4.4); by plotting the natural log of calculated rate constants as an inverse function of temperature we can calculate the activation energy and preexponential factor. The calculated activation barrier for bronze formation is  $E_A = 134 \pm 13$  kJ/mol with a preexponential factor,  $A = 227 \pm 97$  torr<sup>-1</sup>sec<sup>-1</sup>.

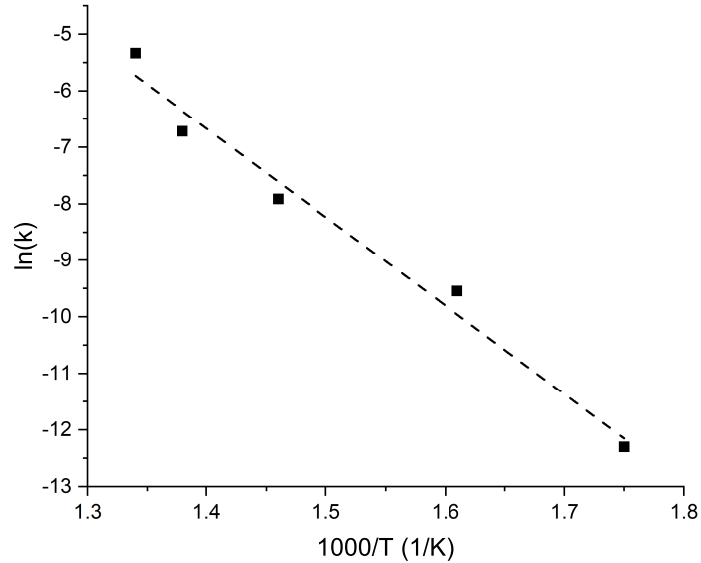


Figure 4.4: Extracting kinetics of oxygen vacancy creation from TGA data between 300°C - 475°C.

Table 4.1 summarized the sequence of elementary steps based on the reaction scheme described for the reaction, when transition states were calculated in the DFT measurements activation energies exist and rate constants were calculated using Eyring equation<sup>229</sup> and where no transition states were calculated that step was assumed to be quasi equilibrated. In order to complete the microkinetic model we needed the initial oxygen coverage. Assuming the reactor modeled as a transient CSTR and run the model we can achieve an initial oxygen coverage of  $6.5 \times 10^{-7}$  (*c.f.* Figure 4.5).

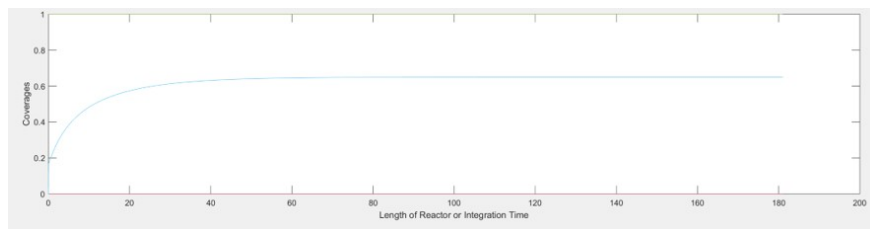


Figure 4.5: Initial oxygen coverage calculated from microkinetic model assuming the reactor is a transient CSTR.

Table 4.1: Sequence of elementary steps on the bronze surface

Step	Reaction
Acrolein adsorption and allyl alcohol production	
1	$C_3H_4O + W_3O_8H_t \rightleftharpoons C_3H_4O-W_3O_8H_t$
2	$C_3H_4O-W_3O_8H_t \longrightarrow C_3H_5O-W_3O_8$
3	$C_3H_5O-W_3O_8 + \frac{1}{2} H_2 \longrightarrow C_3H_5O-W_3O_8H_b$
4	$C_3H_5O-W_3O_8H_b \rightleftharpoons C_3H_5OH-W_3O_8$
5	$C_3H_5OH-W_3O_8 \longrightarrow C_3H_5OH + W_3O_8$
Propylene production	
6	$C_3H_5O-W_3O_8 + \frac{1}{2} H_2 \rightleftharpoons C_3H_5O-W_3O_8H_t$
7	$C_3H_5O-W_3O_8H_t \rightleftharpoons C_3H_6-W_3O_9$
8	$C_3H_6-W_3O_9 \longrightarrow C_3H_6 + W_3O_9$
Propanol production	
9	$C_3H_6 + W_3O_9 + \frac{1}{2} H_2 \longrightarrow C_3H_6-W_3O_9H_t$
10	$C_3H_6-W_3O_9H_t \rightleftharpoons C_3H_7-W_3O_9$
11	$C_3H_7-W_3O_9 \longrightarrow C_3H_7O-W_3O_8$
12	$C_3H_7O-W_3O_8 + \frac{1}{2} H_2 \rightleftharpoons C_3H_7O-W_3O_8H_b$
13	$C_3H_7O-W_3O_8H_b \rightleftharpoons C_3H_7OH-W_3O_8$
14	$C_3H_7OH-W_3O_8 \rightleftharpoons C_3H_7OH + W_3O_8$
Active site regeneration	
15	$W_3O_8 + \frac{1}{2} H_2 \rightleftharpoons W_3O_8H_t$
16	$W_3O_9 + H_2 \rightleftharpoons W_3O_8 + H_2O$

#### 4.4 Discussion

According to the DFT calculations provided to us production of desired HDO product at 350°C is thermodynamically favorable enough that it is expected to have a ~100% selectivity to propene in which case, microkinetic model (MKM) should successfully predict a product distribution that is in line with the experimental data. This data could not capture the experimental trend of product distribution. The MKM could be used to troubleshoot and find the source of this disagreement; therefore, a sensitivity analysis was performed and we found out that control the rates that govern this product distribution

are steps 2 and 8. Considering that DFT models usually predict the experimental data within  $\pm 30$  kJ the calculated values. Therefore, activation energies of these two steps and binding energies of species involved in them, acrolein, hydrogen and propene, were corrected within the confidence interval of the reported DFT values Table 4.2 to get to a surface coverage regime where catalysis for the products would take place.

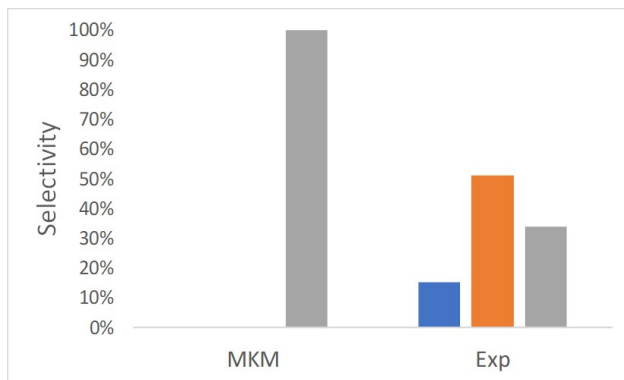


Figure 4.6: Microkinetic (MKM) model prediction of the product distribution based on raw DFT data compared with the experimental data (Exp). Orange is propanol, Blue represent acrolein and gray is propene.  $T = 350^{\circ}\text{C}$ ,  $P_{\text{tot}} = 760$  torr,  $P_{\text{Ac}} = 88$  torr,  $\text{WHSV} = 1800\text{-}3400$   $\text{h}^{-1}$

Table 4.2: Modification to parameters adopted from DFT.

Parameter	BE ( $E_A$ )/ kJ/mol
$\text{BE}_{\text{Acrolein}}$	+50
$\text{BE}_{\text{H}}$	-30
$\text{BE}_{\text{Propene}}$	-30
$\text{TS}_2$	-30
$\text{TS}_8$	-20

Plugging these values into the model resulted in Figure 4.7. This figure shows how MKM can successfully predict the product distribution that was experimentally observed for this reaction at high temperature ( $350^{\circ}\text{C}$ ).

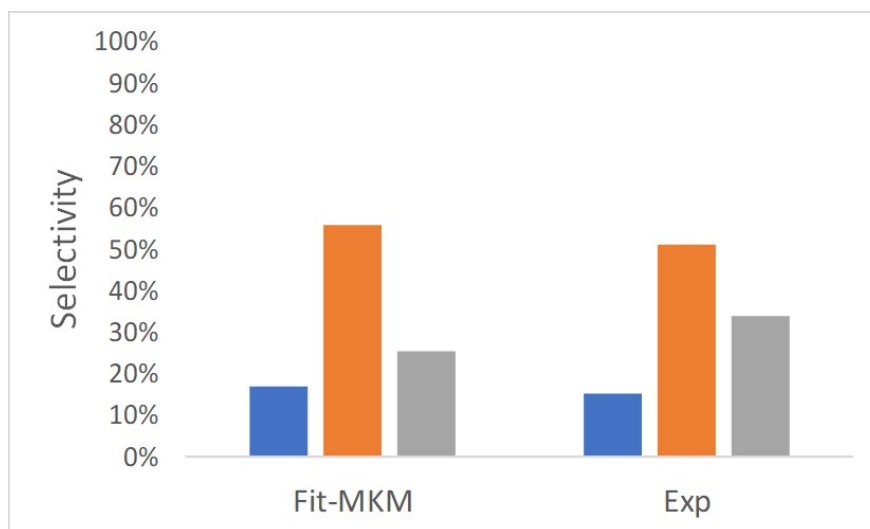


Figure 4.7: Microkinetic model successfully captures the trend of product distribution. Orange is propanol, Blue represent acrolein and gray is propene.  $T = 350^{\circ}\text{C}$ ,  $P_{\text{tot}} = 760$  torr,  $P_{\text{Acr}} = 88$  torr,  $\text{WHSV} = 1800\text{-}3400$   $\text{h}^{-1}$

Now that the MKM can successfully follow the distribution trend reported in the experimental data, the model can be used to investigate the mechanism by calculating the degree of rate control at the reaction conditions for the target products. Table 4.3 reports the results from the degree of rate control analysis<sup>230</sup> for the overall TOF ( $X_{\text{RC}_{\text{TOF}}}$ ), production of acrolein ( $X_{\text{RC}_{\text{Acr}}}$ ), propene ( $X_{\text{RC}_{\text{Ene}}}$ ) and propanol ( $X_{\text{RC}_{\text{Pol}}}$ ). This data suggests that the reaction (propene) is mainly controlled by regenerating the active site rather than breaking the alkoxide bond from tungsten oxide which means that maybe this metal is bonding to the intermediates stronger than expected. Therefore, most abundant surface species present on the surface at the experimental conditions are expected to be these alkoxide species.

## 4.5 Summary

I have developed a microkinetic model, that can be run at different temperatures to study the more favored HYD reactions observed in the experiments at low temperatures as well as HDO product that is more favorable at higher temperatures. The results suggest that oxygen vacancy creation is controlling the rate of the reaction and each of the

Table 4.3: Degree of rate control analysis for routes leading to acrolein, propene and propanol and the overall turn over frequency.

Step	( $X_{RC_{TOF}}$ )	( $X_{RC_{Acr}}$ )	( $X_{RC_{Ene}}$ )	( $X_{RC_{Pol}}$ )
2	0	0	0	0
3	0.19	0.19	0.03	0.28
5	0.10	0.72	0.1	0.38
8	0	0	0	0
9	0	0	0	0
11	0.01	0.01	0	0.02
12	0.62	0.63	1	0.44

observed products are limited by how strong the intermediate alkoxide is bonded to the tungsten surface. The result of this collaboration is in progress for publication and is under review by all collaborating parties.

## REFERENCES

- [1] Pascal Vermeeren, Xiaobo Sun, and F. Matthias Bickelhaupt. Arylic C-X bond activation by palladium catalysts: Activation strain analyses of reactivity trends. *Scientific Reports*, 8(1):1–10, 2018. ISSN 20452322. doi: 10.1038/s41598-018-28998-3.
- [2] Bernard Coq, Gerardo Ferrat, and François Figueras. Conversion of chlorobenzene over palladium and rhodium catalysts of widely varying dispersion. *Journal of Catalysis*, 101(2):434–445, 1986. ISSN 10902694. doi: 10.1016/0021-9517(86)90271-X.
- [3] Hanchi Chen and Shijie Liu. Cooperative adsorption based kinetics for dichlorobenzene dechlorination over Pd/Fe bimetal. *Chemical Engineering Science*, 138:510–515, 2015. ISSN 00092509. doi: 10.1016/j.ces.2015.08.033. URL <http://dx.doi.org/10.1016/j.ces.2015.08.033>.
- [4] Santiago Gómez-Quero, Fernando Cárdenas-Lizana, and Mark A. Keane. Unique selectivity in the hydrodechlorination of 2,4-dichlorophenol over hematite-supported Au. *Journal of Catalysis*, 303:41–49, 2013. ISSN 00219517. doi: 10.1016/j.jcat.2013.03.011.
- [5] V. A. Yakovlev, V. V. Terskikh, V. I. Simagina, and V. A. Likholobov. Liquid phase catalytic hydrodechlorination of chlorobenzene over supported nickel and palladium catalysts: An NMR insight into solvent function. *Journal of Molecular Catalysis A: Chemical*, 153(1-2):231–236, 2000. ISSN 13811169. doi: 10.1016/S1381-1169(99)00352-0.
- [6] Claudia Espro, Bianca Gumina, Emilia Paone, and Francesco Mauriello. Upgrading Lignocellulosic Biomasses: Hydrogenolysis of Platform Derived Molecules Promoted by Heterogeneous Pd-Fe Catalysts. *Catalysts*, 7(12):78, 2017. ISSN 2073-4344. doi: 10.3390/catal7030078. URL <https://www.mdpi.com/2073-4344/7/3/78>.
- [7] P. Mars and D. W. van Krevelen. Oxidations carried out by means of vanadium oxide catalysts. *Chemical Engineering Science*, 3:41–59, 1954. ISSN 00092509. doi: 10.1016/S0009-2509(54)80005-4. URL [http://dx.doi.org/10.1016/S0009-2509\(54\)80005-4](http://dx.doi.org/10.1016/S0009-2509(54)80005-4). The Proceedings of the Conference on Oxidation Processes.
- [8] Artit Ausavasukhi, Yi Huang, Anh T. To, Tawan Sooknoi, and Daniel E. Resasco. Hydrodeoxygenation of m-cresol over gallium-modified beta zeolite catalysts. *Journal of Catalysis*, 290:90–100, 2012. ISSN 00219517. doi: 10.1016/j.jcat.2012.03.003. URL <http://dx.doi.org/10.1016/j.jcat.2012.03.003>.
- [9] Andrey Popov, Elena Kondratieva, Jean Michel Goupil, Laurence Mariey, Philippe Bazin, Jean Pierre Gilson, Arnaud Travert, and Françoise Maugé. Bio-oils hydrodeoxygenation: Adsorption of phenolic molecules on oxidic catalyst supports. *Journal of Physical Chemistry C*, 114(37):15661–15670, 2010. ISSN 19327447. doi: 10.1021/jp101949j. URL <https://doi.org/10.1021/jp101949j>.

- [10] M. J. Mendes, O. A.A. Santos, E. Jordão, and A. M. Silva. Hydrogenation of oleic acid over ruthenium catalysts. *Applied Catalysis A: General*, 217(1-2):253–262, 2001. ISSN 0926860X. doi: 10.1016/S0926-860X(01)00613-5.
- [11] A. van Duijne, V. Ponec, R.M. Koster, R. Pestman, and J.A.Z. Pieterse. Reactions of Carboxylic Acids on Oxides. *Journal of Catalysis*, 168(2):265–272, 2002. ISSN 00219517. doi: 10.1006/jcat.1997.1624.
- [12] Zhong He and Xianqin Wang. Hydrodeoxygenation of model compounds and catalytic systems for pyrolysis bio-oils upgrading. *Catalysis for Sustainable Energy*, 1(2013):28–52, 2013. ISSN 2084-6819. doi: 10.2478/cse-2012-0004. URL <https://www.degruyter.com/view/journals/cse/1/2013/article-p28.xml>.
- [13] Lei Hu, Lu Lin, Zhen Wu, Shouyong Zhou, and Shijie Liu. Recent advances in catalytic transformation of biomass-derived 5-hydroxymethylfurfural into the innovative fuels and chemicals. *Renewable and Sustainable Energy Reviews*, 74:230 – 257, 2017. ISSN 1364-0321. doi: <https://doi.org/10.1016/j.rser.2017.02.042>. URL <http://www.sciencedirect.com/science/article/pii/S1364032117302599>.
- [14] Zhongyi Ma, Lin Wei, Wei Zhou, Litao Jia, Bo Hou, Debao Li, and Yongxiang Zhao. Overview of catalyst application in petroleum refinery for biomass catalytic pyrolysis and bio-oil upgrading. *RSC Advances*, 5:88287–88297, 2015. doi: 10.1039/C5RA17241A. URL <http://dx.doi.org/10.1039/C5RA17241A>.
- [15] Yves Schuurman, Gabriella Fogassy, and Claude Mirodatos. Chapter 10 - Tomorrow's Biofuels: Hybrid Biogasoline by Co-processing in FCC Units. In Kostas S. Triantafyllidis, Angelos A. Lappas, and Michael Stöcker, editors, *The Role of Catalysis for the Sustainable Production of Bio-fuels and Bio-chemicals*, pages 321 – 349. Elsevier, Amsterdam, 2013. ISBN 978-0-444-56330-9. doi: <https://doi.org/10.1016/B978-0-444-56330-9.00010-3>. URL <http://www.sciencedirect.com/science/article/pii/B9780444563309000103>.
- [16] Yeonjoon Kim, Anna E. Thomas, David J. Robichaud, Kristiina Iisa, Peter C. St. John, Brian D. Etz, Gina M. Fioroni, Abhijit Dutta, Robert L. McCormick, Calvin Mukarakate, and Seonah Kim. A perspective on biomass-derived biofuels: From catalyst design principles to fuel properties. *Journal of Hazardous Materials*, 400: 123198, 2020. ISSN 0304-3894. doi: <https://doi.org/10.1016/j.jhazmat.2020.123198>. URL <http://www.sciencedirect.com/science/article/pii/S0304389420311870>.
- [17] Jithin John Varghese. Computational design of catalysts for bio-waste upgrading. *Current Opinion in Chemical Engineering*, 26:20–27, 2019. ISSN 2211-3398. doi: <https://doi.org/10.1016/j.coche.2019.08.002>. URL <http://www.sciencedirect.com/science/article/pii/S2211339819300309>.
- [18] Trevor J. Morgan, Adel Youkhana, Scott Q. Turn, Richard Ogoshi, and Manuel Garcia-Pérez. Review of Biomass Resources and Conversion Technologies for Alternative Jet Fuel Production in Hawai'i and Tropical Regions. *Energy & Fuels*, 33

- (4):2699–2762, 2019. doi: 10.1021/acs.energyfuels.8b03001. URL <https://doi.org/10.1021/acs.energyfuels.8b03001>.
- [19] Amir Izzuddin Adnan, Mei Yin Ong, Saifuddin Nomanbhay, Kit Wayne Chew, and Pau Loke Show. Technologies for Biogas Upgrading to Biomethane: A Review. *Bioengineering (Basel, Switzerland)*, 6, Oct 2019.
- [20] Thomas J. Schwartz, Brandon J. O’Neill, Brent H. Shanks, and James A. Dumesic. Bridging the chemical and biological catalysis gap: Challenges and outlooks for producing sustainable chemicals. *ACS Catalysis*, 4(6):2060–2069, 2014. ISSN 21555435. doi: 10.1021/cs500364y.
- [21] Robert H. Williams and Eric D. Larson. A comparison of direct and indirect liquefaction technologies for making fluid fuels from coal. *Energy for Sustainable Development*, 7(4):103 – 129, 2003. ISSN 0973-0826. doi: [https://doi.org/10.1016/S0973-0826\(08\)60382-8](https://doi.org/10.1016/S0973-0826(08)60382-8). URL <http://www.sciencedirect.com/science/article/pii/S0973082608603828>.
- [22] Yuan Jiang and Debangsu Bhattacharyya. Process modeling of direct coal-biomass to liquids (CBTL) plants with shale gas utilization and CO<sub>2</sub> capture and storage (CCS). *Applied Energy*, 183:1616 – 1632, 2016. ISSN 0306-2619. doi: <https://doi.org/10.1016/j.apenergy.2016.09.098>. URL <http://www.sciencedirect.com/science/article/pii/S030626191631399X>.
- [23] Paul J. Dauenhauer and George W. Huber. Biomass at the shale gas crossroads. *Green Chemistry*, 16:382–383, 2014. doi: 10.1039/C4GC90001D. URL <http://dx.doi.org/10.1039/C4GC90001D>.
- [24] Hu Li, Changhong Wang, Yufei Xu, Zhaozhuo Yu, Shunmugavel Saravanamurugan, Zhilei Wu, Song Yang, and Rafael Luque. Heterogeneous (de)chlorination-enabled control of reactivity in the liquid-phase synthesis of furanic biofuel from cellulosic feedstock. *Green Chemistry*, 22:637–645, 2020. doi: 10.1039/C9GC04092G. URL <http://dx.doi.org/10.1039/C9GC04092G>.
- [25] Haiyan Xia, Siqian Xu, Hong Hu, Jiahuan An, and Changzhi Li. Efficient conversion of 5-hydroxymethylfurfural to high-value chemicals by chemo- and bio-catalysis. *RSC Advances*, 8:30875–30886, 2018. doi: 10.1039/C8RA05308A. URL <http://dx.doi.org/10.1039/C8RA05308A>.
- [26] Pietro Tundo, Liang Nian He, Ekaterina Lokteva, and Claudio Mota. *Chemistry beyond chlorine*. Springer International Publishing, 2016. ISBN 9783319300733. doi: 10.1007/978-3-319-30073-3.
- [27] Satyakrishna Jujjuri, Fernando Cárdenas-Lizana, and Mark A. Keane. Synthesis of group VI carbides and nitrides: Application in catalytic hydrodechlorination. *Journal of Materials Science*, 49(15):5406–5417, 2014. ISSN 15734803. doi: 10.1007/s10853-014-8252-x.

- [28] F. J. Urbano and J. M. Marinas. Hydrogenolysis of organohalogen compounds over palladium supported catalysts. *Journal of Molecular Catalysis A: Chemical*, 173(1-2): 329–345, 2001. ISSN 13811169. doi: 10.1016/S1381-1169(01)00157-1.
- [29] Mark A. Keane. Catalytic Hydrodechlorination : Pollution Abatement Methodology and Serendipitous Carbon Growth. *Energeia*, 12(4):1–6, 2001.
- [30] Binbin Huang, Wentao Qian, Chunxiao Yu, Tao Wang, Guangming Zeng, and Chao Lei. Effective catalytic hydrodechlorination of o-, p- and m-chloronitrobenzene over Ni/Fe nanoparticles: Effects of experimental parameter and molecule structure on the reduction kinetics and mechanisms. *Chemical Engineering Journal*, 306:607–618, 2016. ISSN 13858947. doi: 10.1016/j.cej.2016.07.109. URL <http://dx.doi.org/10.1016/j.cej.2016.07.109>.
- [31] Xuchen Liu, Songtao Wang, Qiguang Dai, and Xingyi Wang. Liquid-phase dechlorination of chlorobenzenes over Pd-doped CoB amorphous catalysts. *Catalysis Communications*, 48:33–37, 2014. ISSN 15667367. doi: 10.1016/j.catcom.2014.01.006. URL <http://dx.doi.org/10.1016/j.catcom.2014.01.006>.
- [32] Santiago Gómez-Quero, Fernando Cárdenas-Lizana, and Mark A. Keane. Liquid phase catalytic hydrodechlorination of 2,4-dichlorophenol over Pd/Al<sub>2</sub>O<sub>3</sub>: Batch vs. continuous operation. *Chemical Engineering Journal*, 166(3):1044–1051, 2011. ISSN 13858947. doi: 10.1016/j.cej.2010.07.032.
- [33] Chen Zhang, Xiaoyan Li, and Hongjian Sun. Palladium-catalyzed hydrodechlorination of ary chlorides and its mechanism. *Inorganica Chimica Acta*, 365(1):133–136, 2011. ISSN 00201693. doi: 10.1016/j.ica.2010.08.031. URL <http://dx.doi.org/10.1016/j.ica.2010.08.031>.
- [34] F. Gioia, E. J. Gallagher, and V. Famiglietti. Effect of hydrogen pressure on detoxification of 1,2,3-trichlorobenzene by catalytic hydrodechlorination with both unsulphided and sulphided NiMo  $\gamma$ -Al<sub>2</sub>O<sub>3</sub>catalyst. *Journal of Hazardous Materials*, 38(2):277–291, 1994. ISSN 03043894. doi: 10.1016/0304-3894(94)90028-0.
- [35] José M. Moreno, Maria A. Aramendía, Alberto Marinas, José M. Marinas, and Francisco J. Urbano. Individual and competitive liquid-phase hydrodechlorination of chlorinated pyridines over alkali-modified Pd/ZrO<sub>2</sub>. *Applied Catalysis B: Environmental*, 76(1-2):34–41, 2007. ISSN 09263373. doi: 10.1016/j.apcatb.2007.05.008.
- [36] Salvador Ordóñez, Fernando V. Díez, and Herminio Sastre. Catalytic Hydrodechlorination of Chlorinated Olefins over a Pd/Al<sub>2</sub>O<sub>3</sub> Catalyst: Kinetics and Inhibition Phenomena. *Industrial & Engineering Chemistry Research*, 41(3): 505–511, 2002. ISSN 0888-5885. doi: 10.1021/ie010679v.
- [37] M. A. Aramendía, V. Boráu, I. M. García, C. Jiménez, A. Marinas, J. M. Marinas, and F. J. Urbano. Liquid-phase hydrodehalogenation of substituted chlorobenzenes

- over palladium supported catalysts. *Applied Catalysis B: Environmental*, 43(1): 71–79, 2003. ISSN 09263373. doi: 10.1016/S0926-3373(02)00279-5.
- [38] Claudia AMORIM, Xiaodong WANG, and Mark A. KEANE. Application of Hydrodechlorination in Environmental Pollution Control: Comparison of the Performance of Supported and Unsupported Pd and Ni Catalysts. *Chinese Journal of Catalysis*, 32(5):746–755, 2011. ISSN 18722067. doi: 10.1016/S1872-2067(10)60228-8. URL <http://linkinghub.elsevier.com/retrieve/pii/S1872206710602288>[http://dx.doi.org/10.1016/S1872-2067\(10\)60228-8](http://dx.doi.org/10.1016/S1872-2067(10)60228-8).
- [39] J. A. Cecilia, A. Infantes-Molina, and E. Rodríguez-Castellón. Hydrodechlorination of polychlorinated molecules using transition metal phosphide catalysts. *Journal of Hazardous Materials*, 296:112–119, 2015. ISSN 18733336. doi: 10.1016/j.jhazmat.2015.04.021. URL <http://dx.doi.org/10.1016/j.jhazmat.2015.04.021>.
- [40] Tadeusz Janiak and Jerzy Błazejowski. Kinetics of 10% Pd/C-catalysed hydrogenolysis of chlorobenzene dissolved in n-heptane by gaseous hydrogen in contact with aqueous NaOH or water. *Applied Catalysis A: General*, 271(1-2): 103–108, 2004. ISSN 0926860X. doi: 10.1016/j.apcata.2004.02.050.
- [41] Satyakrishna Jujjuri and Mark A. Keane. Catalytic hydrodechlorination at low hydrogen partial pressures: Activity and selectivity response. *Chemical Engineering Journal*, 157(1):121–130, 2010. ISSN 13858947. doi: 10.1016/j.cej.2009.11.004.
- [42] Sergei S. Zinovyev, Natalia A. Shinkova, Alvise Perosa, and Pietro Tundo. Liquid phase hydrodechlorination of dieldrin and DDT over Pd/C and Raney-Ni. *Applied Catalysis B: Environmental*, 55(1):39–48, 2005. ISSN 09263373. doi: 10.1016/j.apcatb.2004.06.015.
- [43] Yoshihito Hashimoto, Yoshio Uemichi, and Akimi Ayame. Low-temperature hydrodechlorination mechanism of chlorobenzenes over platinum-supported and palladium-supported alumina catalysts. *Applied Catalysis A: General*, 287(1):89–97, 2005. ISSN 0926860X. doi: 10.1016/j.apcata.2005.03.039.
- [44] J. A. Baeza, L. Calvo, J. J. Rodriguez, E. Carbó-Argibay, J. Rivas, and M. A. Gilarranz. Activity enhancement and selectivity tuneability in aqueous phase hydrodechlorination by use of controlled growth Pd-Rh nanoparticles. *Applied Catalysis B: Environmental*, 168-169:283–292, 2015. ISSN 09263373. doi: 10.1016/j.apcatb.2014.12.042. URL <http://dx.doi.org/10.1016/j.apcatb.2014.12.042>.
- [45] Fabio Murena and Francesco Gioia. Diffusional kinetics in the catalytic hydrodechlorination of chlorobenzene in multiphase aqueous mixtures. *Applied Catalysis A: General*, 271(1-2):145–151, 2004. ISSN 0926860X. doi: 10.1016/j.apcata.2004.02.054.

- [46] Tetsuya Yoneda, Toshio Takido, and Kenji Konuma. Hydrodechlorination of para-substituted chlorobenzenes over a ruthenium/carbon catalyst. *Applied Catalysis B: Environmental*, 84(3-4):667–677, 2008. ISSN 09263373. doi: 10.1016/j.apcatb.2008.05.024.
- [47] Mark A. Keane and Dmitry Yu Murzin. A kinetic treatment of the gas phase hydrodechlorination of chlorobenzene over nickel/silica: Beyond conventional kinetics. *Chemical Engineering Science*, 56(10):3185–3195, 2001. ISSN 00092509. doi: 10.1016/S0009-2509(01)00008-2.
- [48] Eun-jae Shin and Mark A. Keane. Detoxification of dichlorophenols by catalytic hydrodechlorination using a nickel / silica catalyst. *Chemical Engineering Science*, 54(8):1109–1120, April 1999. ISSN 0009-2509. doi: 10.1016/S0009-2509(98)00482-5. URL <https://www.sciencedirect.com/science/article/pii/S0009250998004825>.
- [49] Komandur V.R. Chary, Katar Sri Lakshmi, Pendyala Venkat Ramana Rao, Kamaraju Seetha Rama Rao, and Maria Papadaki. Characterization and catalytic properties of niobia supported nickel catalysts in the hydrodechlorination of 1,2,4-trichlorobenzene. *Journal of Molecular Catalysis A: Chemical*, 223(1-2): 353–361, 2004. ISSN 13811169. doi: 10.1016/j.molcata.2003.09.049.
- [50] Pedro Bodnariuk, Bernard Coq, Gerardo Ferrat, and François Figueras. Carbon-chlorine hydrogenolysis over PdRh and PdSn bimetallic catalysts. *Journal of Catalysis*, 116(2):459–466, 1989. ISSN 10902694. doi: 10.1016/0021-9517(89)90112-7.
- [51] N. Seshu Babu, N. Lingaiah, J. Vinod Kumar, and P. S. Sai Prasad. Studies on alumina supported pd–fe bimetallic catalysts prepared by deposition–precipitation method for hydrodechlorination of chlorobenzene. *Applied Catalysis A: General*, 367(1):70 – 76, 2009. ISSN 0926-860X. doi: <https://doi.org/10.1016/j.apcata.2009.07.031>. URL <http://www.sciencedirect.com/science/article/pii/S0926860X09005432>.
- [52] Valentina I. Simagina and Irina V. Stoyanova. Hydrodechlorination of polychlorinated benzenes in the presence of a bimetallic catalyst in combination with a phase-transfer catalyst. *Mendeleev Communications*, 11(1):38–39, 2001. ISSN 09599436. doi: 10.1070/MC2001v011n01ABEH001302. URL <http://linkinghub.elsevier.com/retrieve/pii/S095994360170702X>.
- [53] N. Seshu Babu, N. Lingaiah, and P. S. Sai Prasad. Characterization and reactivity of Al<sub>2</sub>O<sub>3</sub> supported Pd-Ni bimetallic catalysts for hydrodechlorination of chlorobenzene. *Applied Catalysis B: Environmental*, 111-112:309–316, 2012. ISSN 09263373. doi: 10.1016/j.apcatb.2011.10.013. URL <http://dx.doi.org/10.1016/j.apcatb.2011.10.013>.
- [54] Sujata Mallick, Surjyakanta Rana, and Kulamani Parida. Liquid phase hydrodechlorination of chlorobenzene over bimetallic supported zirconia catalyst.

- Industrial and Engineering Chemistry Research*, 50(22):12439–12448, 2011. ISSN 08885885. doi: 10.1021/ie201142j.
- [55] J. A. Cecilia, A. Infantes-Molina, E. Rodríguez-Castellón, and A. Jiménez-López. Gas phase catalytic hydrodechlorination of chlorobenzene over cobalt phosphide catalysts with different P contents. *Journal of Hazardous Materials*, 260:167–175, 2013. ISSN 03043894. doi: 10.1016/j.jhazmat.2013.05.013. URL <http://dx.doi.org/10.1016/j.jhazmat.2013.05.013>.
- [56] Xuguang Liu, Jixiang Chen, and Jiyan Zhang. Hydrodechlorination of chlorobenzene over silica-supported nickel phosphide catalysts. *Industrial and Engineering Chemistry Research*, 2008. ISSN 08885885. doi: 10.1021/ie7017542.
- [57] Macarena Munoz, Gui Rong Zhang, and Bastian J. M. Etzold. Exploring the role of the catalytic support sorption capacity on the hydrodechlorination kinetics by the use of carbide-derived carbons. *Applied Catalysis B: Environmental*, 203:591–598, 2017. ISSN 09263373. doi: 10.1016/j.apcatb.2016.10.062. URL <http://dx.doi.org/10.1016/j.apcatb.2016.10.062>.
- [58] M. S. Zanuttini, C. D. Lago, C. A. Querini, and M. A. Peralta. Deoxygenation of m-cresol on Pt/ $\gamma$ -Al<sub>2</sub>O<sub>3</sub> catalysts. *Catalysis Today*, 213:9–17, 2013. ISSN 09205861. doi: 10.1016/j.cattod.2013.04.011. URL <http://dx.doi.org/10.1016/j.cattod.2013.04.011>.
- [59] Mika Suvanto, Rätty Jarkko, and Tapani A. Pakkanen. Carbonyl-precursor-based W / Al<sub>2</sub>O<sub>3</sub> and CoW / Al<sub>2</sub>O<sub>3</sub> catalysts : characterization by temperature-programmed methods. *Catalysis Letters*, 62:21–27, 1999. doi: 10.1023/A:1019030518532.
- [60] Aysar T. Jarullah, Iqbal M. Mujtaba, and Alastair S. Wood. Kinetic model development and simulation of simultaneous hydrodenitrogenation and hydrodemetallization of crude oil in trickle bed reactor. *Fuel*, 90(6):2165–2181, 2011. ISSN 00162361. doi: 10.1016/j.fuel.2011.01.025. URL <http://dx.doi.org/10.1016/j.fuel.2011.01.025>.
- [61] Laura Prati and Michele Rossi. Reductive catalytic dehalogenation of light chlorocarbons. *Applied Catalysis B: Environmental*, 23(2-3):135–142, 1999. ISSN 09263373. doi: 10.1016/S0926-3373(99)00071-5.
- [62] Eun Jae Shin and Mark A. Keane. Gas phase catalytic hydrodechlorination of chlorophenols using a supported nickel catalyst. *Applied Catalysis B: Environmental*, 18(3-4):241–250, 1998. ISSN 09263373. doi: 10.1016/S0926-3373(98)00043-5.
- [63] Zhonghao Jin, Chao Yu, Xingyi Wang, Ying Wan, Dao Li, and Guanzhong Lu. Liquid phase hydrodechlorination of chlorophenols at lower temperature on a novel Pd catalyst. *Journal of Hazardous Materials*, 186(2-3):1726–1732, 2011. ISSN 03043894. doi: 10.1016/j.jhazmat.2010.12.058. URL <http://dx.doi.org/10.1016/j.jhazmat.2010.12.058>.

- [64] Ling Cheng, Zhonghao Jin, and Xingyi Wang. Hydrodechlorination of chlorophenols at low temperature over highly defective Pd catalyst. *Catalysis Communications*, 41: 60–64, 2013. ISSN 15667367. doi: 10.1016/j.catcom.2013.06.014. URL <http://dx.doi.org/10.1016/j.catcom.2013.06.014>.
- [65] M. A. Aramendía, V. Boráu, I. M. García, C. Jiménez, J. M. Marinas, and F. J. Urbano. Influence of the reaction conditions and catalytic properties on the liquid-phase hydrodebromination of bromobenzene over palladium supported catalysts: Activity and deactivation. *Applied Catalysis B: Environmental*, 20(2): 101–110, 1999. ISSN 09263373. doi: 10.1016/S0926-3373(98)00097-6.
- [66] Dong Ju Moon, Moon Jo Chung, Kun You Park, and Suk In Hong. Deactivation of pd catalysts in the hydrodechlorination of chloropentafluoroethane. *Applied Catalysis A: General*, 168(1):159 – 170, 1998. ISSN 0926-860X. doi: [https://doi.org/10.1016/S0926-860X\(97\)00352-9](https://doi.org/10.1016/S0926-860X(97)00352-9). URL <http://www.sciencedirect.com/science/article/pii/S0926860X97003529>.
- [67] Sina Behtash, Jianmin Lu, Christopher T. Williams, John R. Monnier, and Andreas Heyden. Effect of palladium surface structure on the hydrodeoxygenation of propanoic acid: Identification of active sites. *Journal of Physical Chemistry C*, 119(4):1928–1942, jan 2015. ISSN 19327455. doi: 10.1021/jp511618u. URL <http://dx.doi.org/10.1021/jp511618u>.
- [68] Xuanxuan Ma, Sujing Liu, Ying Liu, Guodong Gu, and Chuanhai Xia. Comparative study on catalytic hydrodehalogenation of halogenated aromatic compounds over Pd/C and Raney Ni catalysts. *Scientific Reports*, 6(April):1–11, 2016. ISSN 20452322. doi: 10.1038/srep25068. URL <http://dx.doi.org/10.1038/srep25068>.
- [69] Nan Chen, Robert M. Rioux, Luis A. M. M. Barbosa, and Fabio H. Ribeiro. Kinetic and theoretical study of the hydrodechlorination of CH<sub>4</sub>-xCl<sub>x</sub> (x = 1-4) compounds on palladium. *Langmuir*, 26(21):16615–16624, 2010. ISSN 07437463. doi: 10.1021/la1020753.
- [70] Kimberly N. Heck, Michael O. Nutt, Pedro Alvarez, and Michael S. Wong. Deactivation resistance of Pd/Au nanoparticle catalysts for water-phase hydrodechlorination. *Journal of Catalysis*, 267(2):97 – 104, 2009. ISSN 0021-9517. doi: <https://doi.org/10.1016/j.jcat.2009.07.015>. URL <http://www.sciencedirect.com/science/article/pii/S0021951709002504>.
- [71] Michael O. Nutt, Kimberly N. Heck, Pedro Alvarez, and Michael S. Wong. Improved Pd-on-Au bimetallic nanoparticle catalysts for aqueous-phase trichloroethene hydrodechlorination. *Applied Catalysis B: Environmental*, 69(1):115 – 125, 2006. ISSN 0926-3373. doi: <https://doi.org/10.1016/j.apcatb.2006.06.005>. URL <http://www.sciencedirect.com/science/article/pii/S0926337306003018>.
- [72] S. V. Klovov, E. S. Lokteva, E. V. Golubina, P. A. Chernavskii, K. I. Maslakov, T. B. Egorova, S. A. Chernyak, A. S. Minin, and A. S. Konev. Cobalt–carbon

- nanocomposite catalysts of gas-phase hydrodechlorination of chlorobenzene. *Applied Surface Science*, 463(August 2018):395–402, 2019. ISSN 01694332. doi: 10.1016/j.apsusc.2018.08.105. URL <https://doi.org/10.1016/j.apsusc.2018.08.105>.
- [73] Bijan F. Hagh and David T. Allen. Catalytic Hydroprocessing of Chlorinated Benzenes. *Chemical Engineering Science*, 45(8):2695–2701, 1990. doi: 10.1016/0009-2509(90)80160-G.
- [74] George Tavoularis and Mark A. Keane. The gas phase hydrodechlorination of chlorobenzene over nickel/silica. *Journal of Chemical Technology and Biotechnology*, 74(1):60–70, 1999. ISSN 02682575. doi: 10.1002/(SICI)1097-4660(199901)74:1<60::AID-JCTB992>3.0.CO;2-K.
- [75] Claudia Amorim and Mark A. Keane. Catalytic hydrodechlorination of chloroaromatic gas streams promoted by Pd and Ni: The role of hydrogen spillover. *Journal of Hazardous Materials*, 211-212:208–217, 2012. ISSN 03043894. doi: 10.1016/j.jhazmat.2011.08.025. URL <http://dx.doi.org/10.1016/j.jhazmat.2011.08.025>.
- [76] Jixiang Chen, Donghui Ci, Qing Yang, and Kelun Li. Deactivation of Ni<sub>2</sub>P/SiO<sub>2</sub> catalyst in hydrodechlorination of chlorobenzene. *Applied Surface Science*, 320: 643–652, 2014. ISSN 01694332. doi: 10.1016/j.apsusc.2014.09.127. URL <http://www.sciencedirect.com/science/article/pii/S0169433214021187>.
- [77] S. T. Oyama, X. Wang, Y.-K. Lee, K. Bando, and F. G. Requejo. Effect of Phosphorus Content in Nickel Phosphide Catalysts Studied by XAFS and Other Techniques. *Journal of Catalysis*, 210(1):207 – 217, 2002. ISSN 0021-9517. doi: <https://doi.org/10.1006/jcat.2002.3681>. URL <http://www.sciencedirect.com/science/article/pii/S002195170293681X>.
- [78] Milagros Velásquez, Alba B. Vidal, Anelisse Bastardo, Raquel Del Toro, Jesús Rodríguez, Rafael Añez, Paulino Betancourt, Joaquín Brito, Yosslen Aray, and David S. Coll. DFT study of the sulfidation pretreatment of molybdenum carbides in the hydrodechlorination reaction of chlorobenzene. *Journal of Computational Methods in Sciences and Engineering*, 14(1-3):169–177, 2014. ISSN 14727978. doi: 10.3233/JCM-140494.
- [79] Xuandung Le, Yansheng Liu, Xinlin Li, Wei Zhang, and Jiantai Ma. Catalysis of the hydro-dechlorination of 4-chlorophenol and the reduction of 4-nitrophenol by Pd/Fe<sub>3</sub>O<sub>4</sub>@SiO<sub>2</sub>@m-SiO<sub>2</sub>. *New Journal of Chemistry*, 39(8):6474–6481, 2015. ISSN 1144-0546. doi: 10.1039/c5nj01180a.
- [80] Tadeusz Janiak and Jerzy Blaejowski. Hydrogenolysis of chlorobenzene, dichlorobenzenes and chlorotoluenes by in situ generated and gaseous hydrogen in alkaline media and the presence of Pd/C catalyst. *Chemosphere*, 48(10):1097–1102, 2002. ISSN 00456535. doi: 10.1016/S0045-6535(02)00155-8.

- [81] Wenhai Wu and Jie Xu. Liquid-phase hydrodechlorination of chlorinated benzenes over active carbon supported nickel catalysts under mild conditions. *Catalysis Communications*, 5(10):591–595, 2004. ISSN 15667367. doi: 10.1016/j.catcom.2004.07.013.
- [82] Roland Barret. 2 - Importance and Evaluation of the pKa. In Roland Barret, editor, *Therapeutical Chemistry*, pages 21 – 51. Elsevier, 2018. ISBN 978-1-78548-288-5. doi: <https://doi.org/10.1016/B978-1-78548-288-5.50002-0>. URL <http://www.sciencedirect.com/science/article/pii/B9781785482885500020>.
- [83] Zhengping Dong, Xuanduong Le, Chunxu Dong, Wei Zhang, Xinlin Li, and Jiantai Ma. Ni@Pd core-shell nanoparticles modified fibrous silica nanospheres as highly efficient and recoverable catalyst for reduction of 4-nitrophenol and hydrodechlorination of 4-chlorophenol. *Applied Catalysis B: Environmental*, 162: 372–380, 2015. ISSN 09263373. doi: 10.1016/j.apcatb.2014.07.009. URL <http://dx.doi.org/10.1016/j.apcatb.2014.07.009>.
- [84] Akiko Ido, Shinji Ishihara, Akira Kume, Tsuyoshi Nakanishi, Yasunari Monguchi, Hironao Sajiki, and Hisamitsu Nagase. Practical method for PCB degradation using Pd/C-H<sub>2</sub>-Mg system. *Chemosphere*, 90(1):57–64, 2013. ISSN 00456535. doi: 10.1016/j.chemosphere.2012.06.074. URL <http://dx.doi.org/10.1016/j.chemosphere.2012.06.074>.
- [85] Zhicheng Jiang and Changwei Hu. Selective extraction and conversion of lignin in actual biomass to monophenols : A review. *Journal of Energy Chemistry*, 25(6): 947–956, 2016. ISSN 2095-4956. doi: 10.1016/j.jechem.2016.10.008. URL <http://dx.doi.org/10.1016/j.jechem.2016.10.008>.
- [86] Andrew Ng Kay Lup, Faisal Abnisa, Wan Mohd Ashri Wan Daud, and Mohamed Kheireddine Aroua. A review on reactivity and stability of heterogeneous metal catalysts for deoxygenation of bio-oil model compounds. *Journal of Industrial and Engineering Chemistry*, 56:1 – 34, 2017. ISSN 1226-086X. doi: <https://doi.org/10.1016/j.jiec.2017.06.049>. URL <http://www.sciencedirect.com/science/article/pii/S1226086X17303386>.
- [87] Edward Furimsky. Selection of catalysts and reactors for hydroprocessing. *Applied Catalysis A: General*, 171(2):177 – 206, 1998. ISSN 0926-860X. doi: [https://doi.org/10.1016/S0926-860X\(98\)00086-6](https://doi.org/10.1016/S0926-860X(98)00086-6). URL <http://www.sciencedirect.com/science/article/pii/S0926860X98000866>.
- [88] A. V. Bridgwater. Renewable fuels and chemicals by thermal processing of biomass. *Chemical Engineering Journal*, 91(2):87 – 102, 2003. ISSN 1385-8947. doi: [https://doi.org/10.1016/S1385-8947\(02\)00142-0](https://doi.org/10.1016/S1385-8947(02)00142-0). URL <http://www.sciencedirect.com/science/article/pii/S1385894702001420>. Chemreactor - 15 S.I.

- [89] A. V. Bridgwater and M. L. Cottam. Opportunities for biomass pyrolysis liquids production and upgrading. *Energy & Fuels*, 6(2):113–120, 1992. doi: 10.1021/ef00032a001. URL <https://doi.org/10.1021/ef00032a001>.
- [90] Naveenji Arun, Rajesh V. Sharma, and Ajay K. Dalai. Green diesel synthesis by hydrodeoxygenation of bio-based feedstocks: Strategies for catalyst design and development. *Renewable and Sustainable Energy Reviews*, 48:240–255, 2015. ISSN 18790690. doi: 10.1016/j.rser.2015.03.074. URL <http://dx.doi.org/10.1016/j.rser.2015.03.074>.
- [91] Majid Saidi, Fereshteh Samimi, Dornaz Karimipourfard, Tarit Nimmanwudipong, Bruce C. Gates, and Mohammad Reza Rahimpour. Upgrading of lignin-derived bio-oils by catalytic hydrodeoxygenation. *Energy and Environmental Science*, 7(1): 103–129, 2014. ISSN 17545706. doi: 10.1039/c3ee43081b.
- [92] Edward Furimsky. Catalytic hydrodeoxygenation. *Applied Catalysis A: General*, 199(2):147–190, 2000. ISSN 0926860X. doi: 10.1016/S0926-860X(99)00555-4. URL <http://www.sciencedirect.com/science/article/pii/S0926860X99005554>.
- [93] Peter J. Deuss and Katalin Barta. From models to lignin: Transition metal catalysis for selective bond cleavage reactions. *Coordination Chemistry Reviews*, 306(January 2015):510–532, 2016. ISSN 00108545. doi: 10.1016/j.ccr.2015.02.004. URL <http://dx.doi.org/10.1016/j.ccr.2015.02.004>. A Volume in Honor of Peter Ford.
- [94] Qi Song, Feng Wang, Jiaying Cai, Yehong Wang, Junjie Zhang, Weiqiang Yu, and Jie Xu. Lignin depolymerization (LDP) in alcohol over nickel-based catalysts via a fragmentation-hydrogenolysis process. *Energy and Environmental Science*, 6(3): 994–1007, 2013. ISSN 17545692. doi: 10.1039/c2ee23741e.
- [95] Priscilla M. De Souza, Lei Nie, Luiz E. P. Borges, Fabio B. Noronha, and Daniel E. Resasco. Role of oxophilic supports in the selective hydrodeoxygenation of m-cresol on Pd catalysts. *Catalysis Letters*, 144(12):2005–2011, 2014. ISSN 1572879X. doi: 10.1007/s10562-014-1337-y.
- [96] Yongxing Yang, Guangqiang Lv, Liangliang Deng, Boqiong Lu, Jinlong Li, Jiaojiao Zhang, Junyan Shi, and Sujun Du. Renewable aromatic production through hydrodeoxygenation of model bio-oil over mesoporous Ni/SBA-15 and Co/SBA-15. *Microporous and Mesoporous Materials*, 250:47–54, 2017. ISSN 13871811. doi: 10.1016/j.micromeso.2017.05.022. URL <http://dx.doi.org/10.1016/j.micromeso.2017.05.022>.
- [97] Y. Romero, F. Richard, and S. Brunet. Hydrodeoxygenation of 2-ethylphenol as a model compound of bio-crude over sulfided Mo-based catalysts: Promoting effect and reaction mechanism. *Applied Catalysis B: Environmental*, 98(3-4):213–223, 2010. ISSN 09263373. doi: 10.1016/j.apcatb.2010.05.031. URL <http://dx.doi.org/10.1016/j.apcatb.2010.05.031>.

- [98] Sudipta De, Basudeb Saha, and Rafael Luque. Hydrodeoxygenation processes: Advances on catalytic transformations of biomass-derived platform chemicals into hydrocarbon fuels. *Bioresource Technology*, 178:108–118, 2015. ISSN 18732976. doi: 10.1016/j.biortech.2014.09.065. URL <http://dx.doi.org/10.1016/j.biortech.2014.09.065>.
- [99] Cong Wang, Alexander V. Mironenko, Abhishek Raizada, Tianqi Chen, Xinyu Mao, Ashwin Padmanabhan, Dionisios G. Vlachos, Raymond J. Gorte, and John M. Vohs. Mechanistic Study of the Direct Hydrodeoxygenation of m -Cresol over WO<sub>x</sub>-Decorated Pt/C Catalysts. *ACS Catalysis*, 8(9):7749–7759, 2018. ISSN 21555435. doi: 10.1021/acscatal.8b01746. URL <https://doi.org/10.1021/acscatal.8b01746>.
- [100] Liang Wang, Jian Zhang, Guoxiong Wang, Wei Zhang, Chengtao Wang, Chaoqun Bian, and Feng Shou Xiao. Selective hydrogenolysis of carbon-oxygen bonds with formic acid over a Au-Pt alloy catalyst. *Chemical Communications*, 53(18): 2681–2684, 2017. ISSN 1364548X. doi: 10.1039/C6CC09599B. URL <http://dx.doi.org/10.1039/C6CC09599B>.
- [101] C. Sepúlveda, R. García, L.R. Radovic, W.J. DeSisto, K. Leiva, J.L. García Fierro, I.T. Ghampson, and N. Escalona. Hydrodeoxygenation of 2-methoxyphenol over Mo<sub>2</sub>N catalysts supported on activated carbons. *Catalysis Today*, 172(1):232–239, 2011. ISSN 09205861. doi: 10.1016/j.cattod.2011.02.061.
- [102] Huihuang Fang, Junmou Du, Chenchen Tian, Jianwei Zheng, Xinpeng Duan, Linmin Ye, and Youzhu Yuan. Regioselective hydrogenolysis of aryl ether C-O bonds by tungsten carbides with controlled phase compositions. *Chemical Communications*, 53(74):10295–10298, 2017. ISSN 1364548X. doi: 10.1039/c7cc05487d.
- [103] Mingming Li, Jiang Deng, Yikai Lan, and Yong Wang. Efficient Catalytic Hydrodeoxygenation of Aromatic Carbonyls over a Nitrogen-Doped Hierarchical Porous Carbon Supported Nickel Catalyst. *ChemistrySelect*, 2(27):8486–8492, 2017. ISSN 23656549. doi: 10.1002/slct.201701950. URL <https://chemistry-europe.onlinelibrary.wiley.com/doi/abs/10.1002/slct.201701950>.
- [104] Manish Shetty, Daniela Zanchet, William H. Green, and Yuriy Román-Leshkov. Cooperative Co(0)/Co(II) Sites Stabilized by a Perovskite Matrix Enable Selective C-O and C-C bond Hydrogenolysis of Oxygenated Arenes. *ChemSusChem*, 12(0): 1–37, 2019. ISSN 18645631. doi: 10.1002/cssc.201900664. URL <http://doi.wiley.com/10.1002/cssc.201900664>.
- [105] Keiichi Tomishige, Yoshinao Nakagawa, and Masazumi Tamura. Selective hydrogenolysis and hydrogenation using metal catalysts directly modified with metal oxide species. *Green Chemistry*, 19(13):2876–2924, 2017. ISSN 14639270. doi: 10.1039/c7gc00620a.
- [106] M.J Mendes, O.A.A Santos, E Jordão, and A.M Silva. Hydrogenation of oleic acid over ruthenium catalysts. *Applied Catalysis A: General*, 217(1):253 – 262, 2001. ISSN

- 0926-860X. doi: [https://doi.org/10.1016/S0926-860X\(01\)00613-5](https://doi.org/10.1016/S0926-860X(01)00613-5). URL <http://www.sciencedirect.com/science/article/pii/S0926860X01006135>.
- [107] Cody Newman, Xiaobo Zhou, Ben Goundie, I. Tyrone Ghampson, Rachel A. Pollock, Zachery Ross, M. Clayton Wheeler, Robert W. Meulenberg, Rachel N. Austin, and Brian G. Frederick. Effects of support identity and metal dispersion in supported ruthenium hydrodeoxygenation catalysts. *Applied Catalysis A: General*, 477:64–74, 2014. ISSN 0926860X. doi: 10.1016/j.apcata.2014.02.030. URL <http://dx.doi.org/10.1016/j.apcata.2014.02.030>.
- [108] Taiwo Omotoso, Sunya Boonyasuwat, and Steven P. Crossley. Understanding the role of TiO<sub>2</sub> crystal structure on the enhanced activity and stability of Ru/TiO<sub>2</sub> catalysts for the conversion of lignin-derived oxygenates. *Green Chemistry*, 16:645–652, 2014. doi: 10.1039/C3GC41377B. URL <http://dx.doi.org/10.1039/C3GC41377B>.
- [109] Taiwo O. Omotoso, Byeongjin Baek, Lars C. Grabow, and Steven P. Crossley. Experimental and First-Principles Evidence for Interfacial Activity of Ru/TiO<sub>2</sub> for the Direct Conversion of m-Cresol to Toluene. *ChemCatChem*, 9(14):2612, 2017. ISSN 18673899. doi: 10.1002/cctc.201701112.
- [110] Ryan C. Nelson, Byeongjin Baek, Pamela Ruiz, Ben Goundie, Ashley Brooks, M. Clayton Wheeler, Brian G. Frederick, Lars C. Grabow, and Rachel Narehood Austin. Experimental and Theoretical Insights into the Hydrogen-Efficient Direct Hydrodeoxygenation Mechanism of Phenol over Ru/TiO<sub>2</sub>. *ACS Catalysis*, 5(11): 6509–6523, 2015. ISSN 21555435. doi: 10.1021/acscatal.5b01554. URL <https://doi.org/10.1021/acscatal.5b01554>.
- [111] Andrew Ng Kay Lup, Faisal Abnisa, Wan Mohd Ashri Wan Daud, and Mohamed Kheireddine Aroua. Atmospheric hydrodeoxygenation of phenol as pyrolytic-oil model compound for hydrocarbon production using Ag/TiO<sub>2</sub> catalyst. *Asia-Pacific Journal of Chemical Engineering*, 14(July 2018):e2293, 2019. ISSN 19322135. doi: 10.1002/apj.2293. URL <http://doi.wiley.com/10.1002/apj.2293>. e2293 APJ-18-0338.R2.
- [112] Carla Vilela, Andreia F. Sousa, Ana C. Fonseca, Arménio C. Serra, Jorge F. J. Coelho, Carmen S. R. Freire, and Armando J. D. Silvestre. The quest for sustainable polyesters – insights into the future. *Polymymmer Chemistry*, 5:3119–3141, 2014. doi: 10.1039/C3PY01213A. URL <http://dx.doi.org/10.1039/C3PY01213A>.
- [113] Thomas R. Boussie, Eric L. Dias, Zachary M. Fresco, and Vincent J. Murphy. REDUCTION OF ADIPIC ACID AND DERIVATIVES FROM CARBOHYDRATE-CONTAINING MATERIALS, December 2010. URL <https://patentimages.storage.googleapis.com/be/8b/31/f158f025618aa6/US20100317822A1.pdf>.
- [114] Matthew J. Gilkey, Alexander V. Mironenko, Dionisios G. Vlachos, and Bingjun Xu. Adipic Acid Production via Metal-Free Selective Hydrogenolysis of Biomass-Derived

- Tetrahydrofuran-2,5-Dicarboxylic Acid. *ACS Catalysis*, 7(10):6619–6634, 2017. doi: 10.1021/acscatal.7b01753. URL <https://doi.org/10.1021/acscatal.7b01753>.
- [115] Matthew J. Gilkey, Rachana Balakumar, Dionisios G. Vlachos, and Bingjun Xu. Adipic acid production catalyzed by a combination of a solid acid and an iodide salt from biomass-derived tetrahydrofuran-2,5-dicarboxylic acid. *Catalysis Science & Technology*, 8:2661–2671, 2018. doi: 10.1039/C8CY00379C. URL <http://dx.doi.org/10.1039/C8CY00379C>.
- [116] Takehiro Asano, Yoshinao Nakagawa, Masazumi Tamura, and Keiichi Tomishige. Structure and Mechanism of Titania-Supported Platinum-Molybdenum Catalyst for Hydrodeoxygenation of 2-Furancarboxylic Acid to Valeric Acid. *ACS Sustainable Chemistry and Engineering*, 7(10):9601–9612, 2019. ISSN 21680485. doi: 10.1021/acssuschemeng.9b01104.
- [117] Takehiro Asano, Masazumi Tamura, Yoshinao Nakagawa, and Keiichi Tomishige. Selective Hydrodeoxygenation of 2-Furancarboxylic Acid to Valeric Acid over Molybdenum-Oxide-Modified Platinum Catalyst. *ACS Sustainable Chemistry & Engineering*, 4(12):6253–6257, dec 2016. ISSN 2168-0485. doi: 10.1021/acssuschemeng.6b01640. URL <https://pubs.acs.org/doi/10.1021/acssuschemeng.6b01640>.
- [118] Takehiro Asano, Hiroshi Takagi, Yoshinao Nakagawa, Masazumi Tamura, and Keiichi Tomishige. Selective hydrogenolysis of 2-furancarboxylic acid to 5-hydroxyvaleric acid derivatives over supported platinum catalysts. *Green Chemistry*, 21(22): 6133–6145, 2019. ISSN 14639270. doi: 10.1039/c9gc03315g.
- [119] Xuefeng Wei, Xiaoyang Wan, Zhirong Sun, Juan Miao, Ruichang Zhang, and Qingshan Jason Niu. Understanding Electrocatalytic Hydrodechlorination of Chlorophenols on Palladium-Modified Cathode in Aqueous Solution. *ACS Omega*, 3(5):5876–5886, 2018. ISSN 24701343. doi: 10.1021/acsomega.8b00624.
- [120] N. Seshu Babu, N. Lingaiah, Rajesh Gopinath, P. Siva Sankar Reddy, and P. S. Sai Prasad. Characterization and reactivity of alumina-supported Pd catalysts for the room-temperature hydrodechlorination of chlorobenzene. *Journal of Physical Chemistry C*, 111(17):6447–6453, 2007. ISSN 19327447. doi: 10.1021/jp065866r.
- [121] Lang Xu, Xiaoqian Yao, Ahmad Khan, and Manos Mavrikakis. Chloroform Hydrodechlorination over Palladium-Gold Catalysts: A First-Principles DFT Study. *ChemCatChem*, 8(9):1739–1746, 2016. ISSN 18673899. doi: 10.1002/cctc.201600144.
- [122] X. Li, Z. Tang, and X. Zhang. DFT STUDY OF THE C – Cl BOND DISSOCIATION ENTHALPIES AND ELECTRONIC STRUCTURE OF SUBSTITUTED CHLOROBENZENE COMPOUNDS Quantum chemical calculations were used to estimate the bond dissociation energies ( BDEs ) for 13 substituted chlorobenzene compounds . T. *Journal of Structural Chemistry*, 50(1): 40–46, March 2009.

- [123] Tadeusz Janiak and Janina Okal. Effectiveness and stability of commercial Pd/C catalysts in the hydrodechlorination of meta-substituted chlorobenzenes. *Applied Catalysis B: Environmental*, 92(3-4):384–392, 2009. ISSN 09263373. doi: 10.1016/j.apcatb.2009.08.018.
- [124] Ines Del C Figueroa and Milagros S Simmons. Structure-activity relationships of chlorobenzenes using DNA measurement as a toxicity parameter in algae. *Environmental Toxicology and Chemistry*, 10(3):323–329, nov 2018. ISSN 0730-7268. doi: 10.1002/etc.5620100304. URL <https://doi.org/10.1002/etc.5620100304>.
- [125] Claudia Amorim, Guang Yuan, Patricia M. Patterson, and Mark A. Keane. Catalytic hydrodechlorination over Pd supported on amorphous and structured carbon. *Journal of Catalysis*, 234(2):268–281, 2005. ISSN 00219517. doi: 10.1016/j.jcat.2005.06.019.
- [126] A. José Luis Benítez and Gloria Del Angel. TOTAL HYDRODECHLORINATION OF INDUSTRIAL TRANSFORMER OIL ON METAL-SUPPORTED CATALYSTS. *Chemical Engineering Communications*, 196(10):1217–1226, May 2009. doi: 10.1080/00986440902831888. URL <https://doi.org/10.1080/00986440902831888>.
- [127] Wenhei Wu, Jie Xu, and Ryuichiro Ohnishi. Complete hydrodechlorination of chlorobenzene and its derivatives over supported nickel catalysts under liquid phase conditions. *Applied Catalysis B: Environmental*, 60(1):129 – 137, 2005. ISSN 0926-3373. doi: <https://doi.org/10.1016/j.apcatb.2005.03.003>. URL <http://www.sciencedirect.com/science/article/pii/S092633730500130X>.
- [128] N. Chen, R.M. Rioux, and F.H. Ribeiro. Hydrodechlorination reactions of 2-chloro-1,1,1,2-tetrafluoroethane and chloroethane in H<sub>2</sub> and D<sub>2</sub> on Pd catalysts. *Applied Catalysis A: General*, 271(1-2):85–94, sep 2004. ISSN 0926860X. doi: 10.1016/j.apcata.2004.02.049. URL <https://linkinghub.elsevier.com/retrieve/pii/S0926860X04004922>.
- [129] Mark A. Keane, Colin Park, and Claudia Menini. Structure sensitivity in the hydrodechlorination of chlorobenzene over supported nickel. *Catalysis Letters*, 88(1-2):89–94, 2003. ISSN 1011372X. doi: 10.1023/A:1023599203073.
- [130] Nan Chen, Robert M. Rioux, and Fabio H. Ribeiro. Investigation of reaction steps for the hydrodechlorination of chlorine-containing organic compounds on Pd catalysts. *Journal of Catalysis*, 211(1):192–197, 2002. ISSN 00219517. doi: 10.1016/S0021-9517(02)93717-6.
- [131] Rajesh Gopinath, N. Lingaiah, B. Sreedhar, I. Suryanarayana, P. S. Sai Prasad, and Akira Obuchi. Highly stable Pd/CeO<sub>2</sub> catalyst for hydrodechlorination of chlorobenzene. *Applied Catalysis B: Environmental*, 46(3):587–594, 2003. ISSN 09263373. doi: 10.1016/S0926-3373(03)00321-7.
- [132] Mark A. Keane. Advances in greener separation processes ? case study: recovery of chlorinated aromatic compounds. *Green Chemistry*, 5(3):309, 2003. ISSN 1463-9262. doi: 10.1039/b300062c. URL <http://xlink.rsc.org/?DOI=b300062c>.

- [133] C. D. Thompson, R. M. Rioux, N. Chen, and F. H. Ribeiro. Turnover Rate, Reaction Order, and Elementary Steps for the Hydrodechlorination of Chlorofluorocarbon Compounds on Palladium Catalysts. *Journal of Physical Chemistry B*, 104(14): 3067–3077, 2000. ISSN 10895647. doi: 10.1021/jp992888n.
- [134] R. M. Rioux, C. D. Thompson, N. Chen, and F. H. Ribeiro. Hydrodechlorination of chlorofluorocarbons CF<sub>3</sub> – CFC12 and CF<sub>3</sub> – CCl<sub>3</sub> over Pd / carbon and Pd black catalysts. *Catalysis Today*, 62:269–278, November 2000.
- [135] A. H. Weiss and K. A. Krieger. Hydrodechlorination kinetics and reaction mechanisms. *Journal of Catalysis*, 6(2):167 – 185, 1966. ISSN 0021-9517. doi: [https://doi.org/10.1016/0021-9517\(66\)90047-9](https://doi.org/10.1016/0021-9517(66)90047-9). URL <http://www.sciencedirect.com/science/article/pii/0021951766900479>.
- [136] B. Coq, J. Pardillos, and F. Figueras. Isomerization of o-dichlorobenzene over zeolites. Effect of the zeolite structure. *Applied Catalysis*, 62(1):281–294, 1990. ISSN 01669834. doi: 10.1016/S0166-9834(00)82252-6.
- [137] J. H. Sinfelt. Catalytic hydrogenolysis on metals. *Catalysis Letters*, 9(3-4):159–171, 1991. doi: 10.1007/BF00773174. URL <https://doi.org/10.1007/BF00773174>.
- [138] Patrizia Canton, Giuliano Fagherazzi, Marino Battagliarin, Federica Menegazzo, Francesco Pinna, and Nicola Pernicone. Pd/CO Average Chemisorption Stoichiometry in Highly Dispersed Supported Pd/ $\gamma$ -Al<sub>2</sub>O<sub>3</sub> Catalysts. *Langmuir*, 18(17):6530–6535, aug 2002. ISSN 0743-7463. doi: 10.1021/la015650a. URL <https://doi.org/10.1021/la015650a>.
- [139] Cheryl L. M. Joyal and John B. Butt. Chemisorption and disproportionation of carbon monoxide on palladium/silica catalysts of differing percentage metal exposed. *J. Chem. Soc., Faraday Trans. 1*, 83:2757–2764, 1987. doi: 10.1039/F19878302757. URL <http://dx.doi.org/10.1039/F19878302757>.
- [140] K S W Singh, J Rouquerol, G Bergeret, P Gallezot, M Vaarkamp, D C Koningsberger, A K Datye, J W Niemantsverdriet, T Butz, G Engelhardt, G Mestl, H Knözinger, and H Jobic. Characterization of Solid Catalysts: Sections 3.1.1 – 3.1.3, jul 1997. URL <https://doi.org/10.1002/9783527619474.ch3a>.
- [141] N. A. Gaidai, R. V. Kazantsev, N. V. Nekrasov, Yu. M. Shulga, and I. N. Ivleva. KINETICS OF TOLUENE HYDROGENATION OVER PLATINUM-TITANIA CATALYSTS IN CONDITIONS OF STRONG METAL-SUPPORT INTERACTION. *Reaction Kinetics & Catalysis Letters*, 75(1):55–61, January 2002. ISSN 0133-1736.
- [142] Nikolaos E. Tsakoumis, Andrew P. E. York, De Chen, and Magnus Rønning. Catalyst characterisation techniques and reaction cells operating at realistic conditions; towards acquisition of kinetically relevant information. *Catal. Sci. Technol.*, 5(11):4859–4883, 2015. ISSN 2044-4753. doi: 10.1039/C5CY00269A. URL <http://xlink.rsc.org/?DOI=C5CY00269A>.

- [143] Nan Chen. *Kinetics of the hydrodechlorination reaction of chlorinated compounds on palladium catalysts*. PhD thesis, Worcester Polytechnic Institute, 2003. URL <https://www.wpi.edu/Pubs/ETD/Available/etd-0823103-161859/unrestricted/chen.pdf>.
- [144] G. C. Bond, J. J. Philipson, P. B. Wells, and J. M. Winterbottom. Hydrogenation of olefins. Part 3.—Reaction of ethylene and of propylene with deuterium over alumina-supported palladium and rhodium. *Transactions of Faraday Society*, 62: 443–454, 1966. doi: 10.1039/TF9666200443. URL <http://dx.doi.org/10.1039/TF9666200443>.
- [145] J. F. M. Aarts and N. R. M. Sassen. Vibrational spectra of C<sub>6</sub>H<sub>6</sub> and C<sub>6</sub>H<sub>5</sub>D adsorbed on Pd(111): A comparative study of electron energy loss spectra. *Surface Science*, 214:257–275, 1989.
- [146] Deborah E. Hunka, Daniel C. Herman, Liliana I. Lopez, Kara D. Lormand, and Donald P. Land. The adsorption and reaction of HCl on Pd(111). *Journal of Physical Chemistry B*, 105(21):4973–4978, 2002. ISSN 10895647. doi: 10.1021/jp010790e.
- [147] Abdulrahman S. Almithn and David D. Hibbitts. Impact of Metal and Heteroatom Identities in the Hydrogenolysis of C–X Bonds (X = C, N, O, S, and Cl). *ACS Catalysis*, 10(9):5086–5100, 2020. doi: 10.1021/acscatal.0c00481. URL <https://doi.org/10.1021/acscatal.0c00481>.
- [148] M. I. Temkin. The Kinetics of Some Industrial Heterogeneous Catalytic Reactions. *Advances in Catalysis*, 28:173 – 291, 1979. ISSN 0360-0564. doi: [https://doi.org/10.1016/S0360-0564\(08\)60135-2](https://doi.org/10.1016/S0360-0564(08)60135-2). URL <http://www.sciencedirect.com/science/article/pii/S0360056408601352>.
- [149] Sergey M. Kozlov, Hristiyan A. Aleksandrov, and Konstantin M. Neyman. Adsorbed and subsurface absorbed hydrogen atoms on bare and MgO(100)-supported Pd and Pt nanoparticles. *Journal of Physical Chemistry C*, 118(28):15242–15250, 2014. ISSN 19327455. doi: 10.1021/jp502575a.
- [150] M. A. Natal-Santiago, S. G. Podkolzin, R. D. Cortright, and J. A. Dumesic. Microcalorimetric studies of interactions of ethene, isobutene, and isobutane with silica-supported Pd, Pt, and PtSn. *Catalysis Letters*, 45(1-2):155–163, 1997. ISSN 1011372X.
- [151] Charles T. Campbell and Jason R. V. Sellers. The entropies of adsorbed molecules. *Journal of the American Chemical Society*, 134(43):18109–18115, 2012. ISSN 15205126. doi: 10.1021/ja3080117.
- [152] S. C. Fung and J. H. Sinfelt. Hydrogenolysis of Methyl Chloride on Metals. *Journal of Catalysis*, 223:220–223, 1987.
- [153] Nianliu Zhang, Paul Blowers, and James Farrell. Ab initio study of carbon-chlorine bond cleavage in carbon tetrachloride. *Environmental Science and Technology*, 39(2): 612–617, 2005. ISSN 0013936X. doi: 10.1021/es049480a.

- [154] U. Iriarte and I. Sierra. Kinetic and thermodynamic study of chlorobenzene adsorption from aqueous solutions onto granular activated carbon. *Latin American applied research*, 44(2):141–147, 2014. ISSN 0327-0793.
- [155] Michel Boudart, Dj&#xe9, and G. ga Mariadassou. *Kinetics of Heterogeneous Catalytic Reactions*. Princeton University Press, 1984. ISBN null. URL <http://www.jstor.org/stable/j.ctt7zv441>.
- [156] Viktor J. Cybulskis, James W. Harris, Yury Zvinevich, Fabio H. Ribeiro, and Rajamani Gounder. A transmission infrared cell design for temperature-controlled adsorption and reactivity studies on heterogeneous catalysts. *Review of Scientific Instruments*, 87(10):1–12, 2016. ISSN 10897623. doi: 10.1063/1.4963665. URL <http://dx.doi.org/10.1063/1.4963665>.
- [157] Bernard Coq, Francois Figucras, Serge Hub, and Didier Tournigantt. Effect of the Metal-Support Interaction on the Catalytic Properties of Palladium for the Conversion of Difluorodichloromethane with Hydrogen : Comparison of Oxides and Fluorides as Supports. *The Journal of Physical Chemistry*, pages 11159–11166, 1995. doi: 10.1021/j100028a017.
- [158] M. Govindarajan and M. Karabacak. FT-IR, FT-Raman and UV spectral investigation; Computed frequency estimation analysis and electronic structure calculations on 4-hydroxypteridine. *Journal of Molecular Structure*, 1038:114–125, 2013. ISSN 00222860. doi: 10.1016/j.molstruc.2013.01.006. URL <http://dx.doi.org/10.1016/j.saa.2011.11.052>.
- [159] J. F. M. Aarts and K. G. Phelan. Dehalogenation of fluoro- and chlorobenzene on Pd(111) studied by electron energy loss spectroscopy. *Surface Science*, 222(2-3): L853–L860, nov 1989. ISSN 0039-6028. doi: 10.1016/0039-6028(89)90355-5. URL <https://www.sciencedirect.com/science/article/pii/0039602889903555>.
- [160] J. S. Campbell and C. Kemball. Catalytic fission of the carbon-halogen bond. Part 1.-Reactions of ethyl chloride and ethyl bromide with hydrogen on evaporated metal films. *Transactions of the Faraday Society*, 57:809, 1961. ISSN 0014-7672. doi: 10.1039/tf9615700809. URL <http://xlink.rsc.org/?DOI=tf9615700809>.
- [161] Subodh S. Deshmukh, Vladimir I. Kovalchuk, Victor Yu. Borovkov, and Julie L. D’Itri. FTIR Spectroscopic and Reaction Kinetics Study of the Interaction of CF<sub>3</sub> CFCI<sub>2</sub> with  $\gamma$ -Al<sub>2</sub>O<sub>3</sub>. *The Journal of Physical Chemistry B*, 104(6):1277–1284, 2000. ISSN 1520-6106. doi: 10.1021/jp993088f. URL <http://pubs.acs.org/doi/abs/10.1021/jp993088f>.
- [162] Koruga Duro Tamara Jovanovi and Branimir Jovan. The IR Spectra , Molar Absorptivity , and Integrated Molar Absorptivity of the C 76 -D 2 and C 84 -D 2 : 22 Isomers. *Journal of Nanomaterials*, 2017, 2017.

- [163] V. Y. Borovkov, F. Lonyi, and J. L. D'Itri. Fourier Transform Infrared Study of 1,1-Dichlorotetrafluoroethane Adsorption on an Alumina-Supporte dPd Catalyst. *Journal of physical chemistry*, 104:5603, 2000. ISSN 15206106. doi: 10.1021/jp000646d.
- [164] Janine Lichtenberger and Michael D. Amiridis. Catalytic oxidation of chlorinated benzenes over V<sub>2</sub>O<sub>5</sub>/TiO<sub>2</sub> catalysts. *Journal of Catalysis*, 223(2):296–308, 2004. ISSN 00219517. doi: 10.1016/j.jcat.2004.01.032.
- [165] Jun Wang, Vincent F. Kispersky, W. Nicholas Delgass, and Fabio H. Ribeiro. Determination of the Au active site and surface active species via operando transmission FTIR and isotopic transient experiments on 2.3 wt.% Au/TiO<sub>2</sub> for the WGS reaction. *Journal of Catalysis*, 289:171–178, 2012. ISSN 00219517. doi: 10.1016/j.jcat.2012.02.008. URL <http://dx.doi.org/10.1016/j.jcat.2012.02.008>.
- [166] Søren B. Rasmussen, Susana Perez-Ferreras, Miguel A. Bañares, Philippe Bazin, and Marco Daturi. Does pelletizing catalysts influence the efficiency number of activity measurements? Spectrochemical engineering considerations for an accurate operando study. *ACS Catalysis*, 3(1):86–94, 2013. ISSN 21555435. doi: 10.1021/cs300687v.
- [167] Armando Carías-Henriquez, Stan Pietrzyk, and Christophe Dujardin. Modelling and optimization of IR cell devoted to in situ and operando characterization of catalysts. *Catalysis Today*, 205, 2013. ISSN 09205861. doi: 10.1016/j.cattod.2012.08.003.
- [168] Minh-Thong Le. An assessment of the potential for the development of the shale gas industry in countries outside of North America. *Heliyon*, 4:e00516, Feb 2018.
- [169] Beom-Sik Kim, Young-Min Kim, Hyung Won Lee, Jungho Jae, Do Heui Kim, Sang-Chul Jung, Chuichi Watanabe, and Young-Kwon Park. Catalytic Copyrolysis of Cellulose and Thermoplastics over HZSM-5 and HY. *ACS Sustainable Chemistry & Engineering*, 4(3):1354–1363, 2016. doi: 10.1021/acssuschemeng.5b01381. URL <https://doi.org/10.1021/acssuschemeng.5b01381>.
- [170] Keiichi Tomishige, Yoshinao Nakagawa, and Masazumi Tamura. Design of supported metal catalysts modified with metal oxides for hydrodeoxygenation of biomass-related molecules. *Current Opinion in Green and Sustainable Chemistry*, 22: 13–21, 2020. ISSN 24522236. doi: 10.1016/j.cogsc.2019.11.003. URL <https://doi.org/10.1016/j.cogsc.2019.11.003>.
- [171] Yoshinao Nakagawa, Masazumi Tamura, and Keiichi Tomishige. Catalytic Reduction of Biomass-Derived Furanic Compounds with Hydrogen. *ACS Catalysis*, 3(12): 2655–2668, 2013. doi: 10.1021/cs400616p. URL <https://doi.org/10.1021/cs400616p>.
- [172] R. Mariscal, P. Maireles-Torres, M. Ojeda, I. Sádaba, and M. López Granados. Furfural: a renewable and versatile platform molecule for the synthesis of chemicals

- and fuels. *Energy and Environmental Science*, 9:1144–1189, 2016. doi: 10.1039/C5EE02666K. URL <http://dx.doi.org/10.1039/C5EE02666K>.
- [173] Xiaodan Li, Pei Jia, and Tiefeng Wang. Furfural: A Promising Platform Compound for Sustainable Production of C4 and C5 Chemicals. *ACS Catalysis*, 6(11): 7621–7640, 2016. doi: 10.1021/acscatal.6b01838. URL <https://doi.org/10.1021/acscatal.6b01838>.
- [174] Kavita Gupta, Rohit K. Rai, and Sanjay K. Singh. Metal Catalysts for the Efficient Transformation of Biomass-derived HMF and Furfural to Value Added Chemicals. *ChemCatChem*, 10(11):2326–2349, 2018. ISSN 18673899. doi: 10.1002/cctc.201701754.
- [175] Shuo Chen, Robert Wojcieszak, Franck Dumeignil, Eric Marceau, and Sébastien Royer. How Catalysts and Experimental Conditions Determine the Selective Hydroconversion of Furfural and 5-Hydroxymethylfurfural. *Chemical Reviews*, 118(22):11023–11117, 2018. ISSN 15206890. doi: 10.1021/acs.chemrev.8b00134.
- [176] Fei Liu, Qiaoyun Liu, Jinming Xu, Lei Li, Yi-Tao Cui, Rui Lang, Lin Li, Yang Su, Shu Miao, Hui Sun, Botao Qiao, Aiqin Wang, Francois Jérôme, and Tao Zhang. Catalytic cascade conversion of furfural to 1,4-pentanediol in a single reactor. *Green Chemistry*, 20:1770–1776, 2018. doi: 10.1039/C8GC00039E. URL <http://dx.doi.org/10.1039/C8GC00039E>.
- [177] Kefeng Huang, Zachary J. Brentzel, Kevin J. Barnett, James A. Dumesic, George W. Huber, and Christos T. Maravelias. Conversion of Furfural to 1,5-Pentanediol: Process Synthesis and Analysis. *ACS Sustainable Chemistry and Engineering*, 5(6): 4699–4706, 2017. ISSN 21680485. doi: 10.1021/acssuschemeng.7b00059.
- [178] Meredith C. Allen, Alexander J. Hoffman, Tsung-wei Liu, Matthew S. Webber, David Hibbitts, and Thomas J. Schwartz. Highly Selective Cross-Etherification of 5-Hydroxymethylfurfural with Ethanol. *ACS Catalysis*, 10(12):6771–6785, 2020. doi: 10.1021/acscatal.0c01328. URL <https://doi.org/10.1021/acscatal.0c01328>.
- [179] Sara E. Davis, Angelica D. Benavidez, Robert W. Gosselink, Johannes H. Bitter, Krijn P. de Jong, Abhaya K. Datye, and Robert J. Davis. Kinetics and mechanism of 5-hydroxymethylfurfural oxidation and their implications for catalyst development. *Journal of Molecular Catalysis A: Chemical*, 388-389:123–132, 2014. ISSN 1381-1169. doi: <https://doi.org/10.1016/j.molcata.2013.09.013>. URL <http://www.sciencedirect.com/science/article/pii/S1381116913003385>. Special Issue on Biomass Catalysis.
- [180] Mark Douthwaite, Xiaoyang Huang, Sarwat Iqbal, Peter J. Miedziak, Gemma L. Brett, Simon A. Kondrat, Jennifer K. Edwards, Meenakshisundaram Sankar, David W. Knight, Donald Bethell, and Graham J. Hutchings. The controlled catalytic oxidation of furfural to furoic acid using AuPd/Mg(OH)2. *Catalysis Science & Technology*, 7:5284–5293, 2017. doi: 10.1039/C7CY01025G. URL <http://dx.doi.org/10.1039/C7CY01025G>.

- [181] Federica Menegazzo, Michela Signoretto, Tania Fantinel, and Maela Manzoli. Sol-immobilized vs deposited-precipitated Au nanoparticles supported on CeO<sub>2</sub> for furfural oxidative esterification. *Journal of Chemical Technology & Biotechnology*, 92(9):2196–2205, 2017. doi: 10.1002/jctb.5240. URL <https://onlinelibrary.wiley.com/doi/abs/10.1002/jctb.5240>.
- [182] Alessandra Roselli, Yuri Carvalho, Franck Dumeignil, Fabrizio Cavani, Sébastien Paul, and Robert Wojcieszak. Liquid Phase Furfural Oxidation under Uncontrolled pH in Batch and Flow Conditions: The Role of In Situ Formed Base. *Catalysts*, 73(10):1–12, January 2020. ISSN 2073-4344.
- [183] Svenja Werkmeister, Kathrin Junge, Bianca Wendt, Elisabetta Alberico, Haijun Jiao, Wolfgang Baumann, Henrik Junge, Fabrice Gallou, and Matthias Beller. Hydrogenation of Esters to Alcohols with a Well-Defined Iron Complex. *Angewandte Chemie International Edition*, 53(33):8722–8726, 2014. doi: 10.1002/anie.201402542. URL <https://onlinelibrary.wiley.com/doi/abs/10.1002/anie.201402542>.
- [184] Masayuki Naruto, Santosh Agrawal, and Katsuaki Toda & Susumu Saito. Catalytic transformation of functionalized carboxylic acids using multifunctional rhenium complexes. *Scientific Reports*, 7(3425):1–12, June 2017. ISSN 2045-2322. doi: 10.1038/s41598-017-03436-y. URL <https://doi.org/10.1038/s41598-017-03436-y>.
- [185] Bernhard M. Stadler, Pim Puylaert, Justus Diekamp, Richard van Heck, Yuting Fan, Anke Spannenberg, Sandra Hinze, and Johannes G. de Vries. Inexpensive Ruthenium NNS-Complexes as Efficient Ester Hydrogenation Catalysts with High C=O vs. C=C Selectivities. *Advanced Synthesis & Catalysis*, 360(6):1151–1158, 2018. doi: 10.1002/adsc.201701607. URL <https://onlinelibrary.wiley.com/doi/abs/10.1002/adsc.201701607>.
- [186] Shengguang Wang, Vassili Vorotnikov, and Dionisios G. Vlachos. A DFT study of furan hydrogenation and ring opening on Pd(111). *Green Chemistry*, 16:736–747, 2014. doi: 10.1039/C3GC41183D. URL <http://dx.doi.org/10.1039/C3GC41183D>.
- [187] Hilton A. Smith and John F. Fuzek. Catalytic Hydrogenation of Furan and Substituted Furans on Platinum. *Journal of the American Chemical Society*, 71(2): 415–419, 1949. doi: 10.1021/ja01170a013. URL <https://doi.org/10.1021/ja01170a013>.
- [188] Lee J. Durndell, Guchu Zou, Wenfeng Shangguan, Adam F. Lee, and Karen Wilson. Structure-Reactivity Relations in Ruthenium Catalysed Furfural Hydrogenation. *ChemCatChem*, 11(16):3927–3932, 2019. doi: 10.1002/cctc.201900481. URL <https://chemistry-europe.onlinelibrary.wiley.com/doi/abs/10.1002/cctc.201900481>.
- [189] Mei Chia, Yomaira J. Pagán-Torres, David Hibbitts, Qiaohua Tan, Hien N. Pham, Abhaya K. Datye, Matthew Neurock, Robert J. Davis, and James A. Dumesic.

- Selective hydrogenolysis of polyols and cyclic ethers over bifunctional surface sites on rhodium-rhenium catalysts. *Journal of the American Chemical Society*, 133(32): 12675–12689, 2011. ISSN 00027863. doi: 10.1021/ja2038358.
- [190] Mei Chia and James A. Dumesic. Liquid-phase catalytic transfer hydrogenation and cyclization of levulinic acid and its esters to  $\gamma$ -valerolactone over metal oxide catalysts. *Chemical Communications*, 47(44):12233–12235, 2011. ISSN 13597345. doi: 10.1039/c1cc14748j.
- [191] Masazumi Tamura, Yoshinao Nakagawa, and Keiichi Tomishige. Recent Developments of Heterogeneous Catalysts for Hydrogenation of Carboxylic Acids to their Corresponding Alcohols. *Asian Journal of Organic Chemistry*, 9(2):126–143, 2020. ISSN 21935807. doi: 10.1002/ajoc.201900667.
- [192] Takehiro Asano, Yoshinao Nakagawa, Masazumi Tamura, and Keiichi Tomishige. Hydrogenolysis of tetrahydrofuran-2-carboxylic acid over tungsten-modified rhodium catalyst. *Applied Catalysis A: General*, page 117723, 2020. ISSN 0926-860X. doi: 10.1016/j.apcata.2020.117723. URL <http://www.sciencedirect.com/science/article/pii/S0926860X20303161>.
- [193] Theodore W. Walker, Alex K. Chew, Huixiang Li, Benginur Demir, Z. Conrad Zhang, George W. Huber, Reid C. Van Lehn, and James A. Dumesic. Universal kinetic solvent effects in acid-catalyzed reactions of biomass-derived oxygenates. *Energy and Environmental Science*, 11(3):617–628, 2018. ISSN 17545706. doi: 10.1039/c7ee03432f.
- [194] Max A. Mellmer, Canan Sener, Jean Marcel R. Gallo, Jeremy S. Luterbacher, David Martin Alonso, and James A. Dumesic. Solvent effects in acid-catalyzed biomass conversion reactions. *Angewandte Chemie - International Edition*, 53(44): 11872–11875, 2014. ISSN 15213773. doi: 10.1002/anie.201408359.
- [195] Max A. Mellmer, Chotitath Sanpitakseree, Benginur Demir, Peng Bai, Kaiwen Ma, Matthew Neurock, and James A. Dumesic. Solvent-enabled control of reactivity for liquid-phase reactions of biomass-derived compounds. *Nature Catalysis*, 1(3):199–207, 2018. ISSN 25201158. doi: 10.1038/s41929-018-0027-3. URL <http://dx.doi.org/10.1038/s41929-018-0027-3>.
- [196] T. J. Schwartz and J. Q. Bond. A thermodynamic and kinetic analysis of solvent-enhanced selectivity in monophasic and biphasic reactor systems. *Chem. Commun.*, 53(58):8148–8151, 2017. ISSN 1359-7345. doi: 10.1039/C7CC03164E. URL <http://xlink.rsc.org/?DOI=C7CC03164E>.
- [197] Yasuyuki Takeda, Masazumi Tamura, Yoshinao Nakagawa, Kazu Okumura, and Keiichi Tomishige. Hydrogenation of dicarboxylic acids to diols over Re–Pd catalysts. *Catalysis Science & Technology*, 6:5668–5683, 2016. doi: 10.1039/C6CY00335D. URL <http://dx.doi.org/10.1039/C6CY00335D>.

- [198] Rolf Pinkos, Christophe Bauduin, Axel Paul, Gerhard Fritz, and Hans Wagner. PROCESS FOR PREPARING DELTA-VALEROLACTONE IN THE GAS PHASE, September 2011. URL <https://patents.google.com/patent/US20110237806A1/en?q=US20110237806A1>.
- [199] Breaking the Chemical, Engineering Barriers to Lignocellulosic Biofuels, and George W. Huber. *Breaking the chemical and engineering barriers to lignocellulosic biofuels: next generation hydrocarbon biorefineries*. Citeseer, March 2008. URL [https://scholar.google.com/scholar?q=G.W.Huber,in:B.NationalScienceFoundation.Chemical,Environmental,andTransportSystemsDivision,NSF,Washington,DC,2008.#d=gs\\_cit&u=/scholar?q=info:uZ\\_RffacXRYJ:scholar.google.com/&output=cite&scirp=0&hl=en](https://scholar.google.com/scholar?q=G.W.Huber,in:B.NationalScienceFoundation.Chemical,Environmental,andTransportSystemsDivision,NSF,Washington,DC,2008.#d=gs_cit&u=/scholar?q=info:uZ_RffacXRYJ:scholar.google.com/&output=cite&scirp=0&hl=en).
- [200] George W. Huber, Sara Iborra, and Avelino Corma. Synthesis of Transportation Fuels from Biomass: Chemistry, Catalysts, and Engineering. *Chemical Reviews*, 106(9):4044–4098, 2006. doi: 10.1021/cr068360d. URL <https://doi.org/10.1021/cr068360d>. PMID: 16967928.
- [201] Mark Downing, Laurence M. Eaton, Robin Lambert Graham, Matthew H. Langholtz, Robert D. Perlack, Anthony F. Turhollow, Jr, Bryce Stokes, and Craig C. Brandt. U.S. Billion-Ton Update: Biomass Supply for a Bioenergy and Bioproducts Industry. Technical report, Oak Ridge National Laboratory, Oak Ridge, TN. 227p., 8 2011.
- [202] Mukkamala S. Hill N. Joseph J. Baker C. Jensen B. Stemmler E. A. Wheeler M. C. Frederick B. G. van Heiningen A. Berg A. G. Beis, S. H. and W. J. DeSisto. FAST PYROLYSIS OF LIGNINS . *bioresources*, 5(3):1408–1424, 2010. URL [https://bioresources.cnr.ncsu.edu/BioRes\\_05/BioRes\\_05\\_3\\_1408\\_Beis\\_MHJBJSWFHBD\\_Fast\\_Pyrolysis\\_Lignins\\_896.pdf](https://bioresources.cnr.ncsu.edu/BioRes_05/BioRes_05_3_1408_Beis_MHJBJSWFHBD_Fast_Pyrolysis_Lignins_896.pdf).
- [203] Leonard Ingram, Dinesh Mohan, Mark Bricka, Philip Steele, David Strobel, David Crocker, Brian Mitchell, Javeed Mohammad, Kelly Cantrell, and Charles U. Pittman. Pyrolysis of Wood and Bark in an Auger Reactor: Physical Properties and Chemical Analysis of the Produced Bio-oils. *Energy & Fuels*, 22(1):614–625, 2008. doi: 10.1021/ef700335k. URL <https://doi.org/10.1021/ef700335k>.
- [204] Douglas C. Elliott. Historical Developments in Hydroprocessing Bio-oils. *Energy & Fuels*, 21(3):1792–1815, 2007. doi: 10.1021/ef070044u. URL <https://doi.org/10.1021/ef070044u>.
- [205] Dinesh Mohan and Charles U. Pittman. Activated carbons and low cost adsorbents for remediation of tri- and hexavalent chromium from water. *Journal of Hazardous Materials*, 137(2):762 – 811, 2006. ISSN 0304-3894. doi: <https://doi.org/10.1016/j.jhazmat.2006.06.060>. URL <http://www.sciencedirect.com/science/article/pii/S0304389406006996>.
- [206] Jelle Wildschut, Muhammad Iqbal, Farchad H. Mahfud, Ignacio Melián Cabrera, Robbie H. Venderbosch, and Hero J. Heeres. Insights in the hydrotreatment of fast

- pyrolysis oil using a ruthenium on carbon catalyst. *Energy & Environmental Science*, 3:962–970, 2010. doi: 10.1039/B923170F. URL <http://dx.doi.org/10.1039/B923170F>.
- [207] C. Doornkamp and V. Ponec. The universal character of the Mars and Van Krevelen mechanism. *Journal of Molecular Catalysis A: Chemical*, 162(1):19 – 32, 2000. ISSN 1381-1169. doi: [https://doi.org/10.1016/S1381-1169\(00\)00319-8](https://doi.org/10.1016/S1381-1169(00)00319-8). URL <http://www.sciencedirect.com/science/article/pii/S1381116900003198>. In honour of Prof. H. Knozinger on the occasion of his 65th.
- [208] R. Pestman, R. M. Koster, E. Boellaard, A. M. van der Kraan, and V. Ponec. Identification of the Active Sites in the Selective Hydrogenation of Acetic Acid to Acetaldehyde on Iron Oxide Catalysts. *Journal of Catalysis*, 174(2):142 – 152, 1998. ISSN 0021-9517. doi: <https://doi.org/10.1006/jcat.1998.1957>. URL <http://www.sciencedirect.com/science/article/pii/S0021951798919571>.
- [209] Takeshi Matsuda, Yasuyoshi Hirata, Syuya Suga, Hirotohi Sakagami, and Nobuo Takahashi. Effect of H<sub>2</sub> reduction on the catalytic properties of molybdenum oxides for the conversions of heptane and 2-propanol. *Applied Catalysis A: General*, 193(1): 185 – 193, 2000. ISSN 0926-860X. doi: [https://doi.org/10.1016/S0926-860X\(99\)00428-7](https://doi.org/10.1016/S0926-860X(99)00428-7). URL <http://www.sciencedirect.com/science/article/pii/S0926860X99004287>.
- [210] T. Matsuda, H. Shiro, and H. Sakagami & N. Takahashi. Isomerization of heptane on molybdenum oxides treated with hydrogen. *Catalysis Letters*, 47:99–103, September 1997. doi: 10.1023/A:1019048819904. URL <https://doi-org.wv-o-ursus-proxy02.ursus.maine.edu/10.1023/A:1019048819904>.
- [211] Donghai Mei, Ayman M. Karim, and Yong Wang. Density Functional Theory Study of Acetaldehyde Hydrodeoxygenation on MoO<sub>3</sub>. *The Journal of Physical Chemistry C*, 115(16):8155–8164, 2011. doi: 10.1021/jp200011j. URL <https://doi.org/10.1021/jp200011j>.
- [212] Robert K. Grasselli, James D. Burrington, Douglas J. Buttrey, Peter DeSanto Jr., Claus G. Lugmair, and Anthony F. Volpe Jr. & Thomas Weingand. Multifunctionality of Active Centers in (Amm)oxidation Catalysts: From Bi–Mo–O<sub>x</sub> to Mo–V–Nb–(Te, Sb)–O<sub>x</sub>. *Topics in Catalysis*, 23:5–22, August 2003. doi: 10.1023/A:1024859917786. URL <https://link-springer-com.wv-o-ursus-proxy02.ursus.maine.edu/article/10.1023/A:1024859917786#citeas>.
- [213] Robert K. Grasselli. Selective oxidation and ammoxidation of olefins by heterogeneous catalysis. *Journal of Chemical Education*, 63(3):216, 1986. doi: 10.1021/ed063p216. URL <https://doi.org/10.1021/ed063p216>.
- [214] James D. Burrington, Craig T. Kartisek, and Robert K. Grasselli. Aspects of selective oxidation and ammoxidation mechanisms over bismuth molybdate catalysts: II. Allyl

- alcohol as a probe for the allylic intermediate. *Journal of Catalysis*, 63(1):235 – 254, 1980. ISSN 0021-9517. doi: [https://doi.org/10.1016/0021-9517\(80\)90076-7](https://doi.org/10.1016/0021-9517(80)90076-7). URL <http://www.sciencedirect.com/science/article/pii/0021951780900767>.
- [215] James L. Callahan, Robert K. Grasselli, Ernest C. Milberger, and H. Arthur Strecker. Oxidation and ammoxidation of propylene over bismuth molybdate catalyst. *Industrial & Engineering Chemistry Product Research and Development*, 9 (2):134–142, 1970.
- [216] Timothy J. Thibodeau, Alexander S. Canney, William J. Desisto, M. Clayton Wheeler, Francois G. Amar, and Brian G. Frederick. Composition of tungsten oxide bronzes active for hydrodeoxygenation. *Applied Catalysis A: General*, 388(1-2):86–95, 2010. ISSN 0926860X. doi: 10.1016/j.apcata.2010.08.025.
- [217] Daniel R. Moberg, Timothy J. Thibodeau, François G. Amar, and Brian G. Frederick. Mechanism of Hydrodeoxygenation of Acrolein on a Cluster Model of MoO<sub>3</sub>. *The Journal of Physical Chemistry C*, 114(32):13782–13795, 2010. doi: 10.1021/jp104421a. URL <https://doi.org/10.1021/jp104421a>.
- [218] Xin Huang, Hua-Jin Zhai, Jun Li, and Lai-Sheng Wang. On the structure and chemical bonding of tri-tungsten oxide clusters W<sub>3</sub>O<sub>n</sub>- and W<sub>3</sub>O<sub>n</sub> (n=7-10): W<sub>3</sub>O<sub>8</sub> as a potential molecular model for O-deficient defect sites in tungsten oxides. *The journal of physical chemistry. A*, 110:85–92, Jan 2006.
- [219] M. J. Frisch, G. W. Trucks, H. B. Schlegel, G. E. Scuseria, M. A. Robb, J. R. Cheeseman, J. A. Montgomery Jr, T. Vreven, K. N. Kudin, J. C. Burant, et al. *Gaussian 03. Pittsburgh PA: Gaussian*, 2003.
- [220] M. J. E. A. Frisch, G. W. Trucks, H. Bernhard Schlegel, Gustavo E. Scuseria, Michael A. Robb, James R. Cheeseman, et al. *gaussian 09, Revision d. 01, Gaussian*. Gaussian, Inc., 2009.
- [221] Sanja Pudar, Jonas Oxgaard, Kimberly Chenoweth, Adri C. T. van Duin, and William A. Goddard. Mechanism of Selective Oxidation of Propene to Acrolein on Bismuth Molybdates from Quantum Mechanical Calculations. *The Journal of Physical Chemistry C*, 111(44):16405–16415, 2007. doi: 10.1021/jp074452a. URL <https://doi.org/10.1021/jp074452a>.
- [222] George B. Bacskay. A quadratically convergent hartree-fock (QC-SCF) method. Application to open shell orbital optimization and coupled perturbed hartree-fock calculations. *Chemical Physics*, 65(3):383 – 396, 1982. ISSN 0301-0104. doi: [https://doi.org/10.1016/0301-0104\(82\)85211-7](https://doi.org/10.1016/0301-0104(82)85211-7). URL <http://www.sciencedirect.com/science/article/pii/0301010482852117>.
- [223] Konstantin N. Kudin, Gustavo E. Scuseria, and Eric Cancès. A black-box self-consistent field convergence algorithm: One step closer. *The Journal of Chemical Physics*, 116(19):8255–8261, 2002. doi: 10.1063/1.1470195. URL <https://aip.scitation.org/doi/abs/10.1063/1.1470195>.

- [224] Karl K. Irikura, Russell D. Johnson, Raghu N. Kacker, and Rüdiger Kessel. Uncertainties in scaling factors for ab initio vibrational zero-point energies. *The Journal of Chemical Physics*, 130(11):114102, 2009. doi: 10.1063/1.3086931. URL <https://doi.org/10.1063/1.3086931>.
- [225] M. P. Andersson and P. Uvdal. New Scale Factors for Harmonic Vibrational Frequencies Using the B3LYP Density Functional Method with the Triple- $\zeta$  Basis Set 6-311+G(d,p). *The Journal of Physical Chemistry A*, 109(12):2937–2941, 2005. doi: 10.1021/jp045733a. URL <https://doi.org/10.1021/jp045733a>. PMID: 16833612.
- [226] C. Hoang-Van and O. Zegaoui. Studies of high surface area Pt/MoO<sub>3</sub> and Pt/WO<sub>3</sub> catalysts for selective hydrogenation reactions. II. Reactions of acrolein and allyl alcohol. *Applied Catalysis A: General*, 164(1):91 – 103, 1997. ISSN 0926-860X. doi: [https://doi.org/10.1016/S0926-860X\(97\)00160-9](https://doi.org/10.1016/S0926-860X(97)00160-9). URL <http://www.sciencedirect.com/science/article/pii/S0926860X97001609>.
- [227] Chunyang Peng and H. Bernhard Schlegel. Combining Synchronous Transit and Quasi-Newton Methods to Find Transition States. *Israel Journal of Chemistry*, 33(4):449–454, 1993. doi: 10.1002/ijch.199300051. URL <https://onlinelibrary.wiley.com/doi/abs/10.1002/ijch.199300051>.
- [228] Chunyang Peng, Philippe Y. Ayala, H. Bernhard Schlegel, and Michael J. Frisch. Using redundant internal coordinates to optimize equilibrium geometries and transition states. *Journal of Computational Chemistry*, 17(1):49–56, 1996. doi: 10.1002/(SICI)1096-987X(19960115)17:1<49::AID-JCC5>3.0.CO;2-0. URL <https://onlinelibrary.wiley.com/doi/abs/10.1002/%28SICI%291096-987X%2819960115%2917%3A1%3C49%3A%3AAID-JCC5%3E3.0.CO%3B2-0>.
- [229] Henry Eyring. The Activated Complex in Chemical Reactions. *The Journal of Chemical Physics*, 3(2):107–115, 1935. doi: 10.1063/1.1749604. URL <https://doi.org/10.1063/1.1749604>.
- [230] Charles T. Campbell. The Degree of Rate Control: A Powerful Tool for Catalysis Research. *ACS Catalysis*, 7(4):2770–2779, 2017. doi: 10.1021/acscatal.7b00115. URL <https://doi.org/10.1021/acscatal.7b00115>.

## APPENDIX

### REACTOR CONFIGURATION FOR FTIR STUDIES

Heterogeneous catalysis accelerates the reaction by adsorption of and reaction of chemical species involved in the reaction through active sites at the fluid-solid interface. These active sites provide access to new reaction pathways that may otherwise be inaccessible via thermal or homogeneous routes. Several parameters including the number and types of active sites available to different molecules and intermediates as well as the structure of the adsorbed species.<sup>155</sup> Different mechanistic studies on the HDC of PhCl have only speculated the structure of adsorbed chloroaromatics;<sup>62</sup> however, to our knowledge there are no conclusive studies on the nature of PhCl binding to the active site. We propose the use of Fourier Transform Infrared (FTIR) spectroscopy to study how these species bind to the surface, through aromatic ring or through C–Cl bond or a combination of both. Several designs have been proposed for transmission IR gas cells with various capabilities used to study surface chemistries that occur on heterogeneous catalysts. These custom designs include features like operation under vacuum, operation at elevated temperatures, temperature control, and the ability to perform in situ gas treatments. However, these designs often suffer from tedious experimental considerations such as sample preparation or the use of flanges or other measures to secure the IR windows onto the cell. The transmission IR gas cell described here was originally adopted from Gounder's group<sup>156</sup> and modified for our system, incorporates these experimental capabilities along with improved design features to simplify cell operation over a wide experimental range. A key design feature is the modified, hand-tightened Ultra-Torr fittings to provide leak-tight operation and enable rapid removal and loading of catalyst samples with minimal IR cell disassembly. Additionally, catalyst powder samples are utilized as pressed, self-supporting wafers. Figure A.1 shows the experimental set up devised for the FTIR studies.

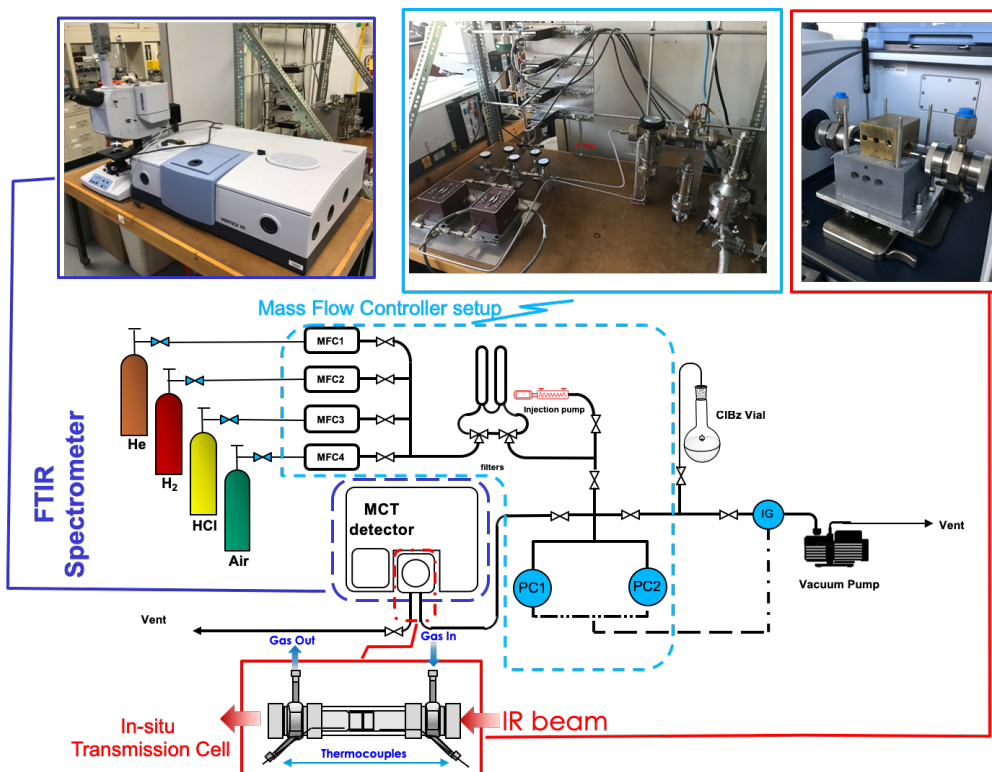


Figure A.1: FTIR experimental set-up equipped with vacuum and a dosing section. In situ transmission cell design was adopted from Cybulskis et al.<sup>156</sup>.

Before starting IR experiments, the system should be leak tested under dynamic vacuum ( $\sim 10^{-2}$ ). First, we close the outlet and evacuate the cell so that our pressure transducer reads 0.0 Torr. Next isolate the system from the vacuum manifold by closing the connecting valve. Now we can monitor the MKS pressure transducer if the pressure did not increase for the period of our reaction then we consider the system leak free.

### A.1 FTIR Dosing Experiment

Two MKS baratron pressure transducers (10 and 1000 Torr) could also be used to initial and final amount of PhCl present in the IR cell manifold. Total volume of the IR cell, transfer line and the dosing manifold is proposed to be measured using a calibration vial of known volume. We will first fill the dosing manifold and the calibration vial with He to a known  $P_i$ , then isolate the calibration vial from the dosing manifold and evacuate. Now by opening the vial's valve the system goes to a final pressure of  $P_f$ . Using the ideal

gas equation of state, we can calculate the total volume  $V_t$  of the system, including the IR cell, the dosing manifold and the transfer lines. Now that we know  $V_t$  and measuring  $P_i$  and  $P_f$  for each dose, assuming there is no adsorption on the lines and the quartz cell, we can calculate the moles of the PhCl adsorbed on the catalysts wafer. For cases where we have the final pressure of 0.0 Torr we can assume total adsorption.

FTIR spectra collected can show us whether the chloroaromatic is adsorbed through a  $\pi$  bond or a  $\sigma$  bond.<sup>64</sup> There are three adsorption configurations of flat, vertical and bridge, for chlorobenzene on different catalysts.<sup>34,157</sup> One possible orientation that we think might be the governing average orientation of the title component on the surface of Pd is the catalyst insertion in the C-Cl bond. Figure A.2 shows the evolution of PhCl on Pd to insertion, the numbers on the bands show bond length in Å.

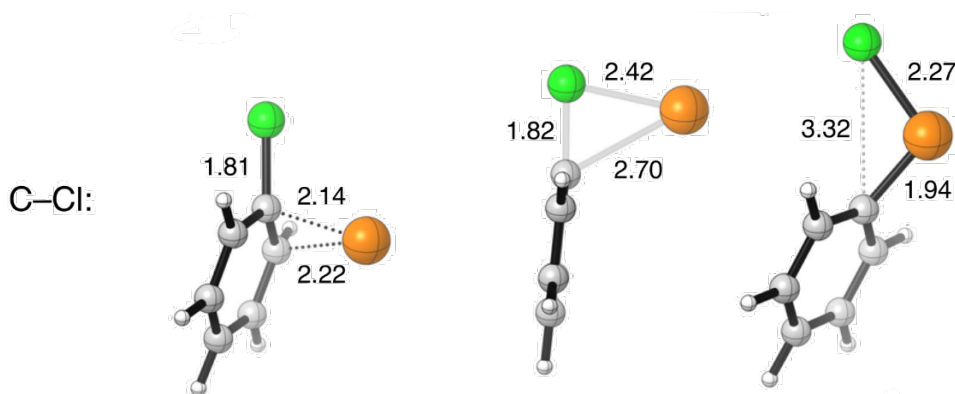


Figure A.2: Pd insertion stages into C-Cl bond in chlorobenzene.<sup>1</sup>

Free chlorobenzene has a planar geometry<sup>158</sup> whose spectrum contains both in-plane and out-of-plane contributions to the IR spectra. In-plane vibrations are responsible for vibrations at  $1588\text{ cm}^{-1}$   $\nu(\text{C}=\text{C})$ . The low-frequency bands at  $690$  and  $774\text{ cm}^{-1}$  correspond to out-of-plane C-H deformations. An IR spectrum after equilibrium adsorption with an increase in out-of-plane vibrations and subsequent decrease in in-plane vibrations could mean vertical orientation while if it is the opposite we expect a parallel orientation. However, as several researchers<sup>62,159,160</sup> have reported, the adsorption orientation of aromatics are often coverage dependent. Therefore, by monitoring the characteristic IR bands for the titled molecules or products after each dose, i.e. varying the coverage, we can

see if the coverage affects the orientation. The effect of Cl coverage will also be investigated by pretreating the surface with HCl before introducing PhCl after which the IR spectra will be collected. Typically chlorobenzene and its derivatives are visible in the range of 400 – 4000 ( $\text{cm}^{-1}$ ).<sup>158</sup> It is expected to see C–Cl stretching vibrations in symmetric and asymmetric modes of 713-762 ( $\text{cm}^{-1}$ ) and 858-982 ( $\text{cm}^{-1}$ ).<sup>161</sup> Through characteristic IR absorption bands, we will be able to calculate the molar extinction coefficient and integrated molar extinction coefficients, which are important for quantitative and qualitative determination our products. Determination of molar absorptivity of our products, in  $\text{Lcm}^{-1}\text{mol}^{-1}$ , at a given wavenumber,  $\epsilon_\lambda$  can be achieved according to Lambert and Beer law, using the absorbance  $A_\lambda$  read at a given wavenumber, b, the path length and c, the analyte concentration:

$$\epsilon_\lambda = A_\lambda \times (bc)^{-1} \quad (\text{A.1})$$

However, the peak height measurements are reported to be very sensitive to the resolution at which the spectra is collected; therefore, the integrated molar extinction coefficients,  $\text{cm}\cdot\text{mol}^{-1}$  which is much less sensitive to the instrumental resolution than the peak height measurement could be used:<sup>162</sup>

$$\Psi = \int \epsilon_\lambda d\lambda \quad (\text{A.2})$$

In this equation  $\lambda$  is the wavelength and  $\epsilon_\lambda$  is the molar absorptivity integrated over the whole band. Subsequently IR spectra could be collected relative to an empty cell background reference under vacuum. Dosing cycles can be repeated until the saturation coverage is observed in the spectra.

## A.2 Steady-State FTIR analysis

Continuous exposure of the chlorine containing material to the catalysts wafer along with dosing exposure were reported before.<sup>163</sup> This is a good tool that will give us insight on the adsorbed species along with kinetics measurement. The IR transmission cell

described before (Figure A.1) would be able to identify species formed in a steady state reaction. However, due to the long effective gas hold up time of 6 s we cannot rely on the kinetics measurements using the same design. In order to investigate the adsorbed species in a steady state (MASIs), we can use the mass flow controller branch in our system. Four MKS mass flow controller will allow us to use hydrogen gas along with helium to adjust the partial pressure of hydrogen. The injection pump will allow us to adjust the flow rate of chlorobenzene. All the lines would be heat traced to prevent condensation of chlorobenzene. Pressure will be monitored using two MKS Barratron pressure transducers. Monitoring for characteristic absorption peaks of Cl-sensitive ( $416\text{-}706\text{ cm}^{-1}$ ) and Pd-H at  $\sim 1952.8\text{ cm}^{-1}$  and parallel configuration of benzene ring at  $\sim 1614\text{ cm}^{-1}$ <sup>164</sup> will enable us to not only identify the most abundant surface intermediates but also help us to identify their orientation on the surface.

### A.3 Time Resolved FTIR Analysis

Another approach that is taken for in situ studies is to collect time resolved data (kinetics data) which would be a good feature in investigating elementary steps and characterizing the active sites. Ribeiro's group<sup>165</sup> showed that kinetics results from in situ IR spectroscopy were comparable with the kinetics results measure in a regular reactor; however, others believe that excessive pelletizing will result in destruction of the pore structure which in turn affects the pore size distribution, leading to the observation of lower activity values.<sup>166</sup> Therefore, the prepared catalyst wafer should also be characterized using CO chemisorption to normalize the rates for the new site density. Moreover, time resolved in situ FTIR analyses requires fast response when changing the flow to be able to monitor the transient state of the reaction. This requires a minimal dead volume and a homogeneous gas velocity in the vicinity of the catalyst surface.<sup>167</sup> Considering the design of the current IR transmission cell is expected to have a large dead volume we need another design for the time resolved studies. There are several designs that focused on decreasing

the dead volume, We propose using the design proposed by Wang et al.<sup>165</sup> that was used to Au active sites and surface active species (Figure A.3).

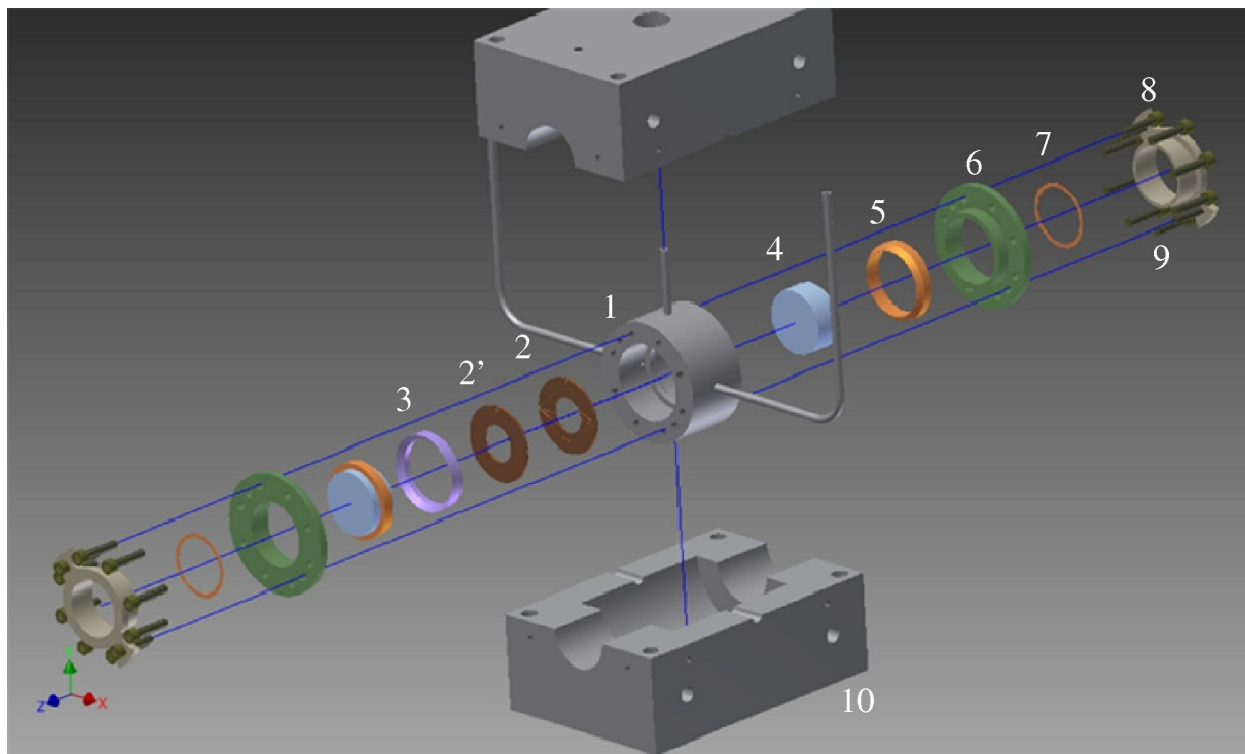


Figure A.3: 3D CAD assembly of the operando transmission IR reactor with heater block ((1) IR cell body; (2) sample holder A; (2') sample holder B; (3) sample holder retainer ring, (4) CaF<sub>2</sub> window; (5) graphite ferrule; (6) window retainer; (7) graphite washer; (8) window retainer; (9) screw set; (10) heater block).<sup>165</sup>

After construction of the cell, which will be a future work, we can simply switch to the new cell and use the mass flow controller branch of our designed system (*c.f.* Figure A.1) for the kinetics measurements. In a typical experiment, the cell will be isolated with beam covers which will retain the continuously fed purged gas through the entire IR beam path length. All lines would be heat trace to prevent condensation of chlorobenzene during the transfer to the cell. The low dead volume of the cell along with fast IR scanning technique will give us unprecedented level of detail the kinetically active surface species and active sites.

#### A.4 Extended Catalytic Systems and Polychlorinated Aromatics

The results of experiments described before will provide a clear picture of the mechanism and kinetics of this reaction. When using different catalysts for this system, e.g. Ni,Coq et al.<sup>136</sup> observed similar rates for both catalysts while Shin and Keane<sup>62</sup> observe a difference in their rates which suggests a different mechanism. Based on the observations in the literature, we hypothesize that there might be differences in the mechanism of hydrodechlorination reactions of chloroaromatics when using Pd and Ni catalysts. We propose the use of kinetics studies coupled with in situ FTIR spectroscopy and isotope labeling to study any differences between the two systems. Finally, as it was suggested by Fabio Ribeiro,<sup>69,130</sup> the rate of hydrodechlorination strongly relies on the C–Cl bond strength. We hypothesize that by increasing the Cl substituents on the benzene rings, caused by change in the molecular electrostatic potential,<sup>158</sup> the rate of the reaction linearly changes with the number of C–Cl bonds on the benzene ring. We propose using chlorobenzene, dichlorobenzene and trichlorobenzene for detailed kinetics measurements to test this hypothesis.

## BIOGRAPHY OF THE AUTHOR

Jalal Tavana was born in Mashhad, Iran on December 18, 1988. He joined Amirkabir University of Technology, also known as Tehran Polytechnic, in the department of Chemical Engineering focused on Petrochemical Industries and graduated with honors in 2011. He then joined one of the leading synthesis groups in the university as a Master's student. Under the supervision of Prof. Mohammad Edrisi to develop nano metallic and bi-metallic oxides for the purpose of removing pollutants from wastewater. In August 2016, he joined "the University of Maine catalysis research group" under the supervision of Dr. Thomas J. Schwartz. Jalal did his research on heterogeneous catalysis focused on biomass upgrading, he was involved in several related hydrogenolysis projects including hydrodechlorination of chlorobenzene and creating biobased polymers through study of hydrodeoxygenation reactions, he was involved in the design and commissioning of multiple instruments like temperature programmed reduction (TPX) setup, FTIR transmission cell and *in situ* spectroscopic setup. Jalal presented his research in several national as well as local conferences. In 2019 he was the recipient of the North American Meeting (NAM26) Kokes Award and in 2020 he won second place for poster competition in the spring meeting of New England Catalysis Society (NECS). Jalal Tavana is a candidate for the Doctor of Philosophy degree in Chemical Engineering from the University of Maine in December 2020.